Hydrogen metabolism in the hindgut of lower termites

Fluxes of hydrogen-dependent and related processes and identification of the homoacetogenic microbiota

Dissertation

zur Erlangung des Doktorgrades der Natuwissenschaften (Dr. rer. nat.)
im Fachbereich Biologie der Philipps-Universität Marburg

vorgelegt von

Michael Pester
aus Wyborg

Marburg/Lahn 2006

Die Untersuchungen zur folgenden Arbeit wurden von September 2003 bis August 2006 am Max-Planck-Institut für terrestrische Mikrobiologie in Marburg unter Leitung von Prof. Dr. Andreas Brune durchgeführt.

Vom Fachbereich Biologie der Philipps-Universität Marburg als Dissertation angenommen am: 23.09.2006

Erstgutachter:	Prof. Dr. Andreas Brune
Zweitgutachter:	Prof. Dr. Rudolf K. Thauer

Tag der Disputation: 30.10.2006

Die in dieser Dissertation beschriebenen Ergebnisse sind in folgenden Publikationen veröffentlicht bzw. zur Veröffentlichung vorgesehen:

Pester, M., and Brune, A. (2006) Expression profiles of *fhs* (FTHFS) genes support the hypothesis that spirochaetes dominate reductive acetogenesis in the hindgut of lower termites. *Environ. Microbiol.* 8: 1261–1270.

Pester, M., and Brune, A. Hydrogen production and efficient recycling during symbiotic lignocellulose degradation in termites. (In Vorbereitung).

Pester, M., Tholen, A., Friedrich, M. W., and Brune, A. Methane oxidation in termite hindguts – absence of evidence and evidence of absence. (In Vorbereitung).

Weiterhin ist folgender Übersichtsartikel (Review) Bestandteil dieser Dissertation:

Brune, A., and Pester, M. (2005) In situ measurements of metabolite fluxes: microinjection of radiotracers into insect guts and other small compartments. In *Methods in Enzymology*. Leadbetter, J. R. (ed). London: Elsevier, pp. 200–212.

Erklärung

Ich versichere, dass ich meine Dissertation

„Hydrogen metabolism in the hindgut of lower termites – fluxes of hydrogen-dependent and related processes and identification of the homoacetogenic microbiota"

selbständig und ohne unerlaubte Hilfe angefertigt habe und mich keiner als der von mir ausdrücklich bezeichneten Quellen und Hilfen bedient habe. Diese Dissertation wurde in der jetzigen oder einer ähnlichen Form noch bei keiner anderen Hochschule eingereicht und hat noch keinen sonstigen Prüfungszwecken gedient.

Marburg, August 2006

Danksagung

An erster Stelle möchte ich mich bei meinem Doktorvater Prof. Dr. Andreas Brune für die Überlassung des Themas sowie die stets offene Tür bei Fragen als auch den Freiraum für die Entfaltung eigener Ideen bedanken.

Herrn Prof. Dr. Rudolf K. Thauer danke ich für die Übernahme des Zweitgutachtens, Herrn Prof. Dr. Ralf Conrad danke ich für die Möglichkeit in seiner Abteilung zu arbeiten.

Weiterer Dank gilt allen Mitgliedern der „Termitengruppe“ für die gute und fröhliche Arbeitsatmosphäre. Im Besonderen danke ich unserer TA Katja Meuser für das reibungslose Managen der vielen kleinen Dinge ohne die ein Labor nicht funktioniert.

Ebenso möchte ich Jared R. Leadbetter und Judith Korb für die Bereitstellung von Termiten danken.

Mein letzter und größter Dank gilt meiner Familie und meiner Freundin für die Unterstützung und Standhaftigkeit in manchmal nicht einfachen Jahren.

Table of contents

1 Introduction

Lower termites and their intriguing biology

Termites are social insects that are thought to have originated in the Late Jurassic period (150 million years ago; Thorne et al., 2000) and since then have successfully colonized about two thirds of Earth's land surface. Their main distribution lies between the latitudes of 48°N and 45°S but they also occur in temperate regions (Lee and Wood, 1971). Currently, seven termite families are recognized, which are summarized in the order Isoptera (Abe et al., 2000) (Fig. 1). Six of these families belong to the phylogenetically lower termites. One of the main features that distinguishes lower termites from the phylogenetically higher termites is the presence of symbiotic protozoa in their enlarged hindgut, which help them to digest lignocellulose, their only food source (Cleveland, 1923; Noirot, 1992).

The wide distribution of termites and their ability to digest lignocellulose in form of wood or grass makes them the most important macroinvertebrates involved in carbon mineralization with the relative contribution of lower termites increasing towards the temperate regions (Sugimoto et al., 2000 and references therein). Despite their role in the carbon cycle, the mere process of lignocellulose degradation is fascinating. The combined efforts of the termite and its hindgut microbiota result in the utilization of 74–99% of the available cellulose and 65–87% of the available hemicellulose of the ingested plant material (based on dry weight, Wood, 1978). However, although it is well established that lower termites depend on their

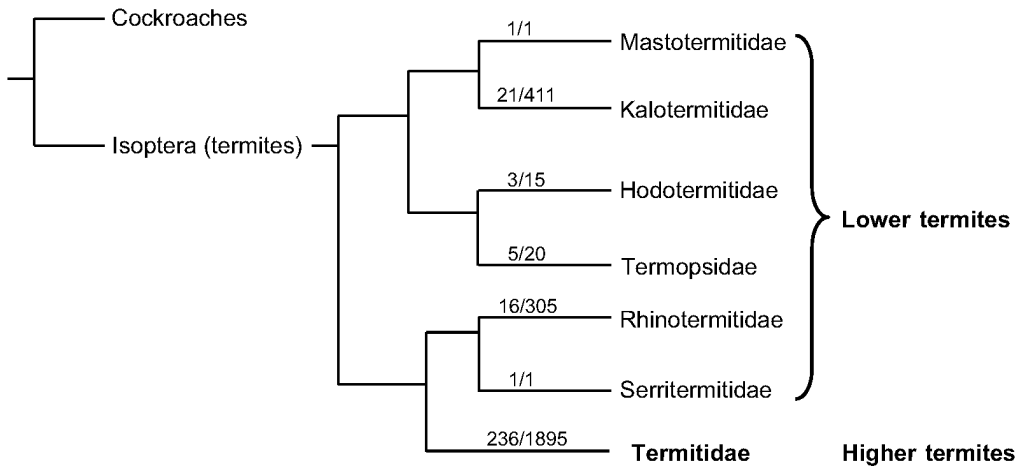

Figure 1. Phylogenetic scheme of termite evolution showing the presumed relationship of the seven termite families, adapted from Higashi and Abe (1997). Numbers superimposed on the single branches represent currently recognized genera/species of the respective families (Abe et al., 2000).

symbiotic microbiota, we are just beginning to understand the individual metabolic interactions in the relationship between the termite, its hindgut protozoa, and the prokaryotes inhabiting the hindgut.

Historical aspects of termite microbiota research

The first report on the intestinal microbiota of lower termites dates back to Lespes in 1856 (see Leidy, 1881), but it took until 1881 for a valid description of hindgut protozoa by Leidy, who initially referred to them as parasites (Leidy, 1881). The symbiotic nature of the hindgut protozoa was discovered by Cleveland in 1923 and described in the upcoming years in a series of publications (Cleveland, 1923; Cleveland, 1924; Cleveland, 1925a; Cleveland, 1925b).

From the work of Hungate, a first mechanistic model of the symbioses emerged as described in the following. Wood particles ingested by the termite pass to the hindgut, where they are ingested by the protozoa and fermented anaerobically to CO_2, H_2, and acetate. The latter compound, after secretion from the protozoa, is absorbed from the hindgut and oxidized aerobically by the termite for energy gain (Hungate, 1939; Hungate, 1943). This model was later supported by data of Odelson and Breznak (1983), who could show that acetate is the dominating volatile fatty acid accumulating in the hindgut fluid and that the production rate of acetate could support 77–100% of the termites energy requirement. In addition, this conclusion was buttressed by the demonstration of acetate in the termite hemolymph but not in the feces and the ability of termite tissue to readily oxidize acetate to CO_2. The main constituents of wood that were utilized for acetate formation were identified using ^{14}C-labeled substrates. About 80% of acetate originated from cellulose and about 20% of acetate originated from hemicellulose (Odelson and Breznak, 1983).

The role of prokaryotes in the hindgut came very late into focus of research and was mainly driven by Breznak and co-workers. Besides a role in the nitrogen economy of the termite, which is discussed later on, hydrogen-driven processes were mainly studied. A major finding was that gut homogenates showed high potential activities of reductive acetogenesis from CO_2 and H_2, which could account for one third of the total acetate production in the hindgut, whereas hydrogenotrophic methanogenesis played only a marginal role (Breznak and Switzer, 1986; Brauman et al., 1992). Based on these experiments, the termite hindgut was proposed to act like an anoxic, homoacetogenic fermentor (Breznak and Switzer, 1986).

Contribution of the termite to wood degradation

The two main contributions of the termite to the breakdown of lignocellulose are the provision of small wood particles and the excretion of endogenous cellulases. The utilized wood is grinded to particles of less than 50 μm in size by the action of the mandibles and the gizzard in the foregut (Fig. 2) (Itakura et al., 1995; Yoshimura et al., 1996). This increases the surface area and, therefore, the

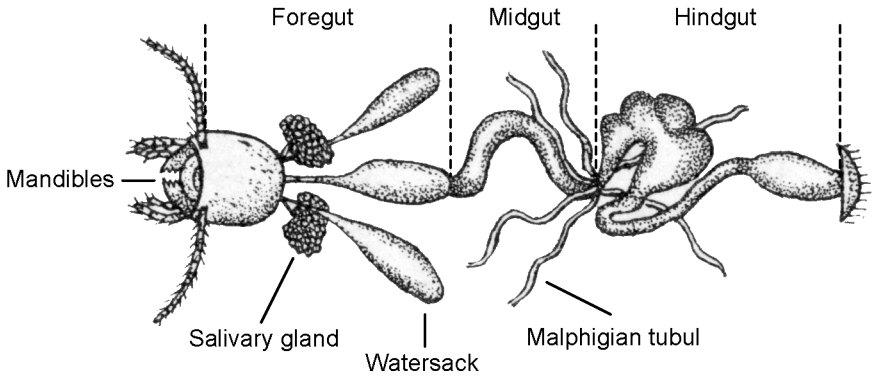

Figure 2. Gut morphology of the lower termite *Reticulitermes lucifugus*. Modified image after Escherich (1909).

accessibility to hydrolyzing enzymes. At the same time, endo-β-1,4-glucanases belonging to the glycosyl hydrolase family 9 (GHF 9) (Tokuda et al., 1997; Watanabe et al., 1997; Lo et al., 2000; Watanabe and Tokuda, 2001; Nakashima et al., 2002a; Tokuda et al., 2004) and β-glucosidases (Inoue et al., 1997; Itakura et al., 1997) are excreted from the salivary glands. However, no cellobiohydrolases were detected so far (Yoshimura, 1995).

Although the excreted cellulases show a high potential hydrolyzing activity on carboxymethyl-cellulose and crystalline cellulose when isolated from the salivary glands, their potential activities drop approximately by one order of magnitude in the fore- and midgut (Tokuda et al., 2005 and references therein). The only exception observed so far is *Coptotermes formosanus*, which shows also a high potential activity in the midgut (Nakashima et al., 2002a; Tokuda et al., 2004). The reason for the general drop of activities in the fore- and midgut is not clear but could, at least in the midgut, be attributed to the simultaneous action of proteinases (Fujita and Abe, 2002). In addition, it should be noted that potential hydrolyzing activities against crystalline cellulose are always higher in the symbiont-packed hindgut even when compared to the high potential activities in the salivary glands (Tokuda et al., 2005).

A similar situation is observed for xylan, the most abundant hemicellulose in wood. There is only little potential activity of endo-β-1,4-xylanase detectable in the salivary glands, the foregut, and the midgut when compared to the hindgut. In the case of β-xylosidase, there is no activity detectable in the salivary glands and the foregut and only in the midgut there is a small potential activity when compared to the hindgut. Removal of protozoa by UV radiation resulted in an almost complete loss of the potential activities of both enzymes in the hindgut, indicating that they are not of termite origin (Inoue et al., 1997).

At present, it is not possible to estimate how much of the wood polysaccharides are actually hydrolyzed during the passage through the fore- and midgut and how much of the mono- and oligosaccharides released are absorbed in the midgut. As

pointed out above, only potential rates were measured and these were generally one order of magnitude lower than in the symbiont-packed hindgut. In addition, the residence time of wood particles in the fore- and midgut is relatively short (<3 h; Kovoor, 1967; Krishna and Singh, 1968; Odelson and Breznak, 1983) when compared to the hindgut (up to 26 h; Breznak and Brune, 1994), where wood particles are retained by ingestion by the protozoa. Summarizing these pieces of circumstantial evidence, it is very likely that the major part of lignocellulose degradation takes place in the hindgut.

Contribution of the hindgut microbiota to the symbiosis

The hindgut microbiota of lower termites consists of up to 20 protozoan species, which differ in number and phylogeny in different termites (ca. 450 protozoan species described, Yamin, 1979), and a great diversity of prokaryotes, with most of them being unique to the termite hindgut (Hongoh et al., 2003; Brune, 2005; Yang et al., 2005). Knowledge on both groups of microorganisms has been extensively reviewed in the last two years (Brune, 2005; Brune and Stingl, 2005; Brugerolle and Radek, 2006) but is mainly descriptive. Based on the large volume protozoa occupy in the hindgut (up to 95% of the hindgut volume, Berchtold et al., 1999), they certainly play the dominant role in the hindgut metabolism. However, one should also consider that a lot of these symbiotic protozoa are themselves hosts to prokaryotes and can be packed with endosymbionts and/or completely covered by ectosymbionts (Fig. 3) (reviewed in Brune and Stingl, 2005). Therefore, prokaryotes seem to play an important role in the hindgut metabolism as well. Unfortunately, not much is known yet about the physiology of the individual microbial species. The pieces of information that were obtained so far are summarized in the following.

The best-established trait of the symbiotic protozoa is that they are primarily

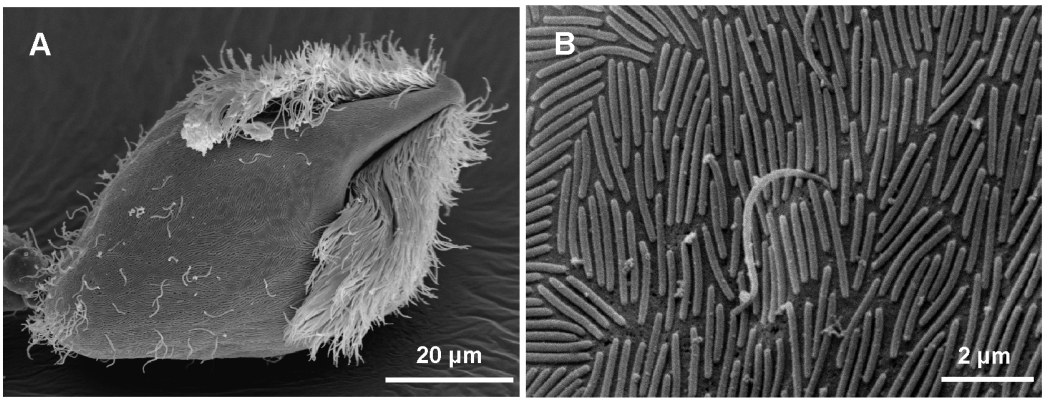

Figure 3. Scanning electron micrograph of the protozoan *Staurojoenina* sp. from the termite *Neotermes cubanus*. (A) Overview of the *Staurojoenina* cell with numerous bacterial rods and occasional spirochetes attached to its surface. (B) Close-up of the cell surface showing in detail the bacterial rods, which were described as *Candidatus* Vestibaculum illigatum and represent a novel lineage of the Bacteroidales. Images were taken from Stingl et al. (2004).

involved in the degradation of wood polysaccharides. This is evidenced by the simple observation that wood particles entering the hindgut are phagocytized immediately by the larger protozoa. As mentioned above, this increases the retention time of wood particles in the hindgut tremendously and allows for a longer activity of the hydrolyzing enzymes. So far, it was possible to test only one axenic protozoan culture for its hydrolyzing enzymes. Crude cell extracts of *Trichomitopsis termopsidis* possessed endo-β-1,4-glucanase and cellobiohydrolase activities but were also able to hydrolyze crystalline cellulose, Douglas fir powder, and xylan (Yamin and Trager, 1979; Odelson and Breznak, 1985a). Recently, the advance of molecular techniques allowed the identification of additional protozoan cellulases, which belong to the GHF 5, GHF 7, and GHF 45 families and which generally act as endo-β-1,4-glucanases (Ohtoko et al., 2000; Nakashima et al., 2002b; Watanabe et al., 2002; Inoue et al., 2005). Based on the observation that in *Coptotermes formosanus* no cellulases of termite origin were detected in the hindgut and vice versa no protozoan cellulases were detected in the foregut or midgut, Nakashima et al. (2002a) proposed a dual cellulose-digesting system with both types of cellulases acting separately in the different gut sections. In *Mastotermes darwiniensis*, a different situation was observed. Here, two of the wood-phagocytizing protozoa were shown to contain – in addition to their own cellulases – also cellulases that were clearly of termite origin (Li et al., 2003). These results were in favor of the hypothesis of Yamaoka and Nagatani (1975), who proposed that cellulases of termite and protozoan origin act simultaneously and synergistically in the hindgut. Unfortunately, there is no information on protozoan enzymes hydrolyzing hemicelluloses yet. However, Inoue et al. (1997) observed that among the 13 protozoa inhabiting the hindgut of *Reticulitermes speratus* only *Dinenympha parva* survived over a longer period of time when termites were fed a strict diet of xylan, indicating that there might be protozoa specialized on hemicellulose utilization.

Early work of Hungate on a mixed culture of termite protozoa and prokaryotes indicated that protozoa ferment the hydrolyzed wood polysaccharides mainly to acetate, CO_2, and H_2 (Hungate, 1943). This result was corroborated later by two axenic cultures of *Trichonympha sphaerica* (Yamin, 1981) and *T. termopsidis* (Yamin, 1980; Odelson and Breznak, 1985b), although it is not clear whether *T. sphaerica* was really devoid of endosymbionts. Keeping in mind that about 450 species of termite protozoa (Yamin, 1979) have been described so far and even more await identification, it seems unlikely that all protozoa have the same metabolism. Evidence pointing towards this direction is the short description of *Tricercomitus divergens* by Yamin (1978), who stated that this protozoan does not utilize cellulose but survives solely on fetal calf serum and yeast extract.

As mentioned before, prokaryotes can often be found in association with protozoa as endo- and ectosymbionts, but they also occur free-living in the hindgut fluid (Brune, 2005; Brune and Stingl, 2005). Among the bacteria, the four major

groups Spirochaetes, Endomicrobia, Firmicutes, and Bacteroidetes are dominating. Nevertheless, other phyla like the Proteobacteria are present to a minor extend as well (Hongoh et al., 2003; Stingl et al., 2005; Yang et al., 2005). The high diversity within these bacterial groups, their unique affiliation to the termite hindgut, and the close association to the protozoa indicate that they also fulfill certain symbiotic functions.

Since lignocellulose is highly depleted in nitrogen, it is not astonishing that prokaryotes play an important role in the nitrogen economy of the termite. It was shown that bacteria enhance the ability of termites to acquire new nitrogen through N_2 fixation and to conserve nitrogen by helping to recycle excretory nitrogen (uric acid and urea) back to the termite for biosynthesis (reviewed by Breznak, 2000). Another important function could be the removal of inflowing oxygen into the hindgut (Brune et al., 1995) and several isolates from lower termites have been shown to do so (Brune, 2005).

The actual contribution of prokaryotes to the degradation of wood polysaccharides or their intermediate fermentation products is not fully understood. Cultivation-based studies indicate that bacteria are not primarily involved in the degradation of cellulose and hemicellulose (Brune, 2005). However, the numerous symbiotic associations with protozoa, which would hamper a cultivation success, should be kept in mind.

Two of the fermentation products originating from protozoa are H_2 and CO_2, and both have been shown to accumulate in the hindgut of *Reticulitermes flavipes* (Ebert and Brune, 1997; Tholen and Brune, 2000). Methanogenic archaea, which utilize both substances, have been found in a variety of lower termites. Depending on the termite species, they are associated either with the hindgut wall (Leadbetter and Breznak, 1996; Leadbetter et al., 1998) or with filamentous prokaryotes attached to the latter (Leadbetter and Breznak, 1996), or occur as ectosymbionts or endosymbionts of certain intestinal flagellates (Lee et al., 1987; Tokura et al., 2000). Despite the common presence of methanogens, methane emission constitutes only a minor fraction of the carbon flow in *R. flavipes* (Odelson and Breznak, 1983). Therefore, methanogenesis plays probably only a minor role, although, it is not firmly established whether methane oxidation occurs in termite hindguts and therefore decreases gross methane emission.

Based on potential rates measured in gut homogenates, reductive acetogenesis seems to be the more important hydrogen-consuming process (Breznak and Switzer, 1986; Brauman et al., 1992). Besides one "classical" homoacetogen belonging to the Clostridia (Kane and Breznak, 1991), also one spirochetes was identified to be able to perform reductive acetogenesis in lower termites (Leadbetter et al., 1999; Graber et al., 2004; Graber and Breznak, 2004). Because of the high abundance of spirochetes (Breznak, 1984; Hongoh et al., 2003; Yang et al., 2005) and the dominance of *fhs* genes attributed to spirochetes in the *fhs*-

gene pool of lower termites, these bacteria were proposed to be mainly responsible for reductive acetogenesis (Salmassi and Leadbetter, 2003). However, this fact still needs to be experimentally proven.

In summary, the physiology of the vast majority of prokaryotes in the termite hindgut is still unclear and awaits its discovery in the future.

Current understanding of the metabolic network in the hindgut

As mentioned earlier, the hindgut of lower termites was proposed to function like an anoxic, homoacetogenic fermentor, in which the wood polysaccharides are hydrolyzed and fermented by protozoa to acetate, CO_2, and H_2, and the latter two products are converted to acetate by homoacetogens (Breznak and Switzer, 1986).

This view has been challenged and modified in the past 10 years mainly by two studies. The introduction of oxygen microsensor studies revealed that the termite hindgut, albeit small is not homogeneous but constitutes a gradient system with oxygen reaching 50–200 µm into the hindgut thereby forming an anoxic and a microoxic zone within the hindgut (Fig. 4) (Brune et al., 1995). Therefore, an influence of oxygen on part of the degradation pathways seemed to be likely. The second major breakthrough was the application of the microinjection method, which allowed injection of minute amounts (50–100 nl) of radiolabeled substrates into dissected termite guts to follow their fate and to measure the underlying processes. The great advantages of this method are that the gut is kept intact as a gradient

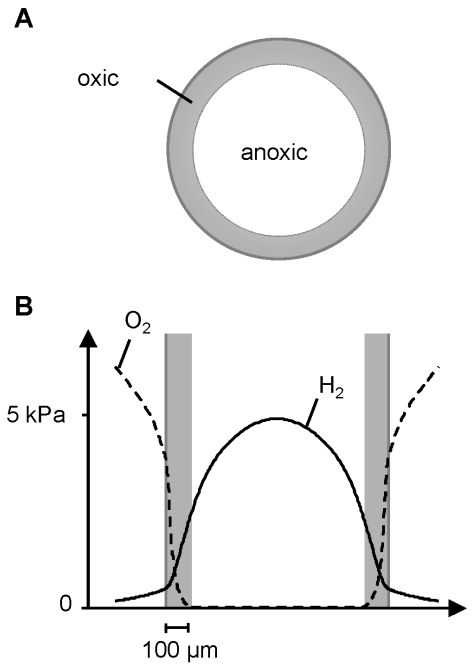

Figure 4. Oxygen status and important metabolite gradients in the agarose-embedded hindgut of the termite *Reticulitermes flavipes*: (A) radial section of the hindgut and (B) oxygen and hydrogen gradients in a radial section. Scheme from Brune and Friedrich (2000).

system, thereby closely mimicking in vivo conditions, and that the injected radiolabeled substrates do not exceed the pool sizes in the gut. This ensures that the conditions of the metabolic network are not brought out of balance (Tholen and Brune, 2000). In a pilot study, the application of the microinjection method to *Reticulitermes flavipes* indicated that lactate is an additional important intermediate but is probably turned over in the microoxic gut periphery and that reductive acetogenesis might indeed play an important role although not that pronounced as proposed previously (Tholen and Brune, 2000). Already these results clearly show that the carbon flow model in the hindgut of lower termites needs to be revised.

The identity of major intermediates in the metabolic network is at the moment still unclear. It is known from previous case studies, which investigated again *R. flavipes*, that hydrogen can accumulate to substantial amounts in the hindgut (Ebert and Brune, 1997) (Fig. 4) but at the same time does not escape by emission to the atmosphere (Odelson and Breznak, 1983). This indicated an efficient recycling of hydrogen but left the questions about the main responsible processes and the extend of the actual hydrogen turnover open. Evidently, there is a need to analyze all hydrogen-utilizing processes in a comprehensive manner and to determine the total hydrogen production rate.

The aims of this study

In this thesis, I investigated three representative species of the Rhinotermitidae, Termitidae, and Kalotermitidae (Fig. 5), the three families of lower termites with the highest species numbers (Kambhampati and Eggleton, 2000). The three termites showed pronounced differences in the degree of hydrogen accumulation in their hindguts, ranging from almost no accumulation to being close to saturation (see chapter 3). Building on this knowledge, all hydrogen-utilizing processes were investigated in a comprehensive manner and the conversion of important fermentation intermediates was analyzed by the microinjection method to establish a robust general model of the metabolic network in the hindgut of lower termites.

The second part of my thesis was concerned with the identity of the organisms responsible for reductive acetogenesis, using the functional gene marker *fhs* (Leaphart and Lovell, 2001; Leaphart et al., 2003; Salmassi and Leadbetter, 2003). Building on the work of Salmassi and Leadbetter (2003), (i) the diversity of homoacetogens, (ii) the relative abundance of homoacetogens, and (iii) the identity of active homoacetogens in the three termites were studied.

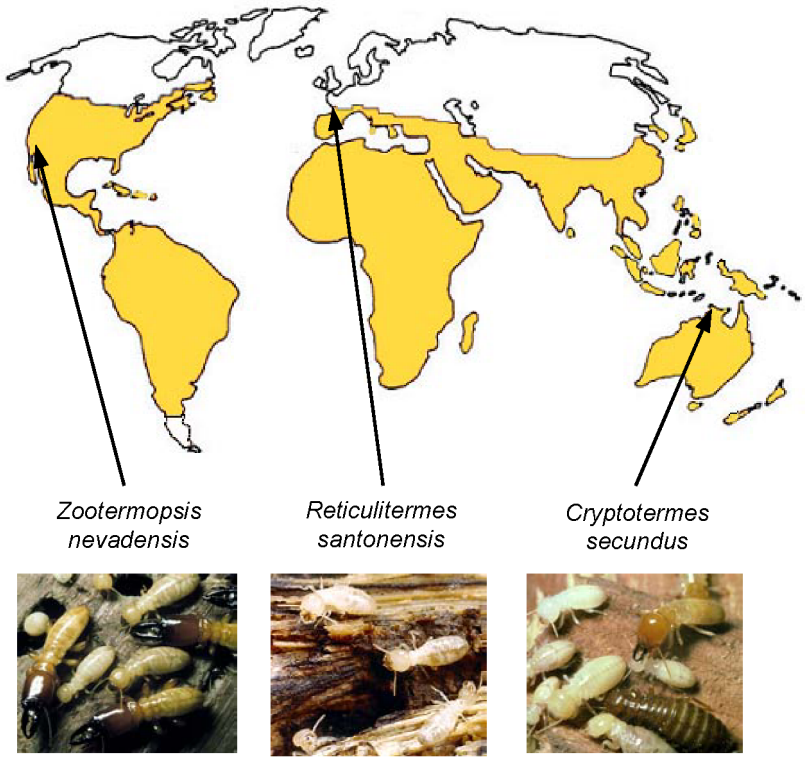

Figure 5. Worldwide distribution of termites (area given in yellow) and the geographical origin of the model termites used in this thesis. *Z. nevadensis* belongs to the Termitidae (rotten-wood termites), *R. santonensis* belongs to the Rhinotermitidae (subterranean termites), and *C. secundus* belongs to the Kalotermitidae (dry-wood termites). Termite images and the earth map were obtained from several sources of the world wide web.

References

1. Abe, T., Bignell, D. E., and Higashi, M. (2000) Termites: evolution, sociality, symbiosis, ecology. Kluwer Academic Publishers, Dordrecht.
2. Berchtold, M., Chatzinotas, A., Schönhuber, W., Brune, A., Amann, R., Hahn, D., and König, H. (1999) Differential enumeration and in situ localization of micro-organisms in the hindgut of the lower termite *Mastotermes darwiniensis* by hybridization with rRNA-targeted probes. *Arch. Microbiol.* 172: 407–416.
3. Brauman, A., Kane, M. D., Labat, M., and Breznak, J. A. (1992) Genesis of acetate and methane by gut bacteria of nutritionally diverse termites. *Science* 257: 1384–1387.
4. Breznak, J. A. (1984) Hindgut spirochetes of termites and *Cryptocercus punctulatus*. In *Bergey's Manual of Systematic Bacteriology*. Krieg, N. R., and Holt, J. G. (eds). Baltimore: Williams & Wilkins, pp. 67–70.
5. Breznak, J. A. (2000) Ecology of prokaryotic microbes in the guts of wood- and litter-feeding termites.In *Termites: Evolution, Sociality, Symbiosis, Ecology*. Abe, T., Bignell, D. E., and Higashi, M. (eds). Dordrecht: Kluwer Academic Publishers, pp. 209–231.
6. Breznak, J. A., and Brune, A. (1994) Role of microorganisms in the digestion of lignocellulose by termites. *Annu. Rev. Entomol.* 39: 453–487.
7. Breznak, J. A., and Switzer, J. M. (1986) Acetate synthesis from H_2 plus CO_2 by termite gut microbes. *Appl. Environ. Microbiol.* 52: 623–630.
8. Brugerolle, G., and Radek, R. (2006) Symbiotic protozoa of termites. In *Soil Biology*. König, H., and Varma, A. (eds). Berlin: Springer-Verlag, pp. 243–269.
9. Brune, A. (2005) Symbiotic associations between termites and prokaryotes. In *The Prokaryotes. An online electronic resource for the microbiological community, 3rd edn.*. Dworkin, M., Falkow, S., Rosenberg, E., Schleifer, K-H., and Stackebrandt, E. (eds). New York: Springer-SBM, http://link.springer-ny.com/link/service/books/10125/
10. Brune, A., and Friedrich, M. (2000) Microecology of the termite gut: structure and function on a microscale. *Curr. Opin. Microbiol.* 3: 263–269.
11. Brune, A., and Stingl, U. (2005) Prokaryotic symbionts of termite gut flagellates: phylogenetic and metabolic implications of a tripartite symbiosis. In *Molecular Basis of Symbiosis*. Overmann, J. (ed). Berlin: Springer, pp. 39–60.
12. Brune, A., Emerson, D., and Breznak, J. A. (1995) The termite gut microflora as an oxygen sink: microelectrode determination of oxygen and pH gradients in guts of lower and higher termites. *Appl. Environ. Microbiol.* 61: 2681–2687.
13. Cleveland, L. R. (1924) The physiological and symbiotic relationships between the intestinal protozoa of termites and their host, with special reference to *Reticulitermes flavipes* Kollar. *Biol. Bull.* 46: 178–227.
14. Cleveland, L. R. (1925) The effects of oxygenation and starvation on the symbiosis between the termite, *Termopsis*, and its intestinal flagellates. *Biol. Bull.* 48: 309–327.
15. Cleveland, L. R. (1925) Toxicity of oxygen for protozoa *in vivo* and *in vitro*: animals defaunated without injury. *Biol. Bull.* 48: 455–468.

16. Cleveland, L.R. (1923) Correlation between the food and morphology of termites and the presence of intestinal protozoa. *Amer. J. Hyg.* 3: 444–461.

17. Ebert, A., and Brune, A. (1997) Hydrogen concentration profiles at the oxic-anoxic interface: a microsensor study of the hindgut of the wood-feeding lower termite *Reticulitermes flavipes* (Kollar). *Appl. Environ. Microbiol.* 63: 4039–4046.

18. Escherich, K. (1909) Die Termiten oder weißen Ameisen. Eine biologische Studie. Leipzig: Klinkhardt Verlag.

19. Fujita, A., and Abe, T. (2002) Amino acid concentration and distribution of lysozyme and protease activities in the guts of higher termites. *Physiol. Entomol.* 27: 76–78.

20. Graber, J. R., and Breznak, J. A. (2004) Physiology and nutrition of *Treponema primitia*, an H_2/CO_2-acetogenic spirochete from termite hindguts. *Appl. Environ. Microbiol.* 70: 1307–1314.

21. Graber, J. R., Leadbetter, J. R., and Breznak, J. A. (2004) Description of *Treponema azotonutricium* sp. nov. and *Treponema primitia* sp. nov., the first spirochetes isolated from termite guts. *Appl. Environ. Microbiol.* 70: 1315–1320.

22. Higashi, M.; Abe, T. (1997) Global diversification of termites driven by the evolution of symbiosis and sociality. In Biodiversity – An Ecological Perspective. Abe, T., Levin, S. A., and Higashi, M. (eds). New York: Springer Verlag, pp. 83–112.

23. Hongoh, Y., Ohkuma, M., and Kudo, T. (2003) Molecular analysis of bacterial microbiota in the gut of the termite *Reticulitermes speratus* (Isoptera; Rhinotermitidae). *FEMS Microbiol. Ecol.* 44: 231–242.

24. Hungate, R. E. (1939) Experiments on the nutrition of *Zootermopsis*. III. The anaerobic carbohydrate dissimilation by the intestinal protozoa. *Ecology* 20: 230–245.

25. Hungate, R. E. (1943) Quantitative analyses of the cellulose fermentation by termite protozoa. *Ann. Entomol. Soc. Am.* 36: 730–739.

26. Inoue, T., Moriya, S., Ohkuma, M., and Kudo, T. (2005) Molecular cloning and characterization of a cellulase gene from a symbiotic protist of the lower termite, *Coptotermes formosanus*. *Gene* 349: 67–75.

27. Inoue, T., Murashima, K., Azuma, J-I., Sugimoto, A., and Slaytor, M. (1997) Cellulose and xylan utilization in the lower termite *Reticulitermes speratus*. *J. Insect Physiol.* 43: 235–242.

28. Itakura, S., Tanaka, H., and Enoki, A. (1997) Distribution of cellulases, glucose and related substances in the body of *Coptotermes formosanus*. *Mater. Org.* 31: 17–29.

29. Itakura, S., Ueshima, K., Tanaka, T., and Enoki, A. (1995) Degradation of wood components by subterranean termite, *Coptotermes formosanus* Shiraki. *Mokuzai Gakkaishi* 41: 580–586.

30. Kambhampati, S., and Eggleton, P. (2000) Taxonomy and phylogenetics of Isoptera. In *Termites: evolution, sociality, symbiosis, ecology*. Abe, T., Bignell, D. E., and Higashi, M. (eds). Dordrecht: Kluwer Academic Publishers, pp. 1–23.

31. Kane, M. D., and Breznak, J. A. (1991) *Acetonema longum* gen. nov. sp. nov., an H_2/CO_2 acetogenic bacterium from the termite *Pterotermes occidentis*. *Arch. Microbiol.* 156: 91–98.

32. Kovoor, J. (1967) Etude radiographique du transit intestinal chez un termite supérieur. *Experientia* 23: 820–821.

33. Krishna, S. S., and Singh, N. B. (1968) Sugar-dye movements through the alimentary canal of *Odontotermes obesus* (Isoptera: Termitidae). *Ann. Entomol. Soc. Am* 61: 230.

34. Leadbetter, J. R., and Breznak, J. A. (1996) Physiological ecology of *Methanobrevibacter cuticularis* sp. nov. and *Methanobrevibacter curvatus* sp. nov., isolated from the hindgut of the termite *Reticulitermes flavipes*. *Appl. Environ. Microbiol.* 62: 3620–3631.

35. Leadbetter, J. R., Crosby, L. D., and Breznak, J. A. (1998) *Methanobrevibacter filiformis* sp. nov., a filamentous methanogen from termite hindguts. *Arch. Microbiol.* 169: 287–292.

36. Leadbetter, J. R., Schmidt, T. M., Graber, J. R., and Breznak, J. A. (1999) Acetogenesis from H_2 plus CO_2 by spirochetes from termite guts. *Science* 283: 686–689.

37. Leaphart, A. B., and Lovell, C. R. (2001) Recovery and analysis of formyltetrahydrofolate synthetase gene sequences from natural populations of acetogenic bacteria. *Appl. Environ. Microbiol.* 67: 1392–1395.

38. Leaphart, A. B., Friez, M. J., and Lovell, C. R. (2003) Formyltetrahydrofolate synthetase sequences from salt marsh plant roots reveal a diversity of acetogenic bacteria and other bacterial functional groups. *Appl. Environ. Microbiol.* 69: 693–696.

39. Lee, K. E. and Wood, T. G. (1971) Termites and soils. Acad. Press, New York.

40. Lee, M. J., Schreurs, P. J., Messer, A. C., and Zinder, S. H (1987) Association of methanogenic bacteria with flagellated protozoa from a termite hindgut. *Curr. Microbiol.* 15: 337–341.

41. Leidy, J. (1881) The parasites of the termites. *J. Acad. Nat. Sci. Philadelphia.* 2nd Ser. VIII: 425–447.

42. Li, L., Fröhlich, J., Pfeiffer, P., and König, H. (2003) Termite gut symbiotic archaezoa are becoming living metabolic fossils. *Eukar. Cell* 2: 1091–1098.

43. Lo, N., Tokuda, G., Watanabe, H., Rose, H., Slaytor, M., Maekawa, K., Bandi, C., and Noda, H. (2000) Evidence from multiple gene sequences indicates that termites evolved from wood-feeding cockroaches. *Curr. Biol.* 10: 801–804.

44. Nakashima, K., Watanabe, H., and Azuma, J.I. (2002) Cellulase genes from the parabasalian symbiont *Pseudotrichonympha grassii* in the hindgut of the wood-feeding termite *Coptotermes formosanus*. *Cell. Mol. Life Sci.* 59: 1554–1560.

45. Nakashima, K., Watanabe, H., Saitoh, H., Tokuda, G., and Azuma, J.-I. (2002) Dual cellulose-digesting system of the wood-feeding termite, *Coptotermes formosanus* Shiraki. *Insect Biochem. Molec. Biol.* 32: 777–784.

46. Noirot, C. (1992) From wood- to humus-feeding: an important trend in termite evolution. In Biology and evolution of social insects. Billen, J. (ed). Leuven, Belgium: Leuven University Press, pp. 107–119.

47. Odelson, D. A., and Breznak, J. A. (1983) Volatile fatty acid production by the hindgut microbiota of xylophagous termites. *Appl. Environ. Microbiol.* 45: 1602–1613.

48. Odelson, D. A., and Breznak, J. A. (1985) Cellulase and other polymer-hydrolyzing activities of *Trichomitopsis termopsidis*, a symbiotic protozoan from termites. *Appl. Environ. Microbiol.* 49: 622–626.

49. Odelson, D. A., and Breznak, J. A. (1985) Nutrition and growth characteristics of *Trichomitopsis termopsidis*, a cellulolytic protozoan from termites. *Appl. Environ. Microbiol.* 49: 614–621.

50. Ohtoko, K.; Ohkuma, M.; Moriya, S.; Inoue, T.; Usami, R.; Kudo, T. (2000) Diverse genes of cellulase homologues of glycosyl hydrolase family 45 from the symbiotic protists in the hindgut of the termite *Reticulitermes speratus*. *Extremophiles* 4: 343–349.

51. Salmassi, T. M., and Leadbetter, J. R. (2003) Molecular aspects of CO_2-reductive acetogenesis in cultivated spirochetes and the gut community of the termite *Zootermopsis angusticollis*. *Microbiology* 149: 2529–2537.

52. Stingl, U., Maass, A., Radek, R., and Brune, A. (2004) Symbionts of the gut flagellate *Staurojoenina* sp. from *Neotermes cubanus* represent a novel, termite-associated lineage of Bacteroidales: Description of '*Candidatus* Vestibaculum illigatum'. *Microbiology* 150: 2229–2235.

53. Stingl, U., Radek, R., Yang, H., and Brune, A. (2005) '*Endomicrobia*': Cytoplasmic symbionts of termite gut protozoa form a separate phylum of prokaryotes. *Appl. Environ. Microbiol.* 71: 1473–1479.

54. Sugimoto, A., Bignell, D. E.; MacDonald, J. A. (2000) Global impact of termites on the carbon cycle and atmospheric trace gases. In Termites: evolution, sociality, symbioses, ecology. Abe, T., Bignell, D. E., and Higashi, M. (eds). Dordrecht: Kluwer Academic Publishers, pp. 409–435.

55. Tholen, A., and Brune, A. (2000) Impact of oxygen on metabolic fluxes and in situ rates of reductive acetogenesis in the hindgut of the wood-feeding termite *Reticulitermes flavipes*. *Environ. Microbiol.* 2: 436–449.

56. Thorne, B. L., and Grimaldi, D. A., and Krishna, K. (2000) Early fossil history of the termites. In Termites: evolution, sociality, symbiosis, ecology. Abe, T., Bignell, D. E., and Higashi, M. (eds). Dordrecht: Kluwer Academic Publishers, pp. 77–93.

57. Tokuda, G, Lo, N, and Watanabe, H (2005) Marked variations in patterns of cellulase activity against crystalline- vs. carboxymethyl-cellulose in the digestive systems of diverse, wood-feeding termites. *Physiol. Entomol.* 30: 372–380.

58. Tokuda, G., Lo, N., Watanabe, H., Arakawa, G., Matsumoto, T., and Noda, H. (2004) Major alteration of the expression site of endogenous cellulases in members of an apical termite lineage. *Mol. Ecol.* 13: 3219–3228.

59. Tokuda, G., Watanabe, H., Matsumoto, T., and Noda, H (1997) Cellulose digestion in the wood-eating higher termite, *Nasutitermes takasagoensis* (Shiraki): distribution of cellulases and properties of endo-β-1,4-glucanase. *Zoolog. Sci.* 14: 83–93.

60. Tokura, M., Ohkuma, M., and Kudo, T. (2000) Molecular phylogeny of methanogens associated with flagellated protists in the gut and with the gut epithelium of termites. *FEMS Microbiol. Ecol.* 33: 233–240.

61. Watanabe, H., and Tokuda, G. (2001) Animal cellulases. *Cell Mol. Life Sci.* 58: 1167–1178.

62. Watanabe, H., Nakamura, M., Tokuda, G., Yamaoka, I., Scrivener, A. M., and Noda, H. (1997) Site of secretion and properties of endogenous endo-β-1,4-glucanase components from *Reticulitermes speratus* (Kolbe), a Japanese subterranean termite. *Insect Biochem. Molec. Biol.* 27: 305–313.

63. Watanabe, H., Nakashima, K., Saito, H., and Slaytor, M. (2002) New endo-beta-1,4-glucanases from the parabasalian symbionts, *Pseudotrichonympha grassii* and *Holomastigotoides mirabile* of *Coptotermes* termites. *Cell. Mol. Life Sci.* 59: 1983-1992.

64. Wood, T.G. (1978) Food and feeding habits of termites. In Production ecology of ants and termites. Brian, MV (ed). Cambridge: Cambridge Univ. Press, pp. 55–80.

65. Yamaoka, I., and Nagatani, Y (1975) Cellulose digestion system in the termite *Reticulitermes speratus* (Kolbe). I. Producing sites and physiological significance of two kinds of cellulose in the worker. *Zool. Mag. (Tokyo)* 84: 23–29.

66. Yamin, M. A. (1978) Axenic Cultivation of the Flagellate Tricercomitus divergens Kirby from the Termite Cryptotermes cavifrons Banks. *J. Parasitol.* 64: 1122-1123.

67. Yamin, M. A. (1980) Cellulose metabolism by the termite flagellate *Trichomitopsis termopsidis*. *Appl. Environ. Microbiol.* 39: 859–863.

68. Yamin, M. A. (1981) Cellulose metabolism by the flagellate *Trichonympha* from a termite is independent of endosymbiotic bacteria. *Science* 211: 58–59.

69. Yamin, M. A., and Trager, W. (1979) Cellulolytic activity of an axenically-cultivated termite flagellate, *Trichomitopsis termopsidis*. *J. Gen. Microbiol.* 113: 417–420.

70. Yamin, M.A. (1979) Termite flagellates. *Sociobiology* 4: 1–119.

71. Yang, H., Schmitt-Wagner, D., Stingl, U., and Brune, A. (2005) Niche heterogeneity determines bacterial community structure in the termite gut (*Reticulitermes santonensis*). *Environ. Microbiol.* 7: 916–932.

72. Yoshimura, T. (1995) Contribution of the protozoan fauna to nutritional physiology of the lower termite, *Coptotermes formosanus* Shiraki (Isoptera: Rhinotermitidae). *Wood Research* 82: 68–129.

73. Yoshimura, T., Fujino, T., Ito, T., Tsunoda, K., and Takahashi, M. (1996) Ingestion and decomposition of wood and cellulose by the protozoa in the hindgut of *Coptotermes formosanus* Shiraki (Isoptera: Rhinotermitidae) as evidenced by polarizing and transmission electron microscopy. *Holzforschung* 50: 99–104.

2 In situ measurements of metabolite fluxes: Microinjection of radiotracers into insect guts and other small compartments

Andreas Brune and Michael Pester.

Published in Methods in Enzymology, 397: 200-212 (2005).

Abstract

In microbial ecology, it is of great interest to determine metabolic activities under *in situ* conditions, i.e., without disturbing the structure of the community and the spatial arrangement of individual populations by experimental manipulation. Microinjection of radiotracers and subsequent analysis using the isotope dilution technique has proven to be a powerful method to measure metabolic fluxes in small biological systems, e.g., the intestinal tract of termites. The large variety of commercially available radiolabeled substrates and the identification and quantitation of radiolabeled products by chromatographic methods allow the investigation of the complete metabolic network in a given system.

Introduction

Most microbial habitats are not homogeneous but are rather characterized by physicochemical gradients of various metabolites. Soils, sediments, microbial mats, and also the intestinal tract of insects are prominent examples of highly structured biological systems where the spatial separation of microbial populations gives rise to steep metabolite gradients and also controls the fluxes between sources and sinks of the respective metabolites (see Kühl and Jørgensen, 1992; Brune et al., 2000).

In the past, metabolic activities in such habitats were often studied with homogenized samples (for examples, see Breznak and Switzer, 1986; Skyring, 1987; Brauman et al., 1992 and references therein). However, homogenization can severely bias the results because it destroys the structure of the original system, increases the distance between microbial cells, and introduces buffer components and substrate concentrations different from those in the natural habitat. Therefore, it is not surprising that metabolic activities obtained with homogenized material often do not mirror the metabolic activities *in situ* (Jørgensen, 1978; Kühl and Jørgensen, 1992; Tholen and Brune, 1999).

Introduction of minute amounts and volumes of radiolabeled substrates into structurally intact systems, e.g., by microinjection, circumvents such experimental constraints. The minimal mechanical disturbance preserves the integrity of the system and ensures that physicochemical gradients and spatial arrangement of

microbial populations are maintained. Since radiolabeled metabolites can be detected with high sensitivity, only minute amounts and volumes of the respective metabolites need to be injected, which avoids undesirable changes in size and concentration of the metabolite pools *in situ*.

There are several prerequisites for the applicability of this method. Most importantly, the system has to be in a steady state, i.e., net changes of metabolite pools and metabolic fluxes during a given time interval should be negligible. Furthermore, the formation rate of a given product can be analyzed only if the label in the product is trapped by dilution in a relatively large product pool, so that the turnover of labeled product is negligible.

Another important consideration concerns the distribution of the label after injection. For systems where the spatial distribution of microbial populations in the system can be considered homogenous at the scale of label distribution, as in the case of a horizontally stratified sediment, integrated rates can be determined even if the injected label is unevenly distributed within each layer — unless the label is carried out of the system during the incubation. However, systems in which the microbial populations are heterogeneously distributed within the range of the injected label, as in the case of insect guts, a fast and even distribution of the injected radiolabel by diffusion and/or advective mixing is required to calculate rates based on the isotope dilution technique.

Microinjection of radiotracers has been applied successfully to determine metabolic rates in various gradient habitats. For example, depth profiles of *in situ* sulfate reduction rates in sediment cores (Moeslund et al., 1994) and cyanobacterial mats (Jørgensen, 1994) were determined by injection of $^{35}SO_4^{2-}$ into different layers. Another example is the measurement of metabolic rates and the respective carbon flux within intact hindguts of various termite species by microinjection of ^{14}C-labeled substrates (Tholen and Brune, 1999; Tholen and Brune, 2000). This chapter will focus on the latter example — the experimental procedure and possible pitfalls will be discussed in detail.

Theoretical background

In small systems with a heterogeneous spatial arrangement of the microbial populations, it is important that the time required for an even distribution of the injected radiolabel is considerably shorter than the time interval used for the determination of the metabolic activity. At short distances, diffusion is the most important transport mechanism, and the time (t) required for a molecule to travel by diffusion a certain distance (s) in space is described by the Einstein-Smoluchowski equation:

$$t = \frac{s^2}{6 \cdot D} \qquad (1)$$

where D is the apparent diffusion coefficient of the injected substrate in a given environment. Based on Eq. (1), and assuming a diffusion coefficient for small molecules in aqueous medium of approximately 10^{-5} cm^2 s^{-1} (Ambrose et al., 1999), it can be estimated that an injected substance travels approximately 1 mm within 60 s after injection. In closed biological systems, the time needed for total mixing is often further reduced by advection, e.g., caused by peristalsis and movements of protists in gut environments. This allows the study of systems even larger than those controlled solely by diffusion. The mathematics of diffusion are covered in detail by Crank (1975).

The determination of metabolic rates in a small, enclosed, and well-mixed system requires knowledge of the size of the respective substrate and product pools. Depending on the size of the substrate pool, two situations can be distinguished:

i. The pool size (N) is small and therefore increased considerably by the injected substrate. In this case, the observed decrease of radiolabel in the substrate pool over time ($\mathrm{d}X_S/\mathrm{d}t$) is directly proportional to the turnover rate of the substrate (R_S):

$$\frac{\mathrm{d}X_S(t)}{\mathrm{d}t} = R_S \cdot A \tag{2}$$

where A is the specific radioactivity of the labeled element in the substrate pool. The increased pool size, however, may remove kinetic constraints of the system, and the resulting potential rates may exceed the *in situ* rates considerably.

ii. The amount of injected label is small and does not greatly increase the size of the substrate pool. In the ideal case, the pool size can be considered constant, and the decrease of radioactivity in the substrate pool (X_S) reflects the dilution of the initially injected label (X_0) by non-labeled substrate entering the pool and labeled substrate leaving the pool (Fig. 1):

$$X_S(t) = X_0 \cdot \mathrm{e}^{\mu \cdot t} \tag{3}$$

where μ is the turnover rate constant. In its logarithmic form, Eq. (3) yields a linear function and the turnover rate constant can be determined from the slope of the linear regression of the experimental data:

$$\ln X_S(t) = \mu \cdot t + \ln X_0 \tag{4}$$

The substrate turnover rate can then be calculated using the experimentally determined pool size and the turnover rate constant:

$$R_S = \mu \cdot N \tag{5}$$

The calculation of the product formation rates is a slightly more complex. The specific radioactivity of the substrate pool is determined by the amount of radiolabel injected into the pool:

$$A = \frac{X}{N} \tag{6}$$

Owing to the washout of radioactivity from the substrate pool (Eq. 3), the specific radioactivity of the pool decreases over time:

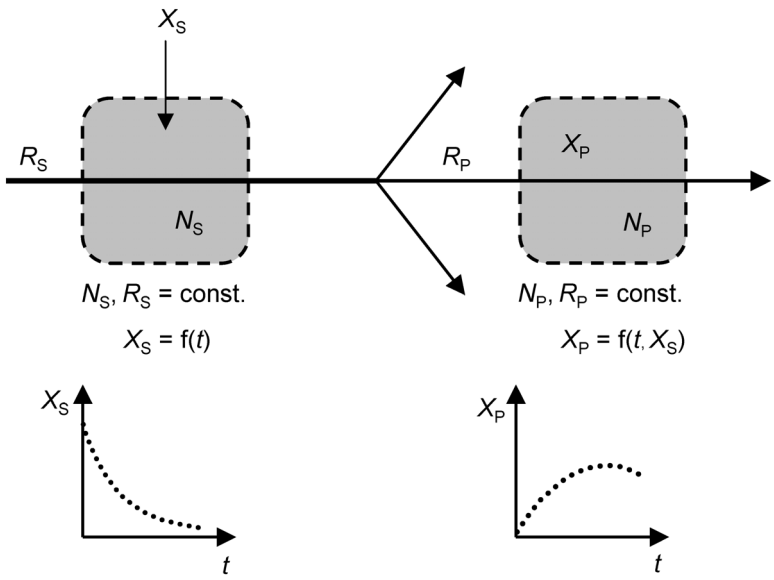

Figure 1. Principle of flux measurements using the isotope dilution technique. At steady-state conditions, the pools of substrate (N_S) and the product(s) (N_P) and the corresponding fluxes through the respective pools (R_S, R_P) are constant parameters. The hypothetical time courses for the washout of injected radiolabeled substrate (X_S) and the accumulation of radiolabeled product (X_P) are indicated; they can be used to calculate turnover rates and metabolic fluxes (see text).

$$A(t) = A_0 \cdot e^{\mu \cdot t} \tag{7}$$

Despite a constant rate of substrate-to-product conversion (steady state), this decrease in the specific radioactivity of the substrate pool causes also a decrease in the formation rate of labeled product [dX_P/dt] (Fig. 1). dX_P/dt is obtained by substituting the specific radioactivity in Eq. (2) by Eq. (7). The resulting Eq. (8) describes the formation of a labeled product as a function of time, turnover-rate constant of the substrate pool, and the turnover rate of this particular product (R_P).

$$\frac{dX_P(t)}{dt} = R_P \cdot A_0 \cdot e^{\mu \cdot t} \tag{8}$$

Integration of Eq. (8) over time ($t_0 = 0$; $X_0 = 0$) yields a new exponential function (Eq. 9), which allows the formation rate of a given product to be calculated from the experimentally obtained data points [X_P; t], the turnover-rate constant, and the initial specific radioactivity of the substrate pool.

$$X_P(t) = \frac{R_P \cdot A_0}{\mu}(e^{\mu \cdot t} - 1) \tag{9}$$

Practical example

The model described above has been successfully applied in a study of metabolite fluxes in the hindgut of the termite *Reticulitermes flavipes*, employing ^{14}C-labeled metabolites (Tholen and Brune, 2000). The hindgut paunch of this termite is characterized by steep gradients of O_2 and H_2 (Ebert and Brune, 1997; Fig. 2) and by a heterogeneous distribution of the microbial community within the gut (Yang et al.,

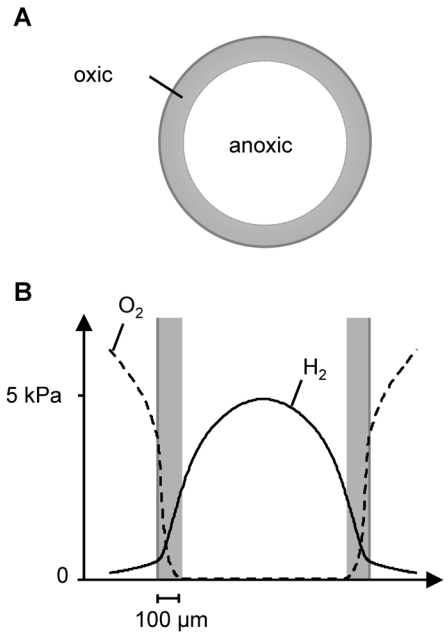

Figure 2. Oxygen status and important metabolite gradients in the agarose-embedded hindgut of the termite *Reticulitermes flavipes*: (A) radial section of the hindgut and (B) oxygen and hydrogen gradients in a radial section. Scheme from Brune and Friedrich (2000).

2005). The lactate pool in the hindgut fluid was rather small (ca. 1 mM), but the rapid washout of injected label from the substrate pool indicates a rapid turnover of lactate (Fig. 3A). The experimentally determined turnover rate constant (Eq. 4), which gave a good fit with the experimental data when inserted into Eq. (3), yielded a high lactate turnover rate (Eq. 5), representing about one-third of the total carbon flux through *R. flavipes*. Acetate was the major product of lactate turnover, and also the experimentally determined product formation rates gave good fits with the experimental data when inserted into Eq. (9). When the experiment was repeated under a nitrogen atmosphere, the lactate turnover rate decreased, and the product formation rates changed fundamentally when compared to the situation under air (Fig. 3B), which provides a perfect example underlining the necessity to determine metabolic fluxes under *in situ* conditions.

Experimental setup

Microinjection apparatus

The introduction of minute volumes of radiotracer (down to sub-microliter amounts) into the sample is accomplished by means of microinjection. The microinjection apparatus is a hydraulic system consisting of a fine-tipped glass capillary filled with light mineral oil ($d_{25\,°C} \approx 0.8$ g ml^{-1}) connected to a microliter syringe. The syringe can be actuated either mechanically or by a motorized mechanism. The positioning of the capillary tip is controlled by a manual micromanipulator (MM 33, Märzhäuser, Wetzlar, Germany) and monitored with the help of a stereomicroscope (Fig. 4A).

A critical point of the microinjection is the accuracy of the volume delivery. During method development, we tested three different variants of the microinjection apparatus. Initially, we used a Microdispenser® (Drummond Scientific Company, Broomall, Pa., USA), which resembles an automatic pipette with a steel piston that inserts directly into the capillary tip, thus creating a direct connection between capillary tip and syringe. However, the volume delivery of the Microdispenser® was not reproducible at volumes <100 nl. In addition, the transmission of mechanical disturbances resulting from the manual operation of the instrument led to uncontrolled movements of the capillary tip, which affected the tip position and the integrity of the sample.

To alleviate these problems, the tip and the actuator were separated by connecting the capillary via hydraulic tubing to a microliter syringe, which was operated manually using a micrometer drive. This variant was applied successfully in several studies (Tholen and Brune, 1999, Tholen and Brune, 2000), but the setup was inferior to the first variant because it was difficult to remove air bubbles introduced into the hydraulic tubing during instrument setup and capillary changes.

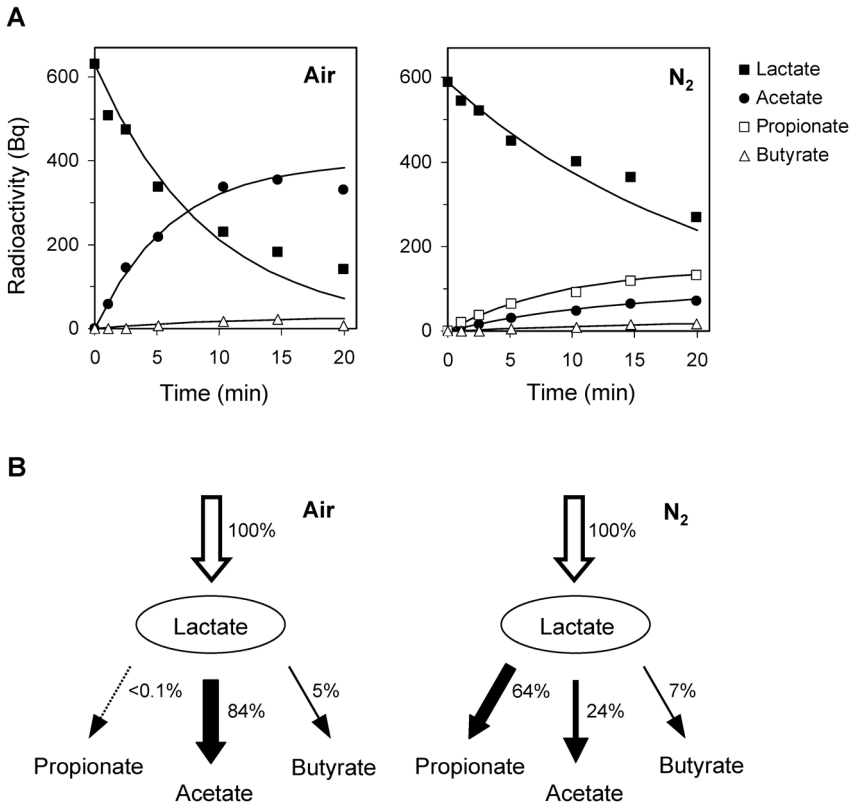

Figure 3. Original data from a microinjection study of lactate turnover in the hindgut of the termite *Reticulitermes flavipes* (Tholen and Brune, 2000). (A) Time course of label distribution among different metabolites after microinjection of ^{14}C-lactate into agarose-embedded guts incubated under air or under a nitrogen atmosphere. Values represent the mean of four injections into separate guts. Predicted curves for radioactive substrate depletion and product formation (solid lines) are based on the kinetic model described in the text [Eqns. (4) and (9)]. (B) Impact of oxygen on the relative rates of product formation from lactate produced in the primary fermentations. The slight imbalance is most likely owing to the formation of CO_2 not being accounted for.

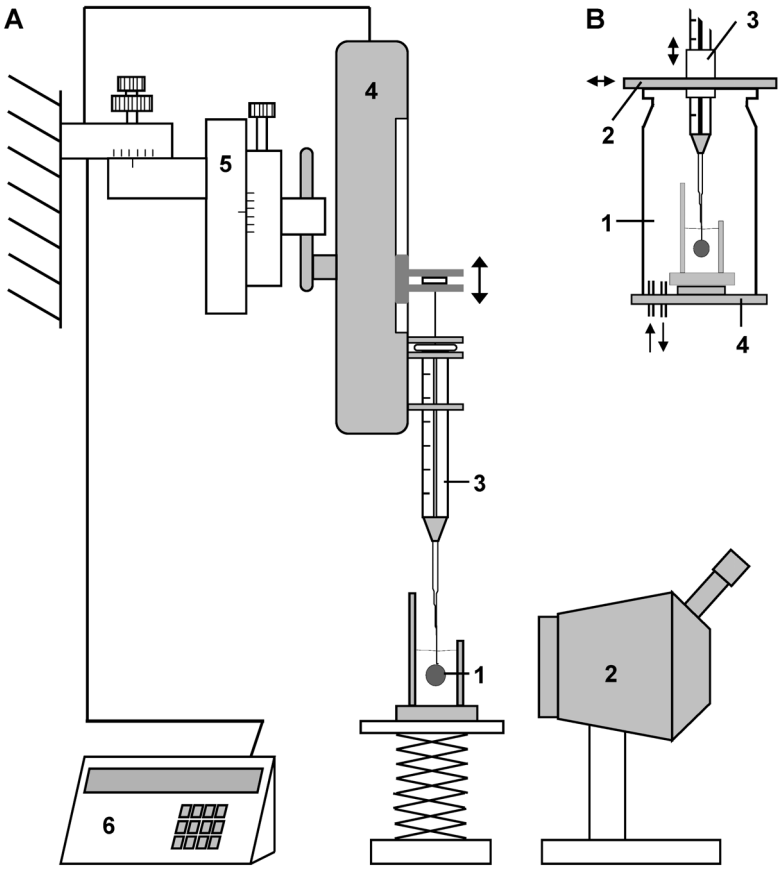

Figure 4. (A) Schematic view of the most advanced setup used for microinjection of radiotracers into insect guts: (1) isolated gut embedded in agarose, placed on a scissor-lift table, (2) stereomicroscope, (3) oil-filled microliter syringe with a fine-tipped glass capillary, (4) motor drive, (5) manual micromanipulator controlling tip position, fixed to a solid steel support, and (6) microprocessor controller for motor drive. (B) Schematic view of the modifications for microinjection under a defined headspace: (1) glass bell, (2) PVC cover plate and (3) shaft, which allow lateral and vertical positioning, and (4) base plate with gas inlet and outlet for continuous flushing.

For this reason, we recently developed a third setup in which the tip was again connected directly to the syringe, but the manual control of the syringe piston was replaced by a microprocessor-controlled stepping motor (Fig. 4A). The current system consists of a 50-µl syringe with a luer-lock connection (Hamilton Company, Reno, Nev., USA) actuated by a Micro Pump II® operated via a Micro4® microprocessor controller (World Precision Instruments, Inc., Sarasota, Fla., USA). This setup is the most accurate and convenient solution to date and allows reproducible injection in the desired volume range (30–50 nl; E. Miambi, A. Fujita, M. Pester, and A. Brune, unpublished results).

For certain applications, microinjection and subsequent incubation must be carried out under a defined atmosphere. For this purpose, samples are placed into a glass bell (inverted membrane filtration funnel; Sartorius, Göttingen, Germany) covered with a round PVC plate (Fig. 4B). The micropipette is inserted through a

small vertical tube glued into a central hole of the PVC plate; the inner diameter of the tube is only slightly larger than the outer diameter of the microliter syringe. The setup is sealed with a thin film of silicone oil applied to all moving parts. With this device, the micropipette tip can be positioned vertically and laterally within the bell, while the headspace of the bell is continuously flushed with the desired gas mixture. At flow rates of 2 ml s^{-1}, the backpressure at the outlet is negligible.

Preparation of fine-tipped capillaries

In addition to the reproducibility of the hydraulic system, the tip of the glass capillary is decisive for a successful microinjection. Prefabricated tips are commercially available (World Precision Instruments, Inc., Sarasota, Fla., USA) but are expensive and do not have an optimal shape.

Custom-made capillaries with the desired tip diameter and length of the taper are constructed by pulling a suitable glass capillary (50 µl; Duran® glass, 1.0 mm I.D, 1.5 mm O.D.), either manually or in a commercial capillary puller. For manual pulling, it is best to first reduce the original diameter of the capillary by gentle, manual pulling after heating the capillary locally with a small gas flame (e.g., of a small soldering torch). The final tip is pulled in a second step using a platinum heating loop and gravitational force. A commercial capillary puller allows tip production in a one-step process and yields more reproducible tapers, but is not essential. Tip diameter and taper length can be varied by changing the heat and the pulling force. The final tip diameter is adjusted by breaking off the tip under a microscope using precision steel tweezers (e.g., Dumont No. 5, Dumont, Montignez, Switzerland).

The connection to the syringe is made by fitting the blunt end of the capillary into a plastic luer-lock adapter. The luer-lock adapter is removed from a disposable syringe needle by briefly heating the steel next to the adaptor (e.g., with a cigarette lighter or the pilot flame of a Bunsen burner) and pulling the adapter and needle apart. The opening in the plastic adaptor is enlarged to the diameter of the glass capillary with a suitable drill bit. The blunt end of the capillary is introduced into the adaptor and connected by carefully melting the plastic with a small flame. A tight seal is crucial and can be improved by applying a fast-curing epoxy glue. Before connection to the syringe, the capillary is filled with the same oil as the syringe.

System check and calibration

The most common problem is an air bubble in the hydraulic system, which is usually introduced when the different parts of the hydraulic system are connected. Because of the large compressibility of air, movements of the piston are not exactly translated into movement of the liquid in the capillary tip, resulting in both inaccurate and poorly reproducible injections.

Therefore, the hydraulic system should be scrutinized for air bubbles, by eye and under a stereomicroscope. Air bubbles are most commonly trapped at the luer-lock

connection between the capillary tip and syringe. Even if no air bubbles are visible, the reproducibility and accuracy of the injections have to be tested. This is done by injecting the desired volume of radiotracer of known volume activity directly into a series of scintillation vials filled with scintillation cocktail and determining the radioactivity using a liquid scintillation counter.

To avoid evaporation of the aqueous sample and to avoid blocking, the tip should be kept immersed in oil between injections.

Radiolabel concentration and injection volumes

To avoid artifacts, the injection should not increase pools sizes or dilute pool concentrations of the metabolites substantially (see earlier discussion). Nevertheless, the label should be sufficient to detect the injected compound and its metabolic products with the analytical equipment available. While the sensitivity of liquid scintillation counting depends mainly on the measuring time, identification and quantitation of metabolites by chromatographic techniques can easily become a limiting factor.

To address both constraints, it is advisable to use the label as supplied by the vendor, i.e., undiluted, and at the highest available specific radioactivity. This is especially important in the case of ^{14}C-labeled compounds. Because of the long half-life time of the ^{14}C isotope, commercial preparations are actually provided at a specific radioactivity that already comes close to the theoretically possible value, where all carbon atoms are labeled (2.3 MBq μmol^{-1} or 62.4 mCi mmol^{-1}). Since microinjection will always involve only minute amounts of a given compound, cost is usually not an issue.

In the example mentioned above (see section IV), we injected 50 nl ^{14}C-lactate (600 Bq) into the hindgut paunch of *R. flavipes* (total volume 0.72 μl). Due to the high specific radioactivity of the lactate preparation (6.1 MBq μmol^{-1}), the amount of lactate injected (0.1 nmol) caused only a relatively small dilution of the intestinal lactate pool (1 nmol). The detection limit of the individual radiolabeled metabolites by high-performance liquid chromatography (HPLC) was in the range of 2–5 Bq per peak (Tholen and Brune, 2000).

Microinjection into termite guts

Ideally, metabolite fluxes should be studied by introducing radiotracer into the gut *in vivo*, i.e., still within the insect body. However, even with immobilized termites, it is impossible to position the capillary tip into a specific gut region. Moreover, the fragile tips break easily when penetrating the cuticle. Therefore, guts have to be isolated from the termites and embedded in agarose made up in Ringer's solution to prevent desiccation and to keep the guts physiologically active. The gut is easily removed from the agarose at the end of the incubation. Both the gut contents and

any radiolabeled metabolites that diffused out of the gut and were trapped in the agarose are available for subsequent analyses.

Sample preparation

Termites are dissected, and guts are embedded in agarose in Ringer's solution (7.5 g NaCl l^{-1}, 0.35 g KCl l^{-1}, and 0.21 g $CaCl_2$ l^{-1}) in a suitable chamber. The bottom and side walls of the chamber are constructed of a U-shaped PVC spacer; front and back walls are made of large microscope cover slips. The termite gut is placed flat and fully extended onto a thin layer of 2% agarose at the bottom of the microchamber and quickly covered with a layer of molten 0.5% agarose (45 °C), which should cool and solidify immediately. Ideally, the overlay should not be thicker than 1–2 mm. Several guts can be prepared in parallel and stored in a moist chamber to avoid desiccation.

Microinjection

A chamber with an embedded gut is placed onto a small scissor-lift table and, if indicated, covered by a glass bell to control the gas headspace (Fig. 4B). Using the micromanipulator, the capillary tip containing the radiotracer is positioned outside of the agarose directly above the gut. Then, the tip is slowly inserted through the agarose into the gut and positioned at the gut center. Usually, the gut wall is indented upon contact with the capillary tip and relaxes after penetration. This visual control is important to avoid injecting the radiotracer into the agarose. With the motorized setup, the injection can be performed at a high rate of volume delivery (e.g., 1000 nl s^{-1}); in that case, also a sudden, barely perceptible increase of the gut volume indicates a successful injection. After injection, the capillary tip is retracted and the gut is placed in a moist chamber for the desired incubation time.

For the interpretation of the results, it is important to determine the exact amount of radiotracer delivered into the gut at the time of injection and the amount of injected tracer that leaks from the gut into the surrounding agarose because of possible damage to the gut caused by the injection procedure. For this purpose, it is convenient to use a compound that does not diffuse across the gut wall and is not metabolized within the gut (e.g., ^{14}C-polyethylene glycol 4000).

Analysis of metabolites

At the end of the incubation, guts are removed from the agarose and immediately placed into a defined volume of ice-cold stopping solution (0.2 M NaOH), and homogenized by sonication with an ultrasonic probe (e.g., Ultraschallprozessor 50 H equipped with a microtip, Dr. Hielscher GmbH, Teltow, Germany). After centrifugation (10 min, 20.000 *g*), the supernatant is analyzed for total radioactivity and individual metabolites. The pellet is washed with stopping solution and then analyzed for residual radioactivity.

The agarose block is placed into an Eppendorf tube containing a defined volume of the stopping solution and stored for a few days at 4 °C to allow metabolites in the agarose to equilibrate with the solution. Cutting the agarose into smaller pieces will speed up the process. After equilibration, the liquid phase is analyzed for total radioactivity and individual metabolites. Volume determination of the remaining agarose block by weighing or analyzing the remaining agarose for total radioactivity allows accurate radioactivity recoveries for the substrate and the single products to be calculated.

The alkaline character of the stopping solution prevents loss of volatile substances, such as CO_2 and short-chain fatty acids. It is advisable to include any metabolites of interest (non-labeled) in the stopping solution to act as internal standard and as a carrier to prevent unspecific loss of the radiotracer.

The overall recovery of radioactivity after microinjection and incubation is determined by liquid scintillation counting (LSC) of aliquots of the gut and agarose samples. Incomplete recovery of the injected radioactivity usually indicates loss of volatile metabolites (e.g., CO_2 or CH_4) during incubation or sample preparation. Individual metabolites are identified and quantitated by high-performance liquid chromatography (HPLC) or gas chromatography (GC) coupled with radioactivity detection. Detection efficiencies and possible quenching effects of the samples have to be considered. Radiolabeled CO_2 is separated from the samples by a flow injection method described by Hall and Aller (1992) and quantitated by LSC.

References

1. Ambrose, D., Berger, L. I., Clay, R. W., Covington, A. K., Eckerman, K. F., and 23 other authors (1999). Handbook of Chemistry and Physics. London: CRC Press.
2. Brauman, A., Kane, M. D., Labat, M., and Breznak, J. A. (1992). Genesis of acetate and methane by gut bacteria of nutritionally diverse termites. *Science* 257: 1384–1387.
3. Breznak, J. A. and Switzer, J. M. (1986). Acetate synthesis from H_2 plus CO_2 by termite gut microbes. *Appl. Environ. Microbiol.* 52: 623–630.
4. Brune, A., Emerson, D., and Breznak, J. A. (1995). The termite gut microflora as an oxygen sink: microelectrode determination of oxygen and pH gradients in guts of lower and higher termites. *Appl. Environ. Microbiol.* 61: 2681–2687.
5. Brune, A., Frenzel, P., and Cypionka, H. (2000). Life at the oxic-anoxic interface: microbial activities and adaptations. *FEMS Microbiol. Rev.* 24: 691–710.
6. Brune, A., and Friedrich, M. (2000). Microecology of the termite gut: structure and function on a microscale. *Curr. Opin. Microbiol.* 3: 263–269.
7. Crank, J. (1975). The Mathematics of Diffusion, 2nd edn. Oxford: Clarendon Press.
8. Ebert, A. and Brune, A. (1997). Hydrogen concentration profiles at the oxic-anoxic interface: a microsensor study of the hindgut of the wood-feeding lower termite *Reticulitermes flavipes* (Kollar). *Appl. Environ. Microbiol.* 63: 4039–4046.

9. Hall, P. O. J. and Aller, R. C. (1992). Rapid, small volume, flow injection analysis of CO_2 and NH_4^+ in marine and freshwaters. *Limnol. Oceanogr.* 37: 1113–1119.

10. Jørgensen, B. B. (1978). A comparison of methods for the quantification of bacterial sulfate reduction in coastal marine sediments. *Geomicrobiol. J.* 1: 11–27.

11. Jørgensen, B. B. (1994). Sulfate reduction and thiosulfate transformations in a cyanobacterial mat during a diel oxygen cycle. *FEMS Microbiol. Ecol.* 13: 303–312.

12. Kühl, M. and Jørgensen, B. B. (1992). Microsensor measurements of sulfate reduction and sulfide oxidation in compact microbial communities of aerobic biofilms. *Appl. Environ. Microbiol.* 58: 1164–1174.

13. Moeslund, L., Thamdrup, B., and Jorgensen, B. B. (1994). Sulfur and iron cycling in a coastal sediment: radiotracer studies and seasonal dynamics. *Biogeochemistry* 27: 129–152.

14. Skyring, G. W. (1987). Sulfate reduction in coastal ecosystems. *Geomicrobiol. J.* 5: 295–374.

15. Tholen, A. and Brune, A. (1999). Localization and in situ activities of homoacetogenic bacteria in the highly compartmentalized hindgut of soil-feeding higher termites (*Cubitermes* spp.). *Appl. Environ. Microbiol.* 65: 4497–4505.

16. Tholen, A. and Brune, A. (2000). Impact of oxygen on metabolic fluxes and in situ rates of reductive acetogenesis in the hindgut of the wood-feeding termite *Reticulitermes flavipes*. *Environ. Microbiol.* 2: 436–449.

17. Yang, H., Schmitt-Wagner, D., Stingl, U., and Brune, A. 2005. Niche heterogeneity determines bacterial community structure in the termite gut (*Reticulitermes santonensis*). *Environ. Microbiol.* 7: 916–932.

3 Hydrogen production and efficient recycling during symbiotic lignocellulose degradation in termites

Michael Pester and Andreas Brune.

In preparation.

Abstract

Termites are the best example in nature for an efficient degradation of lignocellulose, which is the largest organic renewable energy source on earth. Although hydrogen, an emerging "clean" energy carrier, is one of the degradation products during the breakdown of lignocellulose in lower termites, it received so far little attention. To determine the total production of hydrogen as well as to analyze the hydrogen-scavenging processes in a comprehensive manner, we studied representatives from three different lower termite families, which showed pronounced differences in the degree of hydrogen accumulation in their hindgut. Irrespective of the degree of hydrogen accumulation, ranging from almost no accumulation to being close to saturation, the hydrogen pool was rapidly turned over with reductive acetogenesis being the dominating process (18–25% of the total electron flow through the termite). Methanogenesis and aerobic hydrogen oxidation played only a minor role (0–4% and <0.1% of the total electron flow, respectively). The total production of hydrogen in the hindgut depended on the termite species and ranged from 15 to 470 nmol H_2 per hour, which corresponds to up to 34 liters of H_2 produced per liter of termite gut content and day. Interestingly, almost no hydrogen was lost by emission from the termites, documenting an efficient recycling within the hindgut. Since hydrogen was mainly used to produce acetate, which is the main end product of the lignocellulose fermentation and at the same time the major energy substrate of the termites, hydrogen recycling increased the energy yield of the termite by 20%.

Introduction

Hydrogen is viewed as an emerging "clean" energy carrier of the near future and questions are raised how hydrogen could be produced without net CO_2 production (Dunn, 2002). The production from biomass and in particular from lignocellulose as the most abundant renewable organic component in the biosphere has been suggested as one possibility (Claasen et al., 1999). As a model for this process, lower termites received in the last years increasing public attention because of their ability to digest wood with the help of their symbiotic microbiota and the fact that

hydrogen is one of the degradation products (Yamin, 1980; Yamin, 1981; Odelson and Breznak, 1983; Odelson and Breznak, 1985a).

Among the different wood components, lower termites feed on cellulose and hemicellulose, 65–99% of which is degraded during gut passage (reviewed in Breznak and Brune, 1994). Most of this degradation occurs in the hindgut, a microbial bioreactor tightly packed with microorganisms (Brune, 1998). This hindgut microbiota consists of protozoa, which are primarily involved in wood degradation, and a great variety of prokaryotes, whose function is still largely unknown (Brune and Stingl, 2005; Brune, 2005, Brugerolle and Radek, 2006).

In axenic cultures of the protozoa *Trichomitopsis termopsidis* (Yamin, 1980; Odelson and Breznak, 1985a) and *Trichonympha sphaerica* (Yamin, 1981) it has been shown that the main degradation products of cellulose are acetate, CO_2, and H_2 and the combined results of these studies suggest that acetate, CO_2, and H_2 are produced in a molar ratio of 1:1:2. The importance of this metabolic pathway was supported by feeding termites with ^{14}C-labeled cellulose and hemicellulose. Acetate was the almost exclusively formed volatile fatty acid in this experiment (Odelson and Breznak, 1983). Unfortunately, other fermentation products than volatile fatty acids, which could serve as intermediates during the overall fermentation, were not tested. Together with the finding that termite gut homogenates showed high potential activities of reductive acetogenesis, the termite hindgut was initially proposed to act like an anoxic homoacetogenic fermentor (Odelson and Breznak, 1983; Breznak and Switzer, 1986) with acetate being completely taken up by the termite where it can meet 77–100% of the energy requirement of the insect (Odelson and Breznak, 1983).

This model was later challenged in two major ways. The introduction of oxygen microsensor studies revealed that the termite hindgut, albeit small (0.2–8 µl depending on the species; Tholen and Brune, 2000 and this study), is not homogeneous but constitutes a gradient system with oxygen reaching 50–200 µm into the hindgut thereby forming an anoxic and a microoxic zone within the hindgut (Brune et al., 1995). Therefore, an influence of oxygen on part of the degradation pathways seems to be likely. The second major breakthrough was the application of the microinjection method, which allowed injection of minute amounts (50–100 nl) of radiolabeled substrates into dissected termite guts to follow their fate and measure the underlying processes. The great advantages of this method are that the gut is kept intact as a gradient system, thereby closely mimicking in vivo conditions. Furthermore, the injected radiolabeled substrates do not exceed the pool sizes in the gut, which ensures that the conditions of the degradation network are not brought out of balance (Tholen and Brune, 2000; Brune and Pester, 2005). In a pilot study, the application of the microinjection method to *Reticulitermes flavipes* indicated that lactate is an additional important intermediate but is probably turned over in the microoxic gut periphery and that reductive acetogenesis might indeed play an

important role although not that pronounced as proposed previously (Tholen and Brune, 2000). Already these results clearly showed that the carbon flow model in the hindgut of lower termites needs to be revised.

Hydrogen as a potentially major intermediate in this degradation network received even less attention. It is known from previous case studies, which investigated again *R. flavipes*, that hydrogen can accumulate to substantial amounts in the hindgut (Ebert and Brune, 1997) but at the same time does not escape by emission to the atmosphere (Odelson and Breznak, 1983). This indicated an efficient recycling of hydrogen but left the questions about the main responsible processes and the extend of the actual hydrogen turnover open. Evidently, there is a need to analyze all hydrogen-utilizing processes in a comprehensive manner and to determine the total hydrogen production rate.

In this study, we investigate three representative species of the Rhinotermitidae, Termopsidae, and Kalotermitidae, the three families of lower termites with the highest species numbers (Kambhampati and Eggleton, 2000). Preliminary investigations had indicated that the three termite species showed pronounced differences in the degree of hydrogen accumulation in their hindguts ranging from almost no accumulation to being close to saturation. Building on this knowledge, rates of reductive acetogenesis, methanogenesis, and aerobic hydrogen oxidation as well as loss of hydrogen by emission were determined for each termite to identify whether hydrogen is an important intermediate or just an end product accumulating after carbohydrate fermentation. The sum of all hydrogen-utilizing processes was used to estimate the internal hydrogen production rate. In addition, we used the microinjection method to analyze not only acetogenesis from CO_2 but also from lactate and formate thereby adding more robustness to a general model of the degradation network in the hindgut of lower termites.

Results

Characteristics of model termites

Reticulitermes santonensis was the smallest termite studied followed by *Cryptotermes secundus* and *Zootermopsis nevadensis* as indicated by their fresh weight and the volume of their hindgut, which takes up the major part of the abdomen (Table 1). *C. secundus* differed from *R. santonensis* and *Z. nevadensis* in respect to a slightly higher redox potential in the hindgut (Table 1). The composition of metabolite pools in the hindgut consisted of typical fermentation products from carbohydrates and was overall similar in all three termites with acetate (20 mM) and CO_2 (20–30 mM) being the major metabolites (Table 2).

Hydrogen accumulation and emission

The three termites showed pronounced differences in the degree of hydrogen accumulation in their hindguts. The highest values were obtained for the large

Table 1. Characteristics of the studied termites.

Termite	Fresh weight (mg)	Hindgut volume (µl)[a]	Maximum H_2 partial pressure (kPa)[b]	Redox potential (mV)[c]
R. santonensis	2	0.4 ± 0.1	29.8 ± 14.6	–290 to –260
Z. nevadensis	28	7.5 ± 1.1	72.2 ± 28.5	–240 to –210
C. secundus	3	2.2 ± 0.6	1.3 ± 1.1	–130 to –80

a. Volume was determined by geometric approximation.
b. Average and standard deviation of 5 independent measurements. Values were taken from the center of the hindgut.
c. Average and standard deviation of 4 or 5 independent measurements. Measured values were rounded to the nearest decimal

Z. evadensis, often coming close to saturation at the center of the hindgut paunch, the gut region with the largest diameter. While in the paunch of *R. santonensis*, the smallest of the three termites, hydrogen accumulated still to substantial amounts, hydrogen partial pressures in the paunch of *Cryptotermes secundus* were close to the detection limit of the microelectrode (<1 kPa) (Table 1). Axial profiles from the anterior end of the midgut to the posterior end of the hindgut showed that hydrogen accumulated mainly in the enlarged paunch whereas the relatively narrow and tubular-like midgut and colon/rectum region of the hindgut showed no or only minor accumulation of hydrogen. The only exception was the enlarged colon and rectum of *Z. nevadensis*, where hydrogen accumulated as well (Fig. 1). Radial profiles through the paunch of *R. santonensis* and *Z. nevadensis* showed a bell-shaped distribution of hydrogen with the maximum concentration in the center of the paunch and a decrease towards the gut wall (Fig. 2), indicating strong hydrogen-consuming activities in the gut periphery.

Table 2. Metabolites detected in total hindgut extracts of worker termites.

	Pool size (nmol hindgut^{-1})[a]				
Termite	Glucose	Malate	Succinate	Butyrate	Propionate
R. santonensis	2.4 ± 0.8	0.1 ± 0.0	0.4 ± 0.1	0.1 ± 0.0[b]	0.3 ± 0.1
Z. nevadensis[d]	6.0 ± 1.6	0.3 ± 0.2	10.3 ± 4.8	< 0.02	5.1 ± 2.4[b]
C. secundus[e]	0.1 ± 0.1	n. m.[f]	0.2 ± 0.1	0.5[c]	1.0[c]

	Lactate	Acetate	Ethanol	Formate	CO_2
R. santonensis	0.4 ± 0.0	11.3 ± 2.6	0.8 ± 0.6	1.7 ± 0.6	10.7 ± 0.7
Z. nevadensis[d]	2.1 ± 1.2	53.5 ± 13.5[b]	10.4 ± 1.8[b]	26.4 ± 4.8	142.5 ± 33.8[b]
C. secundus[e]	4.0 ± 1.8	38.5[c]	0.8[c]	1.1 ± 0.8	56.4 ± 6.8[b]

a. At least three or more independent measurements were used for determinations of averages and standard deviations. The detection limit was 0.02 nmol.
b. Mean and range of two independent measurements.
c. Single measurement
d. Isovalerate was detected in two independent measurements (10 nmol gut^{-1}, mean).
e. Isovalerate was detected in two independent measurements (0.1 nmol gut^{-1}, mean).
f. Not measured.

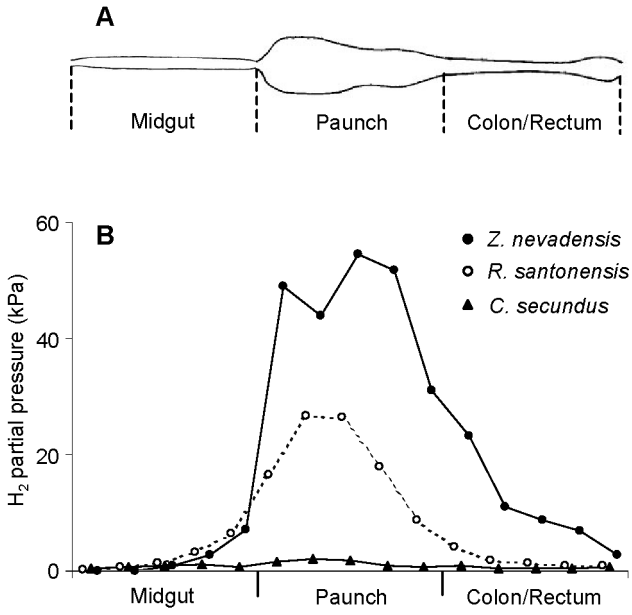

Figure 1. (A) Schematic gut diagram of lower termites showing the midgut and the different hindgut sections paunch and colon/rectum. (B) Typical axial hydrogen profiles along guts embedded in agarose-solidified insect Ringer's solution. Each gut section was divided into 5 subsections where measurements were taken. The subsections were used as normalization standard for the different gut lengths of the three termites.

Emission of hydrogen from living termites was only detected for *R. santonensis* and *Z. nevadensis*, which is in agreement with the hydrogen microsensor measurements. In both termites, the hydrogen emission accounted for 0.1–0.2% of the electron flow through the termite. To determine aerobic hydrogen oxidation, hydrogen emission was measured under an atmosphere of N_2 using the same termites as for the emission measurements under air. However, only a 2-fold to 3-fold stimulation was observed (Fig. 3).

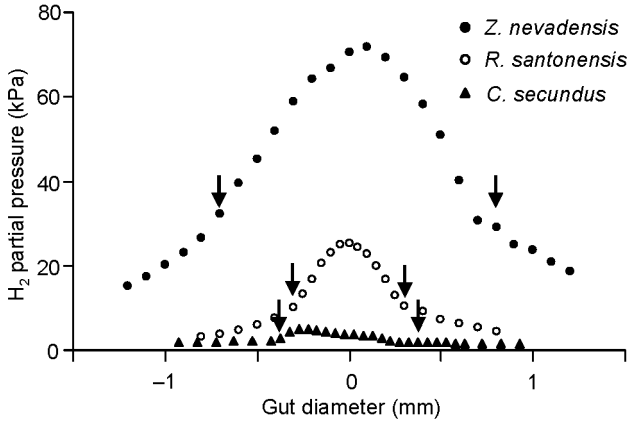

Figure 2. Typical radial profile of hydrogen across the hindgut of the studied termites – arrows indicate the position of the hindgut wall. Guts were embedded in agarose-solidified insect Ringer's solution.

Methane emission and methanogenic archaea

Microscopic observation of F_{420}-autofluorescence was used to localize methanogenic archaea in the three termites. In *R. santonensis*, fluorescent cells were exclusively situated at the microoxic hindgut wall, patchily distributed in microcolonies. Two morphotypes were distinguishable – rod-shaped cells of 1 μm length and coccoid cells of 0.2 μm diameter. In *Z. nevadensis* the situation was completely different. Here, fluorescent cells were detected mainly as endosymbionts of the gut flagellates *Trichomitopsis termopsidis,* which contained ingested wood particles, and *Hexamastix termopsidis* and *Tricercomitus termopsidis*, which contained no ingested wood particles as observed previously (Lee et al., 1987). Only occasionally, fluorescent cells were detected at the hindgut wall but at much smaller densities when compared to *R. santonensis*. Interestingly, no fluorescent cells were detected in *C. secundus*, neither at the gut wall nor in the gut fluid or associated with flagellates.

Methane emission constituted only a minor part of the total electron flow (4%) and carbon flow (2%) in *R. santonensis* and *Z. nevadensis*. Supplementation of H_2 (20%) to the atmosphere surrounding the termites lead to a noticeable stimulation of methane emission (5-fold) in *R. santonensis*. In *Z. nevadensis*, this effect was much less pronounced (Fig. 3). *C. secundus*, in agreement with the microscopy observations, did not emit any methane at all – neither under air nor under air supplemented with H_2 (Fig. 3).

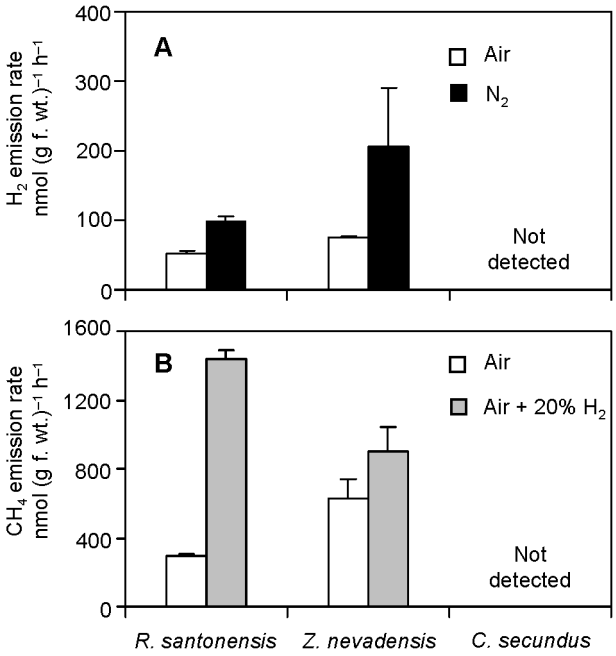

Figure 3. Emission of (A) hydrogen and (B) methane from living termites under different atmospheres. Bars represent averages of at least three independent measurements; standard deviations are given. The only exception is the data on hydrogen emission from *Cryptotermes secundus* where the mean and range of two independent measurements is given and the emission under 100% N_2 was not measured.

Acetogenesis from CO_2

Microinjection of $^{14}CO_3^{2-}$ into intact termite hindguts embedded in a thin layer of agarose-solidified insect Ringer's solution was used to follow the fate of CO_2. The injected $^{14}CO_3^{2-}$ constituted only a fraction of the total CO_2 pool in the hindgut ensuring no substantial increase of the pool size. In all three termites, acetate was the only product detected (Fig. 4). The depletion rates of labeled CO_2 and formation rates of labeled acetate decreased over time, reflecting the decrease in the specific radioactivity (radioactivity per molarity) of the CO_2 pool over time caused by the influx of unlabeled CO_2 from upstream metabolic processes. This was in good agreement with the label dilution model. The depletion rate of labeled CO_2 was generally higher than the formation rate of labeled acetate indicating additional CO_2-utilizing processes. The main additional source of depletion was very likely diffusion

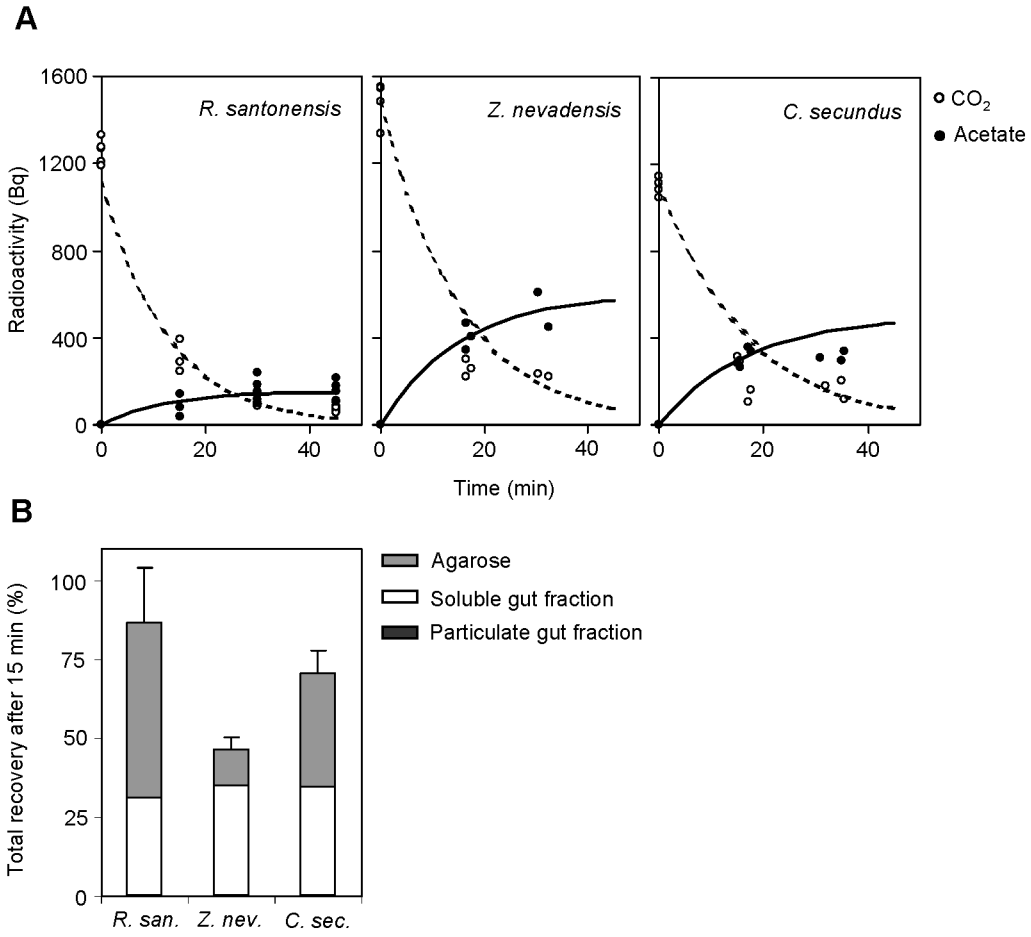

Figure 4. (A)Time-course of label distribution among total CO_2 (CO_2, HCO_3^-, and CO_3^{2-}) and acetate after microinjection of $Na_2{}^{14}CO_3$ into the paunch of agarose-embedded guts of *Reticulitermes santonensis*, *Zootermopsis nevadensis*, and *Cryptotermes secundus*. Each value represents an injection into a separate gut. Expected time curves of substrate depletion (dotted line) and product formation (solid line) were plotted next to the measured values. (B) Total recovery of radioactivity in the different analyzed sample fractions after the first incubation interval. Values are averages of three to five independent injections into separate guts. Error bars give the standard deviation of the total recovery.

of CO_2 into the surrounding agarose and from there partly into the atmosphere as inferred from HPLC analysis of radiolabeled products and total recovery of injected radioactivity in the gut and the surrounding agarose. In *R. santonensis* and *Z. nevadensis*, methanogenesis is likely to be an additional minor CO_2-depleting process but could not be measured due to the experimental setup. Using the label dilution model, rates of acetogenesis from CO_2 were determined to be in the range of 18% and 22% of the electron and carbon flow in *R. santonensis* and *Z. nevadensis*, respectively, and 36% of the electron and carbon flow in *C. secundus* (Table 3).

Table 3. Calculated rates of acetogenesis from CO_2 measured by microinjection of $^{14}CO_3^{2-}$ into hindguts embedded in insect Ringer's solution and comparison to the total CO_2 emission from the termite and processes involved in hydrogen turnover.

	Rate (µmol (g f.wt.)$^{-1}$ h^{-1})		
Termite	Acetogenesis from CO_2 [a]	Methanogenesis	CO_2 emission
R. santonensis	1.46 ± 0.54	0.29 ± 0.01	23.7 ± 0.6
Z. nevadensis	3.44 ± 0.54	0.63 ± 0.11	30.8 ± 5.7
C. secundus	4.26 ± 1.07	0.00 ± 0.00	23.9 ± 0.9
	H_2 emission	H_2 oxidation	Total H_2 turnover [b]
R. santonensis	0.05 ± 0.01	0.05 ± 0.01	7.1
Z. nevadensis	0.08 ± 0.00	0.13 ± 0.09	16.5
C. secundus	0.00 ± 0.00	0.00 ± 0.00	10.5 [c]

a. Calculations are based on the CO_2 pool at the time point of injection (*R. santonensis*, 8.4 nmol; *Z. nevadensis*, 120 nmol; *C. secundus*, 14.0 nmol) and the assumption that both carbon atoms of the acetate molecule stem from CO_2.
b. Sum of hydrogen utilizing processes assuming that acetogenesis from CO_2 is completely hydrogen-dependent. For details see discussion.
c. Calculated using a rate of 3.00 µmol acetate (g f.wt.)$^{-1}$ h^{-1} for acetogenesis from CO_2. For details see discussion.

Acetogenesis from lactate and formate

The same experimental setup as described above was used to inject radiolabeled lactate and radiolabeled formate into hindguts of *R. santonensis* and *C. secundus* (Fig. 5). Injection of labeled lactate into hindguts of *R. santonensis* resulted in substrate depletion and product formation curves that correspond again well to the label dilution model. Lactate was converted to acetate and CO_2 in a molar ratio of 1:1 and the rate of lactate turnover was equal to 10% of the electron and carbon flow. Two thirds of the carbon atoms of lactate were recovered as acetate whereas the remaining carbon atoms were detected in the CO_2 pool (Table 4).

Injection of labeled lactate into hindguts of *C. secundus* gave similar results as obtained for *R. santonensis* (Fig. 5). Due to the larger lactate pool in *C. secundus* (Table 2), the depletion of labeled lactate and the formation of the labeled products acetate and CO_2 were slower when compared to *R. santonensis*. The rate of lactate

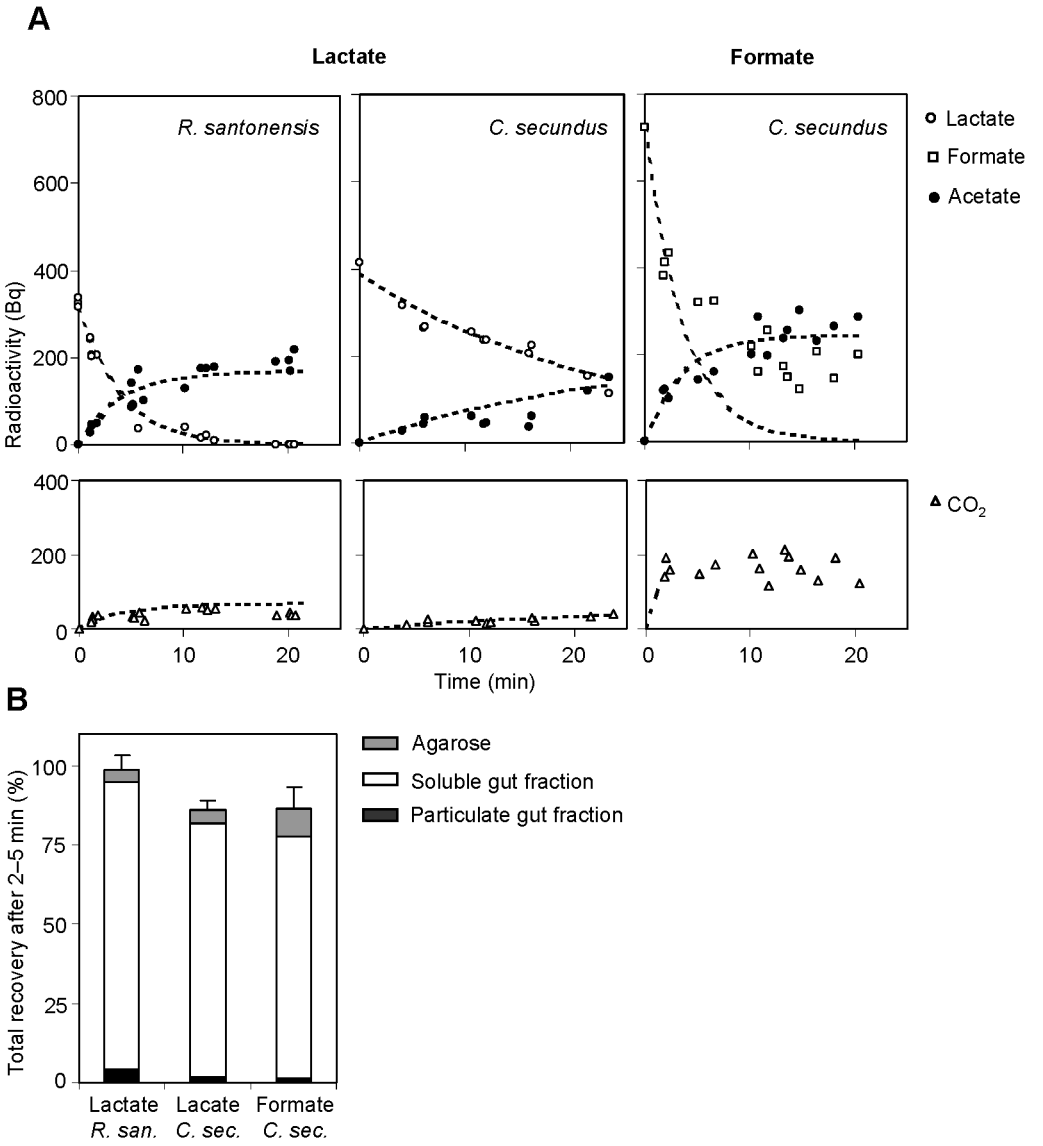

Figure 5. (A) Time-course of label distribution among different metabolites after microinjection of [U-^{14}C]-lactate and ^{14}C-formate into the paunch of agarose embedded guts of *Cryptotermes secundus* and *Reticulitermes santonensis*. Each value represents an injection into a separate gut. Expected time curves of substrate depletion (dotted line) and product formation (solid line) were plotted next to the measured values. (B) Total recovery of radioactivity in the different analyzed sample fractions after the first incubation interval. Values are averages of three to five independent injections into separate guts. Error bars give the standard deviation of the total recovery.

turnover was equal to 11% of the electron and carbon flow. More than half of the carbon atoms of lactate (55%) were recovered as acetate and one tenth of the carbon atoms were detected in the CO_2 pool. The loss of the remaining label was equal to the loss of total recovery of radioactivity indicating formation of a gaseous product – probably CO_2 since methanogenesis was absent – that was lost by diffusion (Table 4).

For *C. secundus*, formate was tested as an additional substrate that could be involved in acetogenesis. Upon injection into hindguts, labeled formate was turned over to acetate and CO_2 (Fig. 5). Interestingly, only the label entering the acetate pool

behaved as predicted by the label dilution model. The injected formate was rapidly metabolized, but the turnover rate slowed down over time when compared to the predictions by the turnover model. In the case of label entering the CO_2 pool, the divergence from the model was even more pronounced. Here, the label in the CO_2 pool was stable over time from the first measuring point on, indicating that labeled CO_2 was entering and leaving the CO_2 pool over time at the same rate. Since turnover of labeled CO_2 entering the large CO_2 pool of the whole hindgut is negligible due to label dilution, this indicates further that the labeled CO_2 entered a smaller, separate CO_2 pool that was turned over faster than it could exchange with the large CO_2 pool of the whole hindgut. Due to the divergence from the model, only the first measurement points (2 min after injection) were used for an estimation of the turnover and formation rates. Rates of formate turnover were in the range of 5% of the electron flow and 11% of the carbon flow. The determination of the acetate and CO_2 formation rates is more complex. After 2 min of injection, 30% of the label of the turned over formate were detected in the acetate pool and 50% were detected in the CO_2 pool. From a mechanistic viewpoint, this indicates that one forth of the formate pool is converted directly to the methyl group of acetate whereas the remaining formate is converted to CO_2 and reducing equivalents. Since the label in the CO_2 pool is constant over time and acetate is the only other product accumulating, the assumption is justified that CO_2 is converted to the carbonyl group of acetate and the produced reducing equivalents are recycled in the acetate formation. Considering these facts, the rate of acetate formation from formate would be 5% of the total electron and carbon flow and the formation rate of CO_2 as an intermediate would be 8% of the total carbon flow (Table 4).

Table 4. Contribution of formate and lactate turnover to acetogenesis as calculated from microinjection data of ^{14}C-labeled metabolites into hindguts embedded in insect Ringer's solution.

Metabolite		Rate (µmol (g f.wt.)$^{-1}$ h^{-1}) [a]	
Injected	Produced	*R. santonensis*	*C. secundus*
Formate		–0.6 [b]	–2.5 [c]
	Acetate	—	0.6 [c,d]
	CO_2	0.5	1.9 [c]
Lactate		–0.8	–0.8
	Acetate	0.8	0.7
	CO_2	0.6	0.2

a. Rates were calculated using the formate pool (*C. secundus*, 0.8 nmol) and lactate pool (*R. santonensis*, 0.2 nmol; *C. secundus*, 1.9 nmol) at the time point of injection.
b. Data from Tholen and Brune (2000) obtained for *Reticulitermes flavipes* a synonymous species to *Reticulitermes santonensis* (Austin et al., 2005).
c. Rates were calculated using only data points obtained within the first 2 min after injection.
d. Assuming that both C-atoms stemmed from formate.

Discussion

This study provided the first experimental determination of hydrogen production and turnover in lower termites, which are regarded as the best natural model system to study efficient lignocellulose degradation. After realizing that different lower termites show different degrees of hydrogen accumulation in their hindgut ranging from nearly saturation to almost no accumulation, the question about the importance of hydrogen during lignocellulose degradation and its total production and turnover in these different lower termites arose. To answer this question, we studied the termites *Reticulitermes santonensis* and *Zootermopsis nevadensis*, which showed a high accumulation of hydrogen, in comparison to *Cryptotermes secundus*, which showed almost no accumulation of hydrogen (Fig. 1, Fig. 2). A cumulative analysis of all hydrogen-utilizing processes was performed to identify the major route of hydrogen turnover and to estimate total hydrogen production in the single termites.

Emission rates of hydrogen from living termites, which constituted 0.0–0.2% of the total electron flow depending on the termite, revealed that hydrogen is not lost by diffusion through the hindgut epithelium but is mainly metabolized within the hindgut. When the same termites were incubated under an atmosphere of N_2, the emission rates increased at most 2 to 3-fold indicating that aerobic oxidation of hydrogen, be it for energy metabolism or oxygen detoxification, plays only a marginal role (Fig. 3). This is in agreement with results obtained for *Reticulitermes flavipes* by Odelson and Breznak (1983), who observed a very low H_2 emission as well and proposed that aerobic hydrogen oxidation is of minor importance based on its theoretical share of the total O_2 consumption by the termite.

A similar situation was observed for methanogenesis. In termite hindguts, methanogenesis is hydrogenotrophic but not aceticlastic, which has been shown in physiological experiments for *R. flavipes* (Breznak and Switzer, 1986) and was corroborated by the isolation of hydrogenotrophic *Methanobrevibacter* spp. (Leadbetter and Breznak, 1996; Leadbetter et al., 1998) as well as by the detection of archaeal 16S rRNA clones in diverse lower termites that could be affiliated only to methanogens which are capable of hydrogenotrophic methanogenesis (Ohkuma et al., 1999; Shinzato et al., 1999; Tokura et al., 2000). Of the three studied termites, only in *R. santonensis* and *Z. nevadensis*, which showed a high accumulation of hydrogen, methane emission (Fig. 3) and the presence of methanogens, as indicated by cells showing F_{420}-autofluorescence, were detected. In both termites, methane emission constituted only 4% of the total electron flow. Since there is cumulative evidence from physiological and molecular studies that there is no methane oxidation in termite guts (Odelson and Breznak, 1983; chapter 4), one can safely assume that the measured net rates of methane emission are equal to the gross rates of methanogenesis within the hindgut. Increasing the hydrogen concentration to 20 kPa in the atmosphere surrounding the termites lead to a 5-fold increase of methane emission from *R. santonensis* indicating that the methanogens, which appear to be

situated at the microoxic hindgut wall in this termite, are hydrogen limited. In *Z. nevadensis*, where the methanogens appear to be endosymbionts of flagellates, the same experiment resulted only in a slight increase of methane emission. Obviously, the high hydrogen concentration in the anoxic center of the hindgut was sufficient for methanogenesis.

In contrast to the above discussed hydrogen utilizing processes, rates of acetogenesis from CO_2 were quite high, ranging from 18–36% of the total carbon flow in the three studied termites and indicating that reductive acetogenesis is the major sink of hydrogen in the termite hindgut. This agrees well with the high potential rates of hydrogen-dependent reductive acetogenesis in gut homogenates of the same three termite species (2–6 μmol acetate (g f. wt.)$^{-1}$ h^{-1}) (Pester and Brune, 2006), which were in the same range as the rates obtained by the microinjection experiments. Despite this cumulative evidence, it is still possible that the measured carbon flow from CO_2 to acetate is not exclusively mediated by hydrogen-dependent reductive acetogenesis but in smaller parts also by homoacetogenic fermentation of lactate or formate-dependent reductive acetogenesis. Because it was not possible to use $^3H_2$ as a tracer due to the experimental setup and its rapid exchange with water in comparison to other conversions (Hungate, 1967), we used microinjection of ^{14}C-labeled lactate and formate to answer this question.

In *R. santonensis*, lactate was turned over to acetate and CO_2 in a molar ratio of 1:1 clearly showing the absence of a complete homoacetogenic turnover. Exactly the same result was obtained previously for the synonymous termite *Reticulitermes flavipes* (Austin et al., 2005). In *R. flavipes*, lactate turnover was also measured under anoxic conditions, where it was turned over to propionate and acetate in a molar ratio of 2:1 (Tholen and Brune, 2000). This shift in fermentation products from oxic to anoxic conditions is typical for propionigenic bacteria (de Vries et al., 1972; Pritchard et al., 1977; Emde and Schink, 1990) but not known for homoacetogens. Therefore, the measured carbon flow from CO_2 to acetate was not partly fueled by lactate turnover. In *R. flavipes*, the turnover of formate was measured as well, resulting in a complete degradation to CO_2. Whether the released reducing equivalents were oxidized by oxygen or were used for reductive acetogenesis or any other process could not be shown (Tholen and Brune, 2000). However, since formate turnover constituted only 2% of the total electron flow (Tholen and Brune, 2000) its possible contribution to reductive acetogenesis is negligible.

In *C. secundus*, lactate was also turned over to acetate and CO_2 and the total carbon flow from lactate to acetate was 5%. A possible contribution of homoacetogenic fermentation to the carbon flow from CO_2 to acetate would result in 1.3% of the carbon flow and would constitute only a minor part when compared to the high rates of reductive acetogenesis. Furthermore, lactate turnover resulted in a similar product

pattern as in *R. santonensis* suggesting that also in *C. secundus* propionigenic bacteria are mainly involved in lactate degradation.

A clear difference to the hindgut metabolism in *R. santonensis* was the fate of formate in *C. secundus*, which was metabolized to acetate and CO_2. Already 2 min after injection, one third of the turned over label from formate appeared in the acetate pool pointing towards a direct contribution to the methyl branch of reductive acetogenesis as carbon and electron donor. Interestingly, the label in the CO_2 pool remained constant over time indicating a small intracellular CO_2 pool with an equal influx and efflux of label, which is turned over faster than it can exchange with the large CO_2 pool of the whole hindgut. Since acetate was the only other product accumulating, the label from this intracellular CO_2 pool must have contributed to the carbonyl branch of reductive acetogenesis. The same is probably true for the intracellular pool of reducing equivalents formed from formate. As a consequence, this would mean that formate-dependent reductive acetogenesis is a minor but completely independent process from hydrogen-dependent reductive acetogenesis in *C. secundus* and follows the following reaction mechanism:

$$4\ HCOOH \rightarrow CH_3COOH + 2\ CO_2 + 2\ H_2O \qquad \text{(Eqn. 1)}$$

The microinjection experiments of lactate and formate served also as an important control for the determined rates of acetogenesis from CO_2. In *R. santonensis*, 10% of the carbon flow went through the lactate pool, which leaves 90% of the remaining polysaccharides to be converted to acetate, CO_2, and H_2 (Eqn. 2) or acetate, formate, and H_2 (Eqn. 3), assuming no other major degradation pathways.

$$n C_6H_{12}O_6 + 2n H_2O \rightarrow 2n CH_3COOH + 2n CO_2 + 4n H_2 \qquad \text{(Eqn. 2)}$$

$$n C_6H_{12}O_6 + 2n H_2O \rightarrow 2n CH_3COOH + 2n HCOOH + 2n H_2 \qquad \text{(Eqn. 3)}$$

Since one third of this remaining carbon flow proceeds to CO_2 or formate and formate was completely turned over to CO_2, 30% of the total carbon were entering the CO_2 pool. Additionally, 3% of the total carbon flow were entering the CO_2 pool from the process of lactate degradation. The sum of influx (33% of the total carbon flow) is in agreement with the efflux from the CO_2 pool, which is the sum of 18% of the carbon flow going to acetate and 2% of the carbon flow going to methane. The resulting difference between influx and efflux is probably released as CO_2 diffusing out of the hindgut (Fig. 6A) or may partly be caused by a slight overestimation of the carbon flux following Eqn. 2. It is likely that the same model applies to *Z. nevadensis* as well because this termite showed similar rates of reductive acetogenesis and methanogenesis and also a high accumulation of hydrogen in the hindgut when compared to *R. santonensis*.

In *C. secundus*, 11% of the carbon flow proceeded through lactate, which leaves 89% of the remaining polysaccharides to be converted according to Eqn. 2 and Eqn. 3, assuming no other major degradation pathways. As described above, one third of the remaining carbon flow would be then converted to CO_2 or formate,

which is equal to 30% of the total carbon flow. The formate microinjection experiments indicated that 11% of the total carbon flow proceed through formate with half of the C-atoms of formate entering the acetate pool and the other half entering the CO_2 pool (each 5.5% of the total carbon flow). Together with the 19%

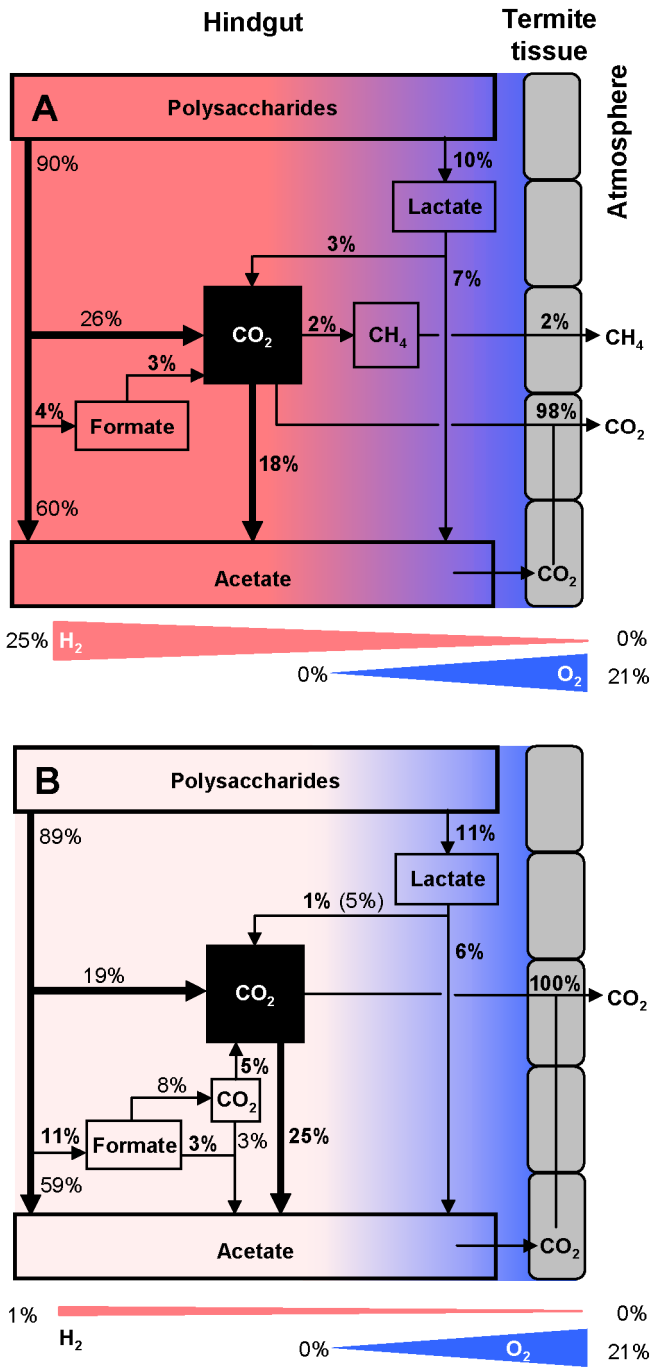

Figure 6. Proposed model of the carbon flow in *R. santonensis* (A) and *C. secundus* (B) based on microinjection experiments using ^{14}C-labeled CO_3^{2-}, formate, and lactate and emission rates of total CO_2 and CH_4. Measured partial fluxes are given in bold. Slight unbalances in the carbon flux are due to rounding errors.

of carbon entering the CO_2 pool directly and the 1% of carbon stemming from lactate degradation this adds up to 25.5% of the carbon flow entering the CO_2 pool. This influx of carbon is lower than the calculated efflux by reductive acetogenesis, which is 36% of the total carbon flow. Since both values underlie certain assumptions for their calculation, they are viewed as lower and upper limit of the actual rate of reductive acetogenesis. We used the more conservative value of 25% of the total carbon flow as the rate of reductive acetogenesis that is implemented in the carbon flow model of the hindgut of *C. secundus* (Fig. 6B).

In summary, hydrogen turned out to be an important intermediate in the hindgut metabolism irrespective of the termite species studied or the amount to which hydrogen accumulated. However, if one takes a closer look, different varieties of hydrogen turnover were observed for *R. santonensis* and *Z. nevadensis* on the one hand and for *C. secundus* on the other hand. In *R. santonensis* and *Z. nevadensis*, where hydrogen accumulated to large amounts, the turnover of the H_2 pool was dominated by reductive acetogenesis with a share of 18% to 22% of the total electron flow depending on the termite followed by methanogenesis with a share of 4% of the total electron flow. The loss by emission from the hindgut and oxidation in the microoxic gut periphery was very small (0.1–0.2% of the total electron flow). The resulting turnover of the H_2 pool equals to 22% and 26% of the total electron flow through the hindgut of *R. santonensis* and *Z. nevadensis*, respectively. This is in good agreement with the estimation of the influx into the H_2 pool. Approximately 28% of the electron flow were estimated to enter the H_2 pool, if one considers that 10% of the electron flow went through the lactate pool, 2% went through the formate pool, and 60% were assumed to enter the acetate pool. The resulting discrepancy of 2–6% of the total electron flow is indicating a slight overestimation of the electron flow through the degradation pathway described by Eqn. 2 on account of alternative pathways, e.g., through malate and succinate or by a direct resorption of glucose and other sugars by the termite in the midgut. The discrepancy might also be partly explained by hydrogen-dependent sulfate reduction. Sulfate reducing bacteria of the genus *Desulfovibrio* have been isolated from the termite hindgut (Brauman et al., 1990; Trinkerl et al., 1990; Kuhnigk et al., 1996; Fröhlich et al., 1999) but molecular studies using cloning and T-RFLP analysis of 16S rRNA genes suggested a very low population density of this metabolic group (Hongoh et al., 2003; Yang et al., 2005). Therefore, the share of hydrogen-dependent sulfate reduction is expected to be very low.

In *C. secundus*, the importance of hydrogen was not that obvious because it accumulated only in low amounts. However, the high rates of hydrogen-dependent reductive acetogenesis clearly indicated a high turnover of this small hydrogen pool. In contrast to *R. santonensis* and *Z. nevadensis*, reductive acetogenesis was the only hydrogen-utilizing process in *C. secundus* with a calculated turnover rate of 36% of the total electron flow. However, as discussed in detail for the carbon flow, the electron

flow through lactate and formate indicated that this rate is overestimated and the actual turnover rate of the H_2 pool is 25% of the electron flow.

The sum of the single hydrogen-utilizing processes including the small loss by emission can be used to calculate the total production rate of hydrogen. Depending on the termite and its hindgut volume, 15–470 nmol of H_2 are produced per hour by the intestinal microbiota. This means that per day up to 34 liters of H_2 can be produced by one liter of termite hindgut content. In comparison, a liter of rumen content of an adult cow produces approximately 10 liters of H_2 per day (Hungate, 1967; Wolin et al., 1997). However, in both intestinal systems hydrogen is not released to the atmosphere but recycled by downstream processes. In contrast to the rumen, where hydrogen mainly fuels methanogenesis and is therefore lost for additional energy recovery (Miller, 1995), in the termite hindgut, hydrogen is mainly converted to acetate by homoacetogens (Leadbetter et al., 1999; Salmassi and Leadbetter, 2003; Graber and Breznak, 2004; Pester and Brune, 2006), thereby increasing the energy yield of the termite from the glycosyl units of lignocellulose by 20%. This makes the termite hindgut not only the smallest (Brune, 1998) but also the most efficient natural bioreactor that delivers in total 80% of the energy stored in the glycosyl units of lignocellulose to the termite in form of acetate.

Materials and methods

Termites

R. santonensis was collected in the Forêt de la Coubre, near Royan, France. *Z. nevadensis* stemmed from the Los Padres National Forest in California, USA, and was kindly provided by Jared R. Leadbetter. *C. secundus* stemmed from a mangrove forest near Darwin, Australia, and was kindly provided by Judith Korb. All termites were kept on a diet of pine wood (*Pinus silvestris* for *R. santonensis* and *Z. nevadensis*, *Pinus radiata* for *C. secundus*). Species affiliation of the termites was confirmed by partially sequencing their cytochrome oxidase II gene (~700 bp, Liu and Beckenbach, 1992) and comparing it to published sequences. Details are described by Pester and Brune (2006).

Hindgut dimensions were determined for each termite species with freshly dissected guts immersed in a drop of insect Ringer's solution (Brune et al., 1995), using a dissecting microscope equipped with a calibrated eyepiece graticule. The gut volume was estimated by approximation to simple geometrical shapes.

Microelectrode measurements

Design and characteristics of polarographic H_2 microelectrodes and redox microelectrodes used in this study were as described by Ebert and Brune (1997). H_2 microelectrodes were calibrated using deionized water that was continuously flushed with an air-hydrogen mixture of different hydrogen partial pressures and gave a linear

response from 0–100 kPa H_2. Redox microelectrodes were calibrated using quinhydrone that was dissolved to saturation in commercial pH calibration solutions (pH 4.0 to 7.0).

Measurements were performed on dissected, fully extended termite guts embedded in agarose-solidified insect Ringer's solution.

Gas emission from termites

Methane was measured by gas chromatography using a Mol Sieve 5A column (30 m × 0.32 mm, 80/100 mesh) and a flame ionization detector. Injector and column temperature were 100 °C and detector temperature was 140 °C. The carrier gas was helium with a flow rate of 20 ml min^{-1}.

Hydrogen was measured by gas chromatography using a Mol Sieve 5A column (70 cm × 6.35 mm, mesh 80/100) and a reduction gas detector containing an HgO bed (RGD2, Trace Analytical, CA, USA). Injector temperature was at room temperature, column temperature was 90 °C, and temperature of the HgO bed was 280 °C. The carrier gas was synthetic air with a flow rate of 20 ml min^{-1}.

Carbon dioxide was measured by gas chromatography using a Porapack Q column (274 cm × 3.18 mm, mesh 80/100) and a methanizer coupled to a flame ionization detector. Column temperature was 80 °C; the carrier gas was 100% hydrogen with a flow rate of 21.5 ml min^{-1}. Samples were directly injected onto the column.

Metabolite pool sizes

Volatile fatty acids and ethanol were measured by gas chromatography using a FFAP column (25 m × 0.32 mm × 0.5 μm) and a flame ionization detector. Injector and detector temperature were 240 °C, column temperature started with 80 °C for 1 min, followed by 80–120 °C with a ramp of 20 °C min^{-1}, 120–205 °C with a ramp of 6.1 °C min^{-1}, and 205 °C for 2 min. The carrier gas was nitrogen with a flow rate of 2 ml min^{-1}. Samples were prepared as described in Tholen and Brune (2000).

For other fermentation products, guts were homogenized in 90 μl ice-cold Millipore-water and centrifuged (10 min, 20.000 *g*, 4 °C). The supernatant was acidified with a H_2SO_4 solution (2 μl, 5 M), centrifuged, and the supernatant analyzed by HPLC on a Grom Resin ZH column (250 mm × 8 mm ID, Grom, Rottenburg, Germany) at 60 °C, using a mobile phase of 5 mM H_2SO_4 (0.6 ml min^{-1}) and a refractive index detector.

For determination of the carbon dioxide pool (H_2CO_3, HCO_3^-, and CO_3^{2-}), hindguts were homogenized in 10 mM NaOH (70 μl) and centrifuged as described above. The supernatant was subjected to flow injection analysis as described by Hall and Aller (1992).

Carbon flow measurements

Metabolite fluxes were measured by microinjection of ^{14}C-labeled compounds as described by Brune and Pester (2005). Briefly, 50–100 nl of ^{14}C-labeled compound were injected into dissected hindguts embedded in agarose-solidified insect Ringer's solution (Brune et al., 1995). The turnover of the injected compound and the formation of its products were monitored over time by HPLC analysis coupled to an online radioactivity detector (Ramona 2000, Raytest, Straubenhardt, Germany). Radiolabeled carbon dioxide was isolated by flow injection analysis as described above and measured by liquid scintillation counting. Recovery of total radioactivity in the samples was measured by liquid scintillation counting.

Rates of substrate turnover and product formation were determined using the label dilution model, which is briefly described in the following. The turnover rate of injected compounds (R_S) was calculated using Eqn. 4 and Eqn. 5:

$$X_S(t) = X_0 \cdot e^{\mu \cdot t} \quad \text{(Eqn. 4)}$$

$$R_S = \mu \cdot N \quad \text{(Eqn. 5)}$$

where X_S is the radioactivity in the substrate pool, X_0 is the radioactivity of the injected substrate at the time point of injection, μ is the turnover rate constant, N is the substrate pool, and t is the time. The formation rate of products (R_P) was calculated using Eqn. 6:

$$X_P(t) = \frac{R_P \cdot A_0}{\mu}(e^{\mu \cdot t} - 1) \quad \text{(Eqn. 6)}$$

where A_0 is the specific radioactivity of the substrate pool at the time point of injection.

The carbon flow and electron flow were calculated using the redox-state of carbon in the glucosyl-units of cellulose as a reference and assuming that all degraded wood polymers and the resulting fermentation products were oxidized to CO_2 by the hindgut microbiota or the termite as shown by Odelson and Breznak (1983). The sum of CO_2, CH_4, and H_2 emission was taken as 100% value of the electron flow and the sum of CO_2 and CH_4 emission was taken as the 100% value of the carbon flow.

Radiochemicals with the following specific and volume activities were used: $Na_2{}^{14}CO_3$, 1.9 MBq μmol^{-1} and 24.4 MBq ml^{-1} (Moravek Biochemicals Inc., Brea, CA, USA); [^{14}C]-Na-formate, 2.2 MBq μmol^{-1} and 7.4 MBq ml^{-1} (GE Healthcare, Little Chalfont, Great Britain); L-[U-^{14}C]-Na-lactate, 5.6 MBq μmol^{-1} and 6.2 MBq ml^{-1} (ARC Inc., St. Louis, MO, USA); [2,3-^{14}C]-succinic acid, 3.1 MBq μmol^{-1} and 3.7 MBq ml^{-1} (ARC Inc.); L-[U-^{14}C]-malic acid, 1.9 MBq μmol^{-1} and 7.4 MBq ml^{-1} (GE Healthcare); [2-^{14}C]-Na-propionate, 2.0 MBq μmol^{-1} and 37.0 MBq ml^{-1} (Moravek Biochemicals Inc.); and [2-^{14}C]-Na-acetate, 2.1 MBq μmol^{-1} and 7.4 MBq ml^{-1} (ARC Inc.). Radiochemical purity was above 95% for all radiochemicals.

References

1. Austin, J. W., Szalanski, A. L., Scheffrahn, R. H., Messenger, M. T., Dronnet, S., and Bagnères, A.-G. (2005) Genetic evidence for the synonymy of two *Reticulitermes* species: *Reticulitermes flavipes* and *Reticulitermes santonensis*. *Ann. Entomol. Soc. Amer.* 98: 395–401.

2. Brauman, A., Kane, M. D., Labat, M., and Breznak, J. A. (1992) Genesis of acetate and methane by gut bacteria of nutritionally diverse termites. *Science* 257: 1384–1387.

3. Brauman, A., Koenig, J. F., Dutreix, J., and Garcia, J. L. (1990) Characterization of two sulfate-reducing bacteria from the gut of the soil-feeding termite, Cubitermes speciosus. *Antonie v. Leeuwenhoek* 58: 271–275

4. Breznak, J. A., and Brune, A. (1994) Role of microorganisms in the digestion of lignocellulose by termites. *Annu. Rev. Entomol.* 39: 453–487

5. Breznak, J. A., and Switzer, J. M. (1986) Acetate synthesis from H_2 plus CO_2 by termite gut microbes. *Appl. Environ. Microbiol.* 52: 623–630.

6. Brugerolle, G., and Radek, R. (2006) Symbiotic protozoa of termites. In: *Soil Biology*. König, H., and Varma, A. (eds). Berlin: Springer-Verlag, pp. 243–269

7. Brune, A. (1998) Termite guts: the world's smallest bioreactors. *Trends. Biotechnol.* 16: 16–21

8. Brune, A. (2005) Symbiotic associations between termites and prokaryotes. In: *The Prokaryotes. An Online Electronic Resource for the Microbiological Community, 3rd edn.* Dworkin, M., Falkow, S., Rosenberg, E., Schleifer, K.-H., and Stackebrandt, E. (eds). New York: Springer-SBM, http://141.150.157.117:8080/prokPUB/index.htm. Springer-SBM, New York.

9. Brune, A., Emerson, D., and Breznak, J. A. (1995) The termite gut microflora as an oxygen sink: microelectrode determination of oxygen and pH gradients in guts of lower and higher termites. *Appl. Environ. Microbiol.* 61: 2681–2687.

10. Brune, A., and Pester, M. (2005) In situ measurements of metabolite fluxes: microinjection of radiotracers into insect guts and other small compartments. In: *Methods in Enzymology*. Leadbetter J. R. (ed). London: Elsevier, pp. 200–212

11. Brune, A., and Stingl, U. (2005) Prokaryotic symbionts of termite gut flagellates: phylogenetic and metabolic implications of a tripartite symbiosis. In: *Molecular Basis of Symbiosis*. Overmann, J. (ed). Berlin: Springer, pp. 39–60

12. Claassen, P. A. M., van Lier, J. B., Lopez Contreras, A. M., van Niel, E. W. J., Sijtsma, L., Stams, A. J. M., de Vries, S. S., and Weusthuis, R. A. (1999) Utilisation of biomass for the supply of energy carriers. *Appl. Microbiol. Biotechnol.* 52: 741–755

13. de Vries, W., Wijck-Kapteijn, W. M., and Stouthamer, A. H. (1972) Influence of oxygen on growth, cytochrome synthesis and fermentation pattern in propionic acid bacteria. *J. Gen. Microbiol.* 71: 515–524

14. Dunn, S. (2002) Hydrogen futures: toward a sustainable energy system. *Int. J. Hydrogen Energy* 27: 235–264

15. Ebert, A., and Brune, A. (1997) Hydrogen concentration profiles at the oxic-anoxic interface: a microsensor study of the hindgut of the wood-feeding lower termite *Reticulitermes flavipes* (Kollar). *Appl. Environ. Microbiol.* 63: 4039–4046.

16. Emde, R., and Schink, B. (1990) Oxidation of glycerol, lactate, and propionate by *Propionibacterium freudenreichii* in a poised-potential amperometric culture system. *Arch. Microbiol.* 153: 506–512

17. Fröhlich, J., Sass, H., Babenzien, H.-D., Kuhnigk, T., Varma, A., Saxena, S., Nalepa, C., Pfeiffer, P., and König, H. (1999) Isolation of *Desulfovibrio intestinalis* sp. nov. from the hindgut of the lower termite *Mastotermes darwiniensis*. *Can. J. Microbiol.* 45: 145–152

18. Graber, J. R., and Breznak, J. A. (2004) Physiology and nutrition of *Treponema primitia*, an H2/CO2-acetogenic spirochete from termite hindguts. *Appl. Environ. Microbiol.* 70: 1307–1314.

19. Hall, P. O. J., and Aller R. C. (1992) Rapid, small volume, flow injection analysis of CO_2 and NH_4^+ in marine and freshwaters. *Limnol. Oceanogr.* 37: 1113–1119.

20. Hongoh, Y., Ohkuma, M., and Kudo, T. (2003) Molecular analysis of bacterial microbiota in the gut of the termite *Reticulitermes speratus* (Isoptera; Rhinotermitidae). *FEMS Microbiol. Ecol.* 44: 231–242.

21. Hungate, R. E. (1967) Hydrogen is an intermediate in the rumen fermentation. *Arch. Microbiol.* 59: 158–164

22. Kambhampati, S., and Eggleton, P. (2000) Taxonomy and phylogenetics of Isoptera. In: *Termites: Evolution, Sociality, Symbiosis, Ecology*. Abe, T., Bignell, D. E., and Higashi, M. (eds.). Dordrecht: Kluwer Academic Publishers, pp. 1–23

23. Kuhnigk, T., Branke, J., Krekeler, D., Cypionka, and H., König, H. (1996) A feasible role of sulfate-reducing bacteria in the termite gut. *System. Appl. Microbiol.* 19: 139–149

24. Leadbetter, J. R., and Breznak, J. A. (1996) Physiological ecology of *Methanobrevibacter cuticularis* sp. nov. and *Methanobrevibacter curvatus* sp. nov., isolated from the hindgut of the termite *Reticulitermes flavipes*. *Appl. Environ. Microbiol.* 62: 3620–3631.

25. Leadbetter, J. R., Crosby, L. D., and Breznak, J. A. (1998) *Methanobrevibacter filiformis* sp. nov., a filamentous methanogen from termite hindguts. *Arch. Microbiol.* 169: 287–292.

26. Leadbetter, J. R., Schmidt, T. M., Graber, J. R., and Breznak, J. A. (1999) Acetogenesis from H_2 plus CO_2 by spirochetes from termite guts. *Science* 283: 686–689.

27. Lee, M. J., Schreurs, P. J., Messer, A. C., Zinder, S. H. (1987) Association of methanogenic bacteria with flagellated protozoa from a termite hindgut. *Curr. Microbiol.* 15: 337–341

28. Liu, H., and Beckenbach, A. T. (1992) Evolution of the mitochondrial cytochrome oxidase II gene among 10 orders of insects. *Mol. Phylogenet. Evol.* 1: 41–52.

29. Miller, T. L. (1995) Ecology of methane production and hydrogen sinks in the rumen. In: *Ruminant physiology: Digestion, Metabolism, Growth and Reproduction*. Engelhardt, W. V., Leonhardt-Marek, S., Breves, G., Gieseke, D. (eds.) Stuttgart: Ferdinand Enke Verlag, pp. 317–331

30. Odelson, D. A., and Breznak, J. A. (1983) Volatile fatty acid production by the hindgut microbiota of xylophagous termites. *Appl. Environ. Microbiol.* 45: 1602–1613

31. Odelson, D. A., and Breznak, J. A. (1985) Nutrition and growth characteristics of *Trichomitopsis termopsidis*, a cellulolytic protozoan from termites. *Appl. Environ. Microbiol.* 49: 614–621

32. Ohkuma, M., Noda, S., and Kudo, T. (1999) Phylogenetic relationships of symbiotic methanogens in diverse termites. *FEMS Microbiol. Lett.* 171: 147–153

33. Pester, M., and Brune, A. (2006) Expression profiles of *fhs* (FTHFS) genes support the hypothesis that spirochaetes dominate reductive acetogenesis in the hindgut of lower termites. *Environ. Microbiol.* 8: 1261–1270

34. Pritchard, G. G., Wimpenny, J. W., Morris, H. A., Lewis, M. W., and Hughes, D. E. (1977) Effects of oxygen on *Propionibacterium shermanii* grown in continuous culture. *J. Gen. Microbiol.* 102: 223–233

35. Salmassi, T. M., and Leadbetter, J. R. (2003) Molecular aspects of CO_2-reductive acetogenesis in cultivated spirochetes and the gut community of the termite *Zootermopsis angusticollis*. *Microbiology* 149: 2529–2537

36. Shinzato, N., Matsumoto, T., Yamaoka, I., Oshima, T., and Yamagishi, A. (1999) Phylogenetic diversity of symbiotic methanogens living in the hindgut of the lower termite *Reticulitermes speratus* analyzed by PCR and in situ hybridization. *Appl. Environ. Microbiol.* 65: 837–840

37. Tholen, A., and Brune, A. (2000) Impact of oxygen on metabolic fluxes and in situ rates of reductive acetogenesis in the hindgut of the wood-feeding termite *Reticulitermes flavipes*. *Environ. Microbiol.* 2: 436–449.

38. Tokura, M., Ohkuma, M., and Kudo, T. (2000) Molecular phylogeny of methanogens associated with flagellated protists in the gut and with the gut epithelium of termites. *FEMS Microbiol. Ecol.* 33: 233–240

39. Trinkerl, M., Breunig, A., Schauder, R., and König, H. (1990) *Desulfovibrio termitidis* sp. nov., a carbohydrate-degrading sulfate-reducing bacterium from the hindgut of a termite. System. *Appl. Microbiol.* 13: 372–377

40. Wolin, M. J., Miller. T. L., and Stewart, C. S. (1997) Microbe-microbe interactions. In: *The rumen microbial ecosystem*. Hobson, P. N., and Stewart, C. S. (eds). London: Blackie Academic and Professional, pp. 478–481

41. Yamin, M. A. (1979) Termite flagellates. *Sociobiology* 4: 1–119

42. Yamin, M. A. (1980) Cellulose metabolism by the termite flagellate *Trichomitopsis termopsidis*. *Appl. Environ. Microbiol.* 39: 859–863.

43. Yamin, M. A. (1981) Cellulose metabolism by the flagellate *Trichonympha* from a termite is independent of endosymbiotic bacteria. *Science* 211: 58–59.

44. Yang, H., Schmitt-Wagner, D., Stingl, U., and Brune, A. (2005) Niche heterogeneity determines bacterial community structure in the termite gut (*Reticulitermes santonensis*). *Environ. Microbiol.* 7: 916–932.

4 Methane oxidation in termite hindguts – absence of evidence and evidence of absence

Michael Pester, Anne Tholen, Michael W. Friedrich, and Andreas Brune.

In preparation.

Abstract

Aerobic methane oxidation is a reaction typical for the oxic–anoxic interface of many habitats. With their counter-gradients of methane and oxygen in the hindgut periphery, also termite hindguts appear to be an ideal habitat for aerobic methane-oxidizing bacteria. However, methane emission rates of living termites increased only slightly when they were shifted from air to a nitrogen atmosphere, indicating that the contribution of methane oxidation to intestinal carbon fluxes is at best only marginal. To test whether these differences could be attributed to methane oxidation or simply to a shift in methane production, living termites were incubated under an atmosphere of air supplemented with $^{14}CH_4$. No conversion of $^{14}CH_4$ to $^{14}CO_2$ occurred, providing clear evidence for the absence of methane oxidation. Screening DNA hindgut extracts of wood-feeding, soil-feeding, and fungus-feeding termites for the *pmo*A gene of methane oxidizing bacteria revealed that methane oxidizers are not just inactive but absent from the termite hindgut. The same result was obtained when screening for the *mcr*A gene of archaea involved in anaerobic methane oxidation. Although at first glance merely an assortment of negative results, this study adds robustness to several important aspects of termite gut microbiology, including the correct determination of gross and net production of the greenhouse gas methane and the elucidation of the metabolic network in the termite hindgut, which improves our understanding of the interactions among the gut microbiota and their role in intestinal carbon flux.

Introduction

Aerobic methane-oxidizing bacteria are typically found at the oxic–anoxic interface of many habitats, e.g., lake sediments, rice field soil, and peat bogs (Hanson and Hanson, 1996), where they thrive on the counter-gradients of methane and oxygen. Hence, also the hindgut of termites would seem an ideal habitat for this metabolic group.

It is well documented that certain termite species emit substantial amounts of methane to the atmosphere, whereas others emit little or no methane (Brauman et al., 1992). Methanogenic archaea, which are easily identified by their F_{420}-autofluoresence, have been located in several microniches within the hindgut

(for a review, see Brune, 2005). Depending on the termite species, they are associated either with the hindgut wall (Leadbetter and Breznak, 1996; Leadbetter et al., 1998; Friedrich et al., 2001) or with filamentous prokaryotes attached to the latter (Leadbetter and Breznak, 1996), or occur as ectosymbionts or endosymbionts of certain intestinal flagellates (Lee et al., 1987, Tokura et al., 2000).

At the gut wall, the outward diffusing methane meets a steep counter-gradient of oxygen, which reaches 50–200 µm into the gut (Brune et al., 1995, Brune and Friedrich, 2000) thereby forming an ideal habitat for methane oxidizing bacteria. A further indication of possible methane oxidation is that the potential methane production rates of methanogens in *Reticulitermes flavipes* exceed the methane emission rates of the termite 3-fold (Leadbetter and Breznak, 1996). Termites emit the greenhouse gas methane to the atmosphere in considerable amounts (2–4 % of the global emission, Sanderson, 1996; Sugimoto et al., 2000) and it is suggestive that aerobic methane-oxidizing bacteria may modulate the gross methane production of the methane-producing populations. However, nobody has ever systematically investigated the presence of methane oxidation in termite hindguts.

In this study, we investigated the presence of methane oxidation in wood-feeding, soil-feeding, and fungus-cultivating termites, which constitute the major feeding guilds among termites. Termites were chosen from the Termitidae or so called higher termites, which represent roughly two thirds of all described termite species, and from the Kalotermitidae, Termopsidae, and Rhinotermitidae, which represent the highest species number among the six families of lower termites (Kambhampati and Eggleton, 2000). Time-course experiments following the turnover of radiolabeled methane were used to measure the process of methane oxidation. Since ammonium is a potential inhibitor of methane-oxidizing bacteria, intestinal ammonium concentrations were determined for most of the species investigated. In addition, DNA extracts of termite hindgut contents were screened for metabolic marker genes of aerobic and anaerobic methane oxidation.

Results

CH_4 emission under air and N_2

All termite species tested emitted CH_4 at a constant rate when incubated under air. Flushing of the headspace with nitrogen evoked a biphasic kinetic of methane emission. Immediately after flushing, the accumulation rates increased slightly but remained constant for approximately 15–20 min. Thereafter, a pronounced increase in methane emission occurred (exemplified in Fig. 1A). The linear increase in single experiments accounted for 13–24% of the methane emission under air depending on the termite (Table 1). However, when compared to the carbon flow through the termite (calculated from the sum of CO_2 and CH_4 emission), the increase of CH_4 emission under 100% N_2 was negligible (Fig. 1B). *Hodotermopsis sjoestedti* was the only termite where a decrease of the CH_4 emission under 100% N_2 was observed.

Table 1. Emission rates of CH_4 and CO_2 of living termites under an atmosphere of air or 100% N_2. Values are means (± SD) for three (CH_4) or four (CO_2) samples.

Termite	CH_4 emission				CO_2 emission	$NH_3 + NH_4^+$
	[nmol (g f.wt.)$^{-1}$ h^{-1}]		% of stimulation in single experiments	% of C flow under air	[µmol (g f.wt.)$^{-1}$ h^{-1}]	(mM)
	Air	N_2			Air	
Reticulitermes santonensis	198 ± 21	261 ± 30	24	0.8	23.7 ± 0.6	0.75 ± 0.08
Zootermopsis nevadensis	493 ± 126	566 ± 135	13	1.6	30.8 ± 5.7	0.23 ± 0.06
Hodotermopsis sjoestedti	1579 ± 276	1517 ± 426	–15	8.6	16.8 ± 3.3	2.15 ± 0.26
Cryptotermes secundus	557 ± 143	607 ± 61	19	2.3	23.9 ± 0.9	n. d.[a]
Cubitermes orthognathus[b]	158 ± 28	160 ± 29	n. d.	4.3	3.7	12 – 121[c]
Macrotermes michaelsenii[d]	31 ± 8	40 ± 14	22	0.5	6.1 ± 0.5	7 – 57[e]

a. Not determined.
b. Data from Schmitt-Wagner and Brune(1999) and Tholen and Brune (1999).
c. Depending on hindgut region: midgut, 34mM; P1 section, 15 mM, P3 section, 12 mM, P4/5 section, 121 mM (data from Ji and Brune, 2006).
d. Starved termites. Measurements were performed 5 days after collection in the field.
e. Depending on the hindgut region: midgut/P1 section, 6.6 mM; P3 section, 18.7 mM; P4 section, 47.4 mM; and P5 section, 57.1 mM.

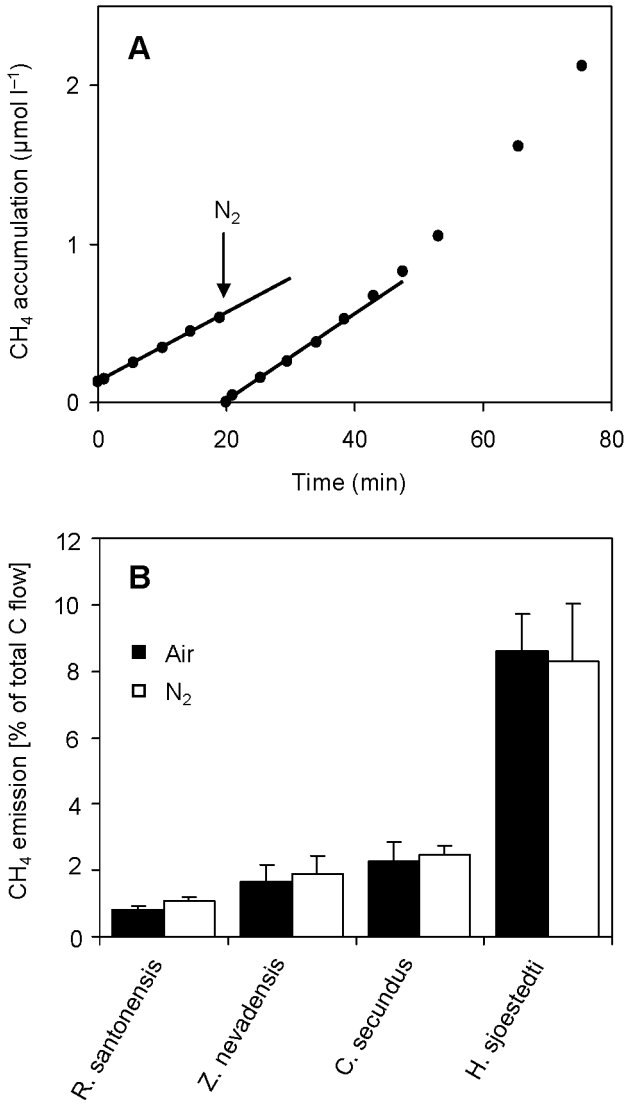

Figure 1. Methane emission by living termites. (A) Time course of CH_4 emission from *Reticulitermes santonensis* incubated under an atmosphere of air, which was replaced by flushing with N_2 for one minute at the time point indicated by the arrow. Similar curves were obtained for other species (data not shown). Rates of CH_4 emission were calculated using the slopes of the linear regression curves under air and N_2. (B) CH_4 emission rates by different termites under air and during the first 15 min after changing the headspace to N_2. Values were normalized to the carbon mineralization flux through the termite (combined CO_2 and CH_4 emission rates under air; Table 1). Bars represent the mean of three independent measurements; standard deviations are given.

CH_4 emission rates of the fungus-cultivating *Macrotermes michaelsenii* were measured as well but were eight times lower than reported previously (Brauman et al., 1992). The reason was very likely the physiological status of the termites, which lacked their symbiotic fungi as food-source in the laboratory. Nevertheless, *M. michaelsenii* also showed only a slight increase of methane emission under 100% N_2 (Table 1).

In vivo incubation with $^{14}CH_4$

Two representative species from the lower and higher termites (*Reticulitermes flavipes* and a *Cubitermes* species, respectively) were incubated for several days in stoppered

glass vials under an atmosphere of air, which was supplemented with $^{14}CH_4$. Shifts in the concentration of $^{14}CH_4$ and $^{14}CO_2$ were monitored over time. However, no decrease of $^{14}CH_4$ or formation of $^{14}CO_2$ could be observed, even when incubated for one week as in the case of *R. flavipes* (Fig. 2).

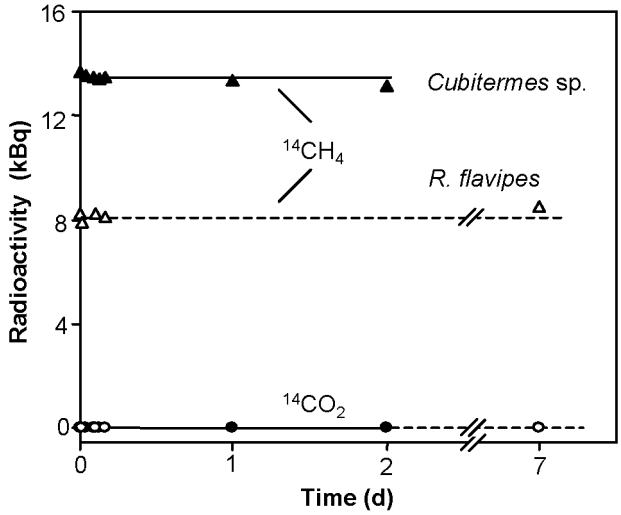

Figure 2. Incubation of living termites under an atmosphere of air supplemented with $^{14}CH_4$. Data shown for the *Cubitermes* species (closed symbols) represent means of two independent measurements, the range is covered by the symbols. Data shown for *R. flavipes* (open symbols) stem from one measurement.

Screening for *pmo*A and *mcr*A genes

DNA was extracted from hindgut contents of termites representing five different families (Table 2) and screened for marker genes coding for enzymes involved in methane oxidation. The *pmo*A gene, which encodes the α-subunit of the particulate methane monooxygenase, was used to target methane-oxidizing bacteria. No PCR products of the expected length were obtained. Only in the case of *R. santonensis*, a PCR product was detected, which was 30–40 bp smaller than the conventional *pmo*A PCR product of the positive control. Cloning of the PCR product obtained from *R. santonensis* hindgut contents revealed an unspecific amplification. Sequences of representative clones had no similarity to sequences of *pmo*A genes or any other genes in public databases (data not shown).

To exclude also the presence of anaerobic methane-oxidizing archaea, two PCR assays were used which specifically amplify the *mcr*A genes of ANME-1 or ANME-2 archaea. This gene encodes the α-subunit of the methyl-coenzyme M reductase. DNA extracts of microbial mats, which showed anaerobic methane oxidation activity (Michaelis et al., 2002), always resulted in a specific PCR product. However, only for the termite *Incisitermes marginipennis*, a PCR product matching the size of the positive control of ANME-2 archaea was observed. Again, this PCR product was cloned but

sequences of representative clones showed no similarity to sequences of *mcr*A genes or any other genes in public databases (data not shown).

Table 2. Termite species from different families and feeding guilds used for functional gene screening.

Family	Species	Feeding guild	Origin
Rhinotermitidae	*Reticulitermes santonensis*	Wood-feeding	Charente maritime, France
	Reticulitermes flavipes	Wood-feeding	Michigan, USA
Termopsidae	*Zootermopsis nevadensis*	Wood-feeding	California, USA
	Hodotermopsis sjoestedtii	Wood-feeding	Yaku-island, Japan
Kalotermitidae	*Cryptotermes secundus*	Wood-feeding	Northern territory, Australia
	Incisitermes marginipennis	Wood-feeding	Mexico [a]
	Neotermes castaneus	Wood-feeding	Florida, USA [a]
Termitidae	*Cubitermes* sp.	Soil-feeding	Busia, Kenya
	Macrotermes michaelsenii	Fungus-cultivating	Kajiado, Kenya

a. Termites were provided by the culture collection of the Federal Institute for Materials Research and Testing, Berlin.

Total ammonia in hindguts

In all lower termites tested, the total ammonia concentration (NH_4^+ and NH_3) ranged from 0.2 to 2.2 mM (Table 1). In the higher termite *Macrotermes michaelsenii*, where the hindgut is axially more differentiated than in lower termites, the concentrations were higher and increased towards the posterior gut sections (7–57 mM, see legend of Table 1 for details).

Discussion

At a first glance, the termite hindgut fulfills all major prerequisites for methane oxidation to take place. Methane is produced by methanogenic archaea associated with gut protozoa (Lee et al., 1987; Tokura et al., 2000) or the gut wall (Leadbetter and Breznak, 1996; Leadbetter et al., 1998; Friedrich et al., 2001) (Fig. 3) The hindgut itself is structured into an anoxic gut center and a microoxic gut periphery (Brune et al., 1995), providing the most important condition for methane oxidation. An inoculation of the hindgut with methanotrophic bacteria is also easily envisaged since the food of termites is in close contact with soil if not soil itself. However, despite these theoretical considerations the results presented in this study

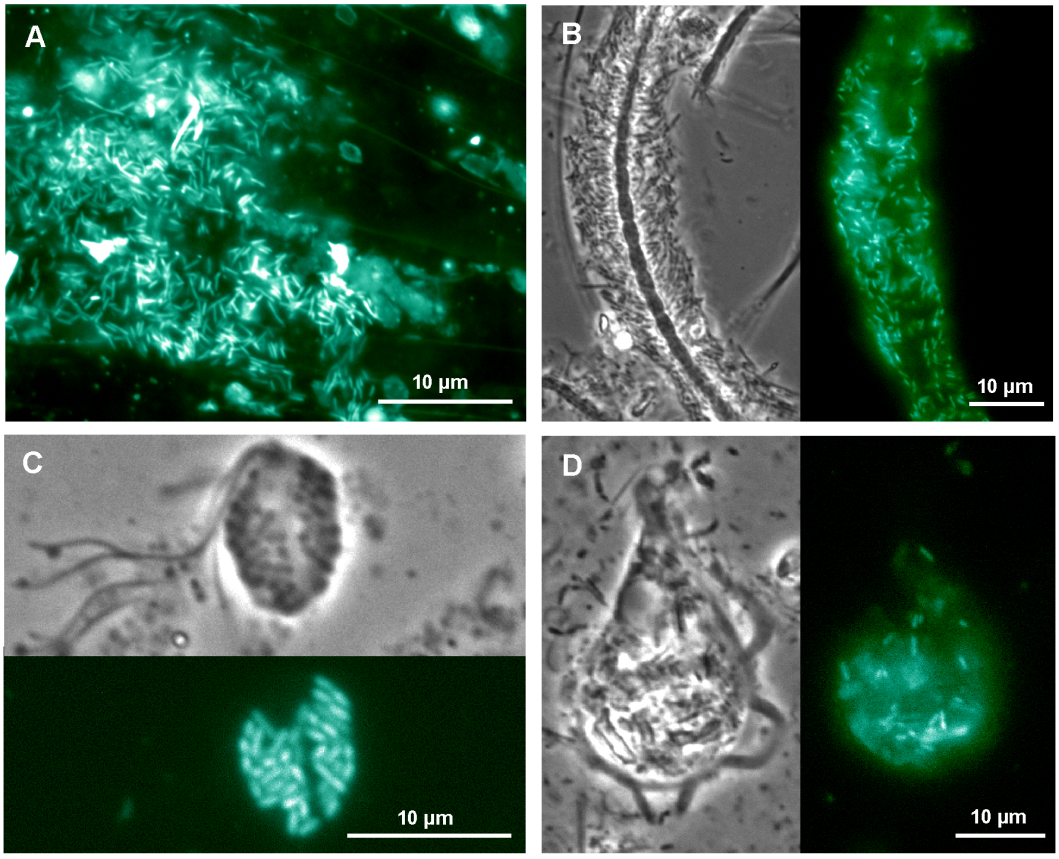

Figure 3. Different habitats of methanogenic archaea observed in the hindgut of termites. (A) F_{420}-autofluorescence of methanogens attached to the hindgut wall of *Reticulitermes santonensis*. (B) Phase contrast image and F_{420}-autofluorescence of methanogens in a biofilm surrounding filamentous prokaryotes in *Schedorhinotermes lamanianus*. (C) Phase contrast image and F_{420}-autofluorescence of methanogens, which are ectosymbionts of a trichomonad flagellate in *Schedorhinotermes lamanianus*. (D) Phase contrast image and F_{420}-autofluorescence of methanogens, which are endosymbionts of the trichomonad flagellate *Trichomitopsis termopsidis* in *Zootermopsis nevadensis*. Images of F_{420}-autofluorescence were taken using a greyscale mode and converted to color images for better visibility.

show cumulative evidence that methane oxidation is not taking place in termite hindguts.

If there were significant rates of aerobic methane oxidation, the methane emission rates of living termites should increase when oxygen is removed from the atmosphere. Although methane emission rates increased slightly after gassing with N_2 for the majority of the termites investigated, this difference accounted at most 0.3% of the total carbon flow through the termite (Fig. 1B). This could indicate the presence of aerobic methane oxidation, which, nevertheless, would be only of minor importance. On the other hand, it is more likely that methanogens, which reside in the microoxic gut periphery, were stimulated by the absence of oxygen (Tholen, 1999). This is supported by the fact that the emitted methane increased first linearly and later exponentially — if absence of aerobic methane oxidation had caused higher methane emission rates, a constant linear increase over time would have been expected.

To gain further insights whether the slight increase of methane emission under N_2 could be attributed to aerobic methane oxidation or whether anaerobic methane oxidation takes place in the anoxic gut center, representative species from the lower and higher termites were incubated for several days under an atmosphere of air supplemented with $^{14}CH_4$. Since $^{14}CH_4$ is diffusing into the hindgut, a turnover of $^{14}CH_4$ to $^{14}CO_2$ should be observed if methane oxidation, aerobic or anaerobic, takes place. One has to point out here that the $^{12}CH_4$ produced in the hindgut and the supplemented $^{14}CH_4$ in the atmosphere behave like two different compounds since the Brownian molecular movement or so called random walk, which describe the movement of a molecule, is by chance and not dependent on the concentration (e.g., Bergethon, 1998). Therefore, $^{12}CH_4$ diffusing out of the hindgut does not hamper a diffusion of $^{14}CH_4$ into the hindgut. In summary, no turnover of $^{14}CH_4$ to $^{14}CO_2$ was observed in the two termite species, giving good evidence that neither aerobic nor anaerobic methane oxidation is taking place. This result is further supported by the fact that in a similar experiment with *Nasutitermes walkeri* (Hill), $^{14}CO_2$ that was supplemented to the atmosphere was converted to ^{14}C-acetate in the hindgut and to termite biomass (Williams et al., 1994). Therefore, the experimental setup did not underlie any constraints.

To make our conclusions more robust, we also tested for the presence of aerobic, methane oxidizing bacteria (MOB) and anaerobic methane oxidizing archaea (ANME) using a molecular, PCR-based approach. The marker genes *pmo*A and *mcr*A were used because they have the advantage to specifically target MOB and ANME-archaea, respectively. Despite the fact that the PCR assays worked very well with environmental samples from lake sediments and marine microbial mats, which served as positive controls, no *mcr*A genes typical for ANME-archaea or *pmo*A genes were detected within the hindgut contents of all tested termites. These results are corroborated by the extensive bacterial 16S rRNA gene clone libraries conducted for *Reticulilermes santonensis* (Yang et al., 2005), *Reticulitermes speratus* and *Microcerotermes* spp. (Hongoh et al., 2003; Hongoh et al., 2005). Among the 2500 clones obtained from these three termites, only one clone from *R. speratus*, clone RS-K73, showed a loose phylogenetic affiliation (96–97% sequence identity) with methanotrophic isolates (*Methylocella* species). A similar situation is observed with the archaeal 16S rRNA gene clones retrieved in various studies from *Reticulitermes speratus* (Ohkuma et al., 1995, Ohkuma et al., 1998, Shinzato et al., 1999, Tokura et al., 2000), *Cryptotermes domesticus* (Ohkuma and Kudo, 1998), *Hodotermopsis sjoestedti*, *Pericapritermes nitobei*, *Odontotermes formosanus*, *Nasutitermes takasagoensis* (Ohkuma et al., 1999, Tokura et al., 2000), *Mastotermes darwiniensis* (www.ncbi.nlm.nih.gov), *Cubitermes orthognathus* (Friedrich et al., 2001), *Cubitermes fungifaber* (Donovan et al., 2004), and *Macrotermes bellicosus* and *Macrotermes subhyalinus* (Eduard Miambi and Andreas Brune, unpublished results), and the three *Methanobrevibacter* spp. isolated from *Reticulitermes flavipes* (Leadbetter and Breznak, 1996, Leadbetter et al., 1998). Here, none of the clones or

isolates fell into the clusters containing ANME-1, ANME-2, or ANME-3 archaea (phylogeny summarized in Meyerdierks et al., 2005) or ANME archaea involved in anaerobic methane oxidation coupled to denitrification (Raghoebarsing et al., 2006). In summary, there is strong evidence that microorganisms involved in methane oxidation are not present in the hindgut of termites.

The fact that methane oxidation does not exist in termite hindguts raises questions concerning reasons for this absence. For both processes, aerobic and anaerobic methane oxidation, only speculative answers can be given. It is well known that aerobic methane oxidation is inhibited by high ammonia concentrations (Whittenbury et al., 1970; O'Neill et al., 1977; Carlsen et al., 1991; King and Schnell, 1994; King and Schnell, 1998). In the soil-feeding *Cubitermes* species and the fungus-cultivating *Macrotermes michaelsenii*, the two higher termites analyzed, such an explanation appears plausible since the total ammonia concentrations in these termites range from 10 mM to 120 mM, depending on the gut section (Ji and Brune, 2006; this study). In wood-feeding termites, however, total ammonia concentrations are consistently lower, ranging from 0.2 to 2.2 mM in the lower wood-feeding termites (this study) and 3 mM in the higher wood-feeding termite *Nasutitermes walkeri* (Hill) (Slaytor and Chapell, 1994). Since there is indirect evidence that aerobic methane oxidation is inhibited by ammonia by a competitive inhibition (Bodelier and Laanbroek, 2004), it is hard to judge whether the present ammonia concentrations could totally inhibit aerobic methane oxidation or whether the inhibitory effect is compensated by high in situ methane concentrations, as observed in other studies (Bosse et al., 1993; King and Schnell, 1994).

In the case of anaerobic methane oxidation, the answer would be even more speculative since for this metabolic process the underlying biochemistry is still under debate (Nauhaus et al., 2005 and references therein) and it is not clear whether ANME-archaea depend on a syntrophic association, e.g., with sulfate reducing bacteria (Strous and Jetten, 2004; Eller et al., 2005).

Also other reasons than inhibition by metabolites or lack of a symbiotic partner could be responsible for the absence of methane oxidation. One of the most limiting factors in the hindgut is space. It is possible that methane oxidizers are simply outgrown or washed out during the gut passage. An even more complex issue is the question whether the termite host can influence its symbiotic microbiota. However, nobody has addressed this question yet.

In summary, the cumulative evidence provided in this study documents (i) that methane is not oxidized in the termite hindgut and (ii) that aerobic and anaerobic methane-oxidizing microorganisms are absent, irrespective of phylogenetic status and feeding guild of the host. The obtained results add a further piece to the puzzle of elucidating the metabolic network in termite hindguts. This will help to understand the intestinal symbioses of these ecologically important soil arthropods, which are the dominating macrofauna involved in carbon mineralization in tropical and subtropical

ecosystems, contributing 1–20% to total carbon mineralization depending on the ecosystem (Lavelle et al., 1997; Sugimoto et al., 2000).

Materials and methods

Termites

The termite species used in this study are listed in Table 2 together with their phylogenetic affiliation, feeding guild, and geographic origin. Wood-feeding termites were held on pinewood and formed stable colonies. Soil-feeding termites were held on soil from the location where they were collected from and could be maintained for up to six months. Fungus-cultivating termites were held on moist filter paper for several days. Experiments reported here were done 4–5 days after collection in the field. Only worker caste termites were used for experiments.

Preparation of $^{14}CH_4$

^{14}C-labeled methane was produced using a culture of *Methanobrevibacter arboriphilus* (DSM 744) grown in anoxic, bicarbonate-buffered mineral medium (AM-4; Brune et al., 1995) supplemented with yeast extract and Casamino acids (Difco; each 0.1%, w/v) and incubated under an H_2–CO_2 atmosphere (80:20, v/v). Cells in the late exponential growth phase were harvested by centrifugation (6000 × *g*, 20 min) and were washed and resuspended twice in anoxic potassium phosphate buffer (0.1 M, pH 7.4) that contained resazurin (10 mg l^{-1}) and was reduced with DTT (0.1 mM). Cell suspensions (7 ml, 3.5 mg cells dry weight) were transferred to 25-ml serum bottles containing a H_2 atmosphere, supplemented with 0.2 ml of an anoxic $NaH^{14}CO_3$ solution (20 µmol, 42 MBq), and incubated on a rotary shaker (140 rpm) at 30°C in the dark. Incubations were stopped after 10 days by adding 0.5 ml NaOH (2 M). The headspace was transferred to a separate bottle, and the produced $^{14}CH_4$ was tested for radiochemical purity, specific radioactivity, and volume radioactivity by gas chromatography (see below).

Analytical techniques

Methane was measured using a gas chromatograph equipped with a Mol Sieve 5A column (30 m × 0.32 mm), a methanizer (for the catalytic reduction of CO_2 to CH_4), and a flame ionization detector. Injector and column temperature were 100 °C, detector temperature was 140 °C. The carrier gas was helium at a flow rate of 20 ml min^{-1}.

Carbon dioxide was measured with a gas chromatograph (SRI instruments, model 9300A) with methanizer, flame ionization detector, and a Porapack Q column (274 cm × 3.18 mm, mesh 80/100). Column temperature was 80 °C; the carrier gas was 100% hydrogen with a flow rate of 21.5 ml min^{-1}. Samples were directly injected onto the column.

Radioactive gases ($^{14}CH_4$ and $^{14}CO_2$) were detected using a radioactivity monitor (RAGA 2026; Raytest, Straubenhardt, Germany). Radiolabeled products were identified by co-chromatography with labeled and unlabeled standards. The detection limit was 25 Bq for each gas.

Total ammonia (NH_3 and NH_4^+) in gut homogenates was measured by flow injection analysis as described by Ji and Brune (2006).

Molecular analysis

DNA extraction from termite hindgut contents (Pester and Brune, 2006) and the PCR assay targeting the *pmo*A gene (Pester et al., 2004) were performed as previously described. DNA from Lake Constance sediment and *pmo*A clones from the same study served as positive control (Pester et al., 2004). The PCR assay targeting the *mcr*A gene of archaea involved in anaerobic methane oxidation (ANME) was performed using the primers ANME1-724f (5'-GGY ATG CAG GTC GGR ATG WC-3') and ANME1-1557r (5'-CAT CTC GAA TGG CAT TCC CTC-3') for ANME1-archaea, and the primers ANME2-813f (5'-AGA TGG CTG AGA TGC TTC-3') and ANME2-1315r (5'-GTG CAG GTA CAT CGA CAT-3') for ANME2-archaea. Primers were constructed on the basis of publicly available metagenomic data of ANME-archaea. Thermal cycling started with an initial denaturation for 2 min at 94 °C and proceeded with 35 cycles of denaturation for 30 sec at 94 °C, annealing for 45 sec at 55 °C, and elongation for 1 min at 72 °C. The final elongation step lasted 7 min. PCR products were checked by standard agarose gel electrophoresis. DNA extracted from microbial mats from the Black Sea served as positive control (Michaelis et al., 2002).

The phylogenetic relationship between methane oxidizing bacteria and bacterial 16S rRNA gene clones of termite hindgut contents as well as archaea involved in anaerobic methane oxidation and archaeal 16S rRNA gene clones obtained from termite hindgut contents was analyzed using the ARB software package (Ludwig et al., 2004). The basal tree was obtained from the 16S/18S rRNA database from January 2004, which is available for download from the ARB homepage (www.arb-home.de). Sequences of interest were aligned to the existing database and added to the basal tree by the ARB parsimony tool (Ludwig et al., 2004) using phylum-specific 50% conservation filters.

Acknowledgements

We thank Judith Korb, Roland Brandl, and Horst Hertel for providing living termites and David Kamanda Ngugi, Hamadi Boga, Sybille Frankenberg, and Mahesh Desai for donating some of their DNA preparations. The excellent technical assistance of Katja Meuser is gratefully acknowledged.

References

1. Bergethon, P. R. 1998. The random walk: a molecular picture of movement. In *The physical basis of biochemistry: the foundations of molecular biophysics*. Bergethon, P. R. (ed). New York: Springer, pp. 448–451.

2. Bodelier, P. L. E., and Laanbroek, H. J. 2004. Nitrogen as a regulatory factor of methane oxidation in soils and sediments. *FEMS Microbiol. Ecol.* 47: 265–277.

3. Bosse, U., Frenzel, P., and Conrad, R. 1993. Inhibition of methane oxidation by ammonium in the surface layer of a littoral sediment. *FEMS Microbiol. Ecol.* 13: 123–134.

4. Brauman, A., Kane, M. D., Labat, M., and Breznak, J. A. 1992. Genesis of acetate and methane by gut bacteria of nutritionally diverse termites. *Science* 257: 1384–1387.

5. Brauman, A., Koenig, J. F., Dutreix, J., and Garcia, J. L. 1990. Characterization of two sulfate-reducing bacteria from the gut of the soil-feeding termite, *Cubitermes speciosus*. *Antonie v. Leeuwenhoek* 58: 271–275.

6. Brune, A. 2005, posting date. Symbiotic associations between termites and prokaryotes. In *The Prokaryotes. An online electronic resource for the microbiological community, 3rd edn. [Online.]*. Dworkin, M., Falkow, S., Rosenberg, E., Schleifer, K-H., and Stackebrandt, E. (eds). New York: Springer-SBM. http://141.150.157.117:8080/prokPUB/index.htm.

7. Brune, A., and Friedrich, M. W. 2000. Microecology of the termite gut: structure and function on a microscale. *Curr. Opin. Microbiol.* 3: 263–269.

8. Brune, A., Emerson, D., and Breznak, J. A. 1995. The termite gut microflora as an oxygen sink: microelectrode determination of oxygen and pH gradients in guts of lower and higher termites. *Appl. Environ. Microbiol.* 61: 2681–2687.

9. Brune, A., Miambi, E., and Breznak, J. A. 1995. Roles of oxygen and the intestinal microflora in the metabolism of lignin-derived phenylpropanoids and other monoaromatic compounds by termites. *Appl. Environ. Microbiol.* 61: 2688–2695.

10. Carlsen, H. N., Jorgensen, L., and Degn, H. 1991. Inhibition by ammonia of methane utilization of *Methylococcus capsulatus* (Bath). *Appl. Microbiol. Biotechnol.* 35: 124–127.

11. Donovan, S. E., Purdy, K. J., Kane, M. D., and Eggleton, P. 2004. Comparison of *Euryarchaea* strains in the guts and food-soil of the soil-feeding termite *Cubitermes fungifaber* across different soil types. *Appl. Environ. Microbiol.* 70: 3884–3892.

12. Dröge, S., Limper, U., Emtiazi, F., Schönig, I., Pavlus, N., Drzyzga, O., Fischer, U., and König, H. 2005. In vitro and in vivo sulfate reduction in the gut contents of the termite *Mastotermes darwiniensis* and the rose-chafer *Pachnoda marginata*. *J. Gen. Appl. Microbiol.* 51: 57–64.

13. Eller, G., Kanel, L., and Krüger, M. 2005. Cooccurrence of aerobic and anaerobic methane oxidation in the water column of Lake Plusssee. *Appl. Environ. Microbiol.* 71: 8925–8928.

14. Friedrich, M. W., Schmitt-Wagner, D., Lüders, T., and Brune, A. 2001. Axial differences in community structure of *Crenarchaeota* and *Euryarchaeota* in the highly compartmentalized gut of the soil-feeding termite *Cubitermes orthognathus*. *Appl. Environ. Microbiol.* 67: 4880–4890.

15. Fröhlich, J., Sass, H., Babenzien, H.-D., Kuhnigk, T., Varma, A., Saxena, S., Nalepa, C., Pfeiffer, P., and König, H. 1999. Isolation of *Desulfovibrio intestinalis* sp. nov. from the hindgut of the lower termite *Mastotermes darwiniensis*. *Can. J. Microbiol.* 45: 145–152.

16. Hanson, R. S., and Hanson, T. S. 1996. Methanotrophic bacteria. *Microbiol. Rev.* 60: 439–471.

17. Hongoh, Y., Deevong, P., Inoue, T., Moriya, S., Trakulnaleamsai, S., Ohkuma, M., Vongkaluang, C., Noparatnaraporn, N., and Kudo, T. 2005. Intra- and interspecific comparisons of bacterial diversity and community structure support coevolution of gut microbiota and termite host. *Appl. Environ. Microbiol.* 71: 6590–6599.

18. Hongoh, Y., Ohkuma, M., and Kudo, T. 2003. Molecular analysis of bacterial microbiota in the gut of the termite *Reticulitermes speratus* (Isoptera; Rhinotermitidae). *FEMS Microbiol. Ecol.* 44: 231–242.

19. Ji, R., and Brune, A. 2006. Nitrogen mineralization, ammonia accumulation, and emission of gaseous NH_3 by soil-feeding termites. *Biogeochemistry* 78: 267–283.

20. Kambhampati, S., and Eggleton, P. 2000. Taxonomy and phylogenetics of Isoptera. In *Termites: Evolution, Sociality, Symbiosis, Ecology*. Abe, T., Bignell, D. E., and Higashi, M. (eds). Dordrecht: Kluwer Academic Publishers, pp. 1–23.

21. King G. M., and Schnell, S. 1998. Effects of ammonium and non-ammonium salt additions on methane oxidation by *Methylosinus trichosporium* OB3b and Maine forest soils. *Appl. Environ. Microbiol.* 64: 253–257.

22. King, G. M., and Schnell, S. 1994. Ammonium and nitrite inhibition of methane oxidation by *Methylobacter albus* BG8 and *Methylosinus trichosporium* OB3b at low methane concentrations. *Appl. Environ. Microbiol.* 60: 3508–3513.

23. Kuhnigk, T., Branke, J., Krekeler, D., Cypionka, H., and König, H. 1996. A feasible role of sulfate-reducing bacteria in the termite gut. *System. Appl. Microbiol.* 19: 139–149.

24. Lavelle, P., Bignell, D., Lepage, M., Wolters, V., Roger, P., Ineson, P., Heal, O. W., and Dhillion, S. 1997. Soil function in a changing world: the role of invertebrate ecosystem engineers. *Eur. J. Soil Biol.* 33: 159–193.

25. Leadbetter, J. R., and Breznak, J. A. 1996. Physiological ecology of *Methanobrevibacter cuticularis* sp. nov. and *Methanobrevibacter curvatus* sp. nov., isolated from the hindgut of the termite *Reticulitermes flavipes*. *Appl. Environ. Microbiol.* 62: 3620–3631.

26. Leadbetter, J. R., Crosby, L. D., and Breznak, J. A. 1998. *Methanobrevibacter filiformis* sp. nov., a filamentous methanogen from termite hindguts. *Arch. Microbiol.* 169: 287–292.

27. Lee, M. J., Schreurs, P. J., Messer, A. C., and Zinder, S. H. 1987. Association of methanogenic bacteria with flagellated protozoa from a termite hindgut. *Curr. Microbiol.* 15: 337–341.

28. Ludwig, W., Strunk, O., Westram, R., Richter, L., Meier, H., and 27 other authors. 2004. ARB: a software environment for sequence data. *Nucleic Acids Res.* 32: 1363–1371.

29. Meyerdierks, A., Kube, M., Lombardot, T., Knittel, K., Bauer, M., Glockner, F. O., Reinhardt, R., and Amann, R. 2005. Insights into the genomes of archaea mediating the anaerobic oxidation of methane. *Environ. Microbiol.* 7: 1937–1951.

30. Michaelis, W., Seifert, R., Nauhaus, K., Treude, T., Thiel, V., Blumenberg, M., Knittel, K., Gieseke, A., Peterknecht, K., Pape, T., Boetius, A., Amann, R., Jorgensen, B. B., Widdel, F., Peckmann, J., Pimenov, and N. V., and Gulin, M. B. 2002. Microbial reefs in the black sea fueled by anaerobic oxidation of methane. *Science* 297: 1013–1015.

31. Nauhaus, K., Treude, T., Boetius, A., and Krüger, M. 2005. Environmental regulation of the anaerobic oxidation of methane: a comparison of ANME-I and ANME-II communities. *Environ. Microbiol.* 7: 98–106.

32. Ohkuma, M., and Kudo, T. 1998. Phylogenetic analysis of the symbiotic intestinal microflora of the termite *Cryptotermes domesticus*. *FEMS Microbiol. Lett.* 164: 389–395.

33. Ohkuma, M., Noda, S., and Kudo, T. 1999. Phylogenetic relationships of symbiotic methanogens in diverse termites. *FEMS Microbiol. Lett.* 171: 147–153.

34. Ohkuma, M., Noda, S., Horikoshi, K., and Kudo, T. 1995. Phylogeny of symbiotic methanogens in the gut of the termite *Reticulitermes speratus*. *FEMS Microbiol. Lett.* 134: 45–50.

35. Ohkuma, M., Ohtoko, K., Grunau, C., Moriya, S., and Kudo, T. 1998. Phylogenetic identification of the symbiotic hypermastigote *Trichonympha agilis* in the hindgut of the termite *Reticulitermes speratus* based on small-subunit rRNA sequence. *J. Euk. Microbiol.* 45: 439–444.

36. O'Neill, G. J., and Wilkinson, J. F. 1977. Oxidation of ammonia by methane oxidizing bacteria and the effects of ammonia on methane oxidation. *J. Gen. Microbiol.* 100: 407–412.

37. Orphan, V. J., Hinrichs, K. U., Ussler, W. 3rd, Paull, C. K., Taylor, L. T., Sylva, S. P., Hayes, J. M., and Delong, E. F. 2001. Comparative analysis of methane-oxidizing archaea and sulfate-reducing bacteria in anoxic marine sediments. *Appl. Environ. Microbiol.* 67: 1922–1934.

38. Pester, M., and Brune, A. 2006. Expression profiles of *fhs* (FTHFS) genes support the hypothesis that spirochaetes dominate reductive acetogenesis in the hindgut of lower termites. *Environ. Microbiol.* 8: 1261–1270

39. Pester, M., Friedrich, M. W., Schink, B., and Brune, A. 2004. *pmoA*-based analysis of methanotrophs in a littoral lake sediment reveals a diverse and stable community in a dynamic environment. *Appl. Environ. Microbiol.* 70: 3138–3142.

40. Platen, H., and Schink, B. 1987. Methanogenic degradation of acetone by an enrichment culture. *Arch. Microbiol.* 149: 136–141.

41. Raghoebarsing, A. A., Pol, A., van de Pas-Schoonen, K. T., Smolders, A. J., Ettwig, K. F., Rijpstra, W. I., Schouten, S., Damste, J. S., Op den Camp, H. J., Jetten. M. S., and Strous, M. 2006. A microbial consortium couples anaerobic methane oxidation to denitrification. *Nature* 440: 918–921.

42. Sanderson, M.G. 1996. Biomass of termites and their emissions of methane and carbon dioxide: A global database. *Global Biogeochem. Cycles* 10: 543–557.

43. Schmitt-Wagner, D., and Brune, A. 1999. Hydrogen profiles and localization of methanogenic activities in the highly compartmentalized hindgut of soil-feeding higher termites (*Cubitermes* spp.). *Appl. Environ. Microbiol.* 65: 4490–4496.

44. Shinzato, N., Matsumoto, T., Yamaoka, I., Oshima, T., and Yamagishi, A. 1999. Phylogenetic diversity of symbiotic methanogens living in the hindgut of the lower termite *Reticulitermes speratus* analyzed by PCR and in situ hybridization. *Appl. Environ. Microbiol.* 65: 837–840.

45. Slaytor, M., and Chappell, D. J. 1994. Nitrogen metabolism in termites. *Comp. Biochem. Physiol.* 107: 1–10.

46. Strous, M., and Jetten, M. S. 2004. Anaerobic oxidation of methane and ammonium. *Annu. Rev. Microbiol.* 58: 99–117.

47. Sugimoto, A., Bignell, D. E., and MacDonald, J. A. 2000. Global impact of termites on the carbon cycle and atmospheric trace gases In *Termites: Evolution, Sociality, Symbioses, Ecology.* Abe, T., Bignell, D. E., and Higashi, M. (eds). Dordrecht: Kluwer Academic Publishers, pp. 409–435.

48. Tholen, A. 1999. Ph.D. thesis. University of Constance, Germany. Der Termitendarm als strukturiertes Ökosystem: Untersuchung der Mikrobiota und der Stoffflüsse im Darm von *Reticulitermes flavipes* und *Cubitermes* spp.

49. Tholen, A., and Brune; A. 1999. Localization and in situ activities of homoacetogenic bacteria in the highly compartmentalized hindgut of soil-feeding higher termites (*Cubitermes* spp.). *Appl. Environ. Microbiol.* 65: 4497–4505.

50. Tokura, M., Ohkuma, M., and Kudo; T. 2000. Molecular phylogeny of methanogens associated with flagellated protists in the gut and with the gut epithelium of termites. *FEMS Microbiol. Ecol.* 33: 233–240.

51. Whittenbury, R., Phillips, K. C., and Wilkinson; J. F. 1970. Enrichment, isolation, and some properties of methane-utilizing bacteria. *J. Gen. Microbiol.* 61: 205–218.

52. Williams, C. M., Veivers, P. C., Slaytor, M., and Cleland, S. V. 1994. Atmospheric carbon dioxide and acetogenesis in the termite *Nasutitermes walkeri* (Hill). *Comp. Biochem. Physiol.* 107: 113–118.

53. Yang, H., Schmitt-Wagner, D., Stingl, U., and Brune, A. 2005. Niche heterogeneity determines bacterial community structure in the termite gut (*Reticulitermes santonensis*). *Environ. Microbiol.* 7: 916–932.

5 Expression profiles of *fhs* (FTHFS) genes support the hypothesis that spirochetes dominate reductive acetogenesis in the hindgut of lower termites

Michael Pester and Andreas Brune.

Published in Environmental Microbiology, 8: 1261–1270 (2006).

Abstract

Reductive acetogenesis is an important metabolic process in the hindgut of wood-feeding termites. We analyzed diversity and expression profiles of the bacterial *fhs* gene, a marker gene encoding a key enzyme of reductive acetogenesis, formyl tetrahydrofolate synthetase (FTHFS), to identify the active homoacetogenic populations in representatives of three different termite families. Clone libraries of PCR-amplified *fhs* genes from hindgut contents of *Reticulitermes santonensis* (Rhinotermitidae) and *Cryptotermes secundus* (Kalotermitidae) were compared to previously published *fhs* gene sequences obtained from *Zootermopsis nevadensis* (Termopsidae). Most of the clones clustered among the 'Termite Treponemes', which comprise also the *fhs* genes of the two strains of the homoacetogenic spirochete *Treponema primitia*. The high abundance of treponemal *fhs* genes in all clone libraries was in agreement with the results of DNA-based terminal-restriction fragment length polymorphism (T-RFLP) analyses. Moreover, in mRNA-based T-RFLP profiles of the three termites, only expression of *fhs* genes of 'Termite Treponemes' was detected, albeit at different levels. In *C. secundus*, only one of the dominating phylotypes was transcribed, while in *R. santonensis*, the apparently less abundant *fhs* genes were the most actively expressed. Our results strongly support the hypothesis that spirochetes are responsible for reductive acetogenesis in the hindgut of lower, wood-feeding termites.

Introduction

Most lower termites feed on wood or plant litter and contribute to the turnover of dead plant material in many ecosystems (Wood, 1978; Wood and Johnson, 1986). The major metabolic intermediate of the plant fiber degradation is acetate, which accumulates in the hindgut of all lower termites investigated so far (Brune, 2006). The acetate concentration in the gut fluid is in the range of several tens of millimolar and forms the bulk of the volatile fatty acid pool in the hindgut (Odelson and Breznak, 1983; Tholen and Brune, 2000); acetate is considered the most important substrate in energy metabolism of the termite. High potential

activities of CO_2 reduction to acetate in termite gut homogenates indicate that reductive acetogenesis contributes considerably to acetate production (Brauman et al., 1992), and *in situ* measurements of reductive acetogenesis in *Reticulitermes flavipes* document that approximately 10% of the carbon flow proceeds through this process (Tholen and Brune, 2000).

Information about the bacteria responsible for reductive acetogenesis in lower termites is scarce. In the literature, such microorganisms are called homoacetogenic bacteria (Schink and Bomar, 1992), or simply acetogenic bacteria (Drake et al., 2001), because of their ability to use carbon dioxide as an electron sink and to reduce it via the carbon monoxide dehydrogenase system, producing acetate as the typical fermentation product. Most of the homoacetogens isolated from termites belong to the Clostridiales and, with the exception of *Acetonema longum*, stem from higher termites (Breznak et al., 1988; Kane and Breznak, 1991; Kane et al., 1991; Boga et al., 2003). However, several years ago Breznak and co-workers succeeded in isolating the first homoacetogenic spirochete, *Treponema primitia*, from a lower termite. This finding and the high abundance of spirochetes in the hindgut (Breznak, 1984) led to the hypothesis that *Treponema* species mainly contribute to reductive acetogenesis in lower termites (Leadbetter et al., 1999; Graber et al., 2004; Graber and Breznak, 2004).

Identification of homoacetogens by their 16S rRNA genes is hindered by their polyphyletic nature. However, the bacterial formyl tetrahydrofolate synthetase (FTHFS, EC 6.3.4.3, also known as formate tetrahydrofolate ligase), a structurally and functionally conserved enzyme in the acetyl-CoA pathway, can be used to identify homoacetogens (Leaphart and Lovell, 2001; Leaphart et al., 2003). The FTHFS encoding gene, *fhs*, can serve as a functional marker for reductive acetogenesis, and its phylogeny allows homoacetogenic and non-homoacetogenic bacteria to be distinguished (Leaphart and Lovell, 2001; Leaphart et al., 2003). Interestingly, primers based on the *fhs* gene sequences of homoacetogenic Clostridiales also amplify *fhs* genes of *Treponema* spp. isolated from the termite gut (Leaphart et al., 2003; Salmassi and Leadbetter, 2003) that fall within the phylogenetic radiation of the *fhs* genes of homoacetogenic Clostridiales.

An inventory of bacterial *fhs* genes in the hindgut of a *Zootermopsis* species revealed that 77% of the clones clustered with the *fhs* gene of the homoacetogenic *Treponema primitia* ('Termite treponeme cluster'), while the rest fell among *fhs* genes of homoacetogenic Clostridiales and other, non-homoacetogenic species (Salmassi and Leadbetter, 2003). This is an indication that treponemes are indeed responsible for reductive acetogenesis in *Zootermopsis* species, but it remained to be shown whether the genes are actually expressed and whether reductive acetogenesis in wood-feeding lower termites is generally catalyzed by treponemes.

Determination of mRNA levels provides information about specific gene expression and can be used as an indicator of the activity of a given metabolic

pathway (Conway and Schoolnik, 2003). This principle has been successfully applied in a number of studies targeting functional genes of prokaryotes such as *nif*H in termite guts and lake water (Noda et al., 1999; Zani et al., 2000), *nah*A (Wilson et al., 1999) and *pmo*A (Cheng et al., 1999) in groundwater, and *nar*G, *nap*A, *nir*S, *nir*K, and *nos*Z in estuarine sediments (Nogales et al., 2002).

In this study, we investigated the diversity and expression of bacterial *fhs* genes in hindgut contents of lower, wood-feeding termites representing three different families. Clone libraries were constructed from hindgut contents of *Reticulitermes santonensis* and *Cryptotermes secundus* and sequences were compared to previously published bacterial *fhs* sequences obtained from *Zootermopsis nevadensis* (Salmassi and Leadbetter, 2003). Furthermore, relative abundance of *fhs* genes and their expression in all three termites was analyzed by DNA-based and mRNA-based T-RFLP analyses.

Results

Identification of termites

Termites were identified by their morphological features. The identification was supported by sequence analysis of their cytochrome oxidase II (COII) genes. The deduced amino acid sequence from *Reticulitermes santonensis* fell into a cluster of published sequences from *R. santonensis* and *R. flavipes*, which are synonymous species of different geographic origin (Austin et al., 2005). The sequence from *Cryptotermes secundus* was closely related to a previously published sequence of *C. secundus* (99.4% sequence identity) and well separated from other species of the same genus (details not shown).

The deduced amino acid sequence from the *Zootermopsis* species was only distantly related (90% sequence identity) to the published COII sequence from *Zootermopsis angusticollis* (Liu and Beckenbach, 1992). The morphology of the subsidiary tooth of the right mandible, a differential trait distinguishing the three currently recognized *Zootermopsis* species (Thorne and Haverty, 1989), clearly identified the termites used in this study as *Zootermopsis nevadensis*. Moreover, the COII sequence from *Z. nevadensis* (this study) was identical to that from the *Zootermopsis* sp. used in the study of Salmassi and Leadbetter (2003), which was later identified as *Z. nevadensis*, and not *Z. angusticollis* (J. R. Leadbetter, personal communication).

Potential rates of reductive acetogenesis

Rates of reductive acetogenesis were measured following the conversion of $^{14}CO_2$ to ^{14}C-acetate in hindgut homogenates. Highest rates per gut were observed with the large *Z. nevadensis*, whereas lower rates were observed with the smaller *C. secundus* and *R. santonensis* (Table 1). However, when based on the fresh weight of the respective termite, all rates were in a similar range, albeit significantly lower in *C. secundus*.

Table 1. Potential rates of reductive acetogenesis from $^{14}CO_2$ in hindgut homogenates of the three termite species. Rates are averages of results obtained with two sets of termites.

Termite species	^{14}C-acetate formation	
	Rate per gut [nmol h^{-1}]	Specific rate [µmol (g fresh wt.)$^{-1}$ h^{-1}]
Reticulitermes santonensis	8.3 ± 1.9	4.1 ± 0.9
Cryptotermes secundus	7.2 ± 0.0	2.2 ± 0.2
Zootermopsis nevadensis	438 ± 246	5.9 ± 1.9

All homogenates also formed substantial amounts of labeled formate, a phenomenon reported by Breznak and Switzer (1986) for homogenates of *Reticulitermes flavipes*, *Prorhinotermes simplex*, and *Zootermopsis angusticollis*. Formate formation rates from $^{14}CO_2$ were in a similar range as acetate formation rates in *C. secundus* and *Z. nevadensis*, and roughly twice as high in *R. santonensis* (details not shown).

fhs clone libraries

Nucleic acid extracts from hindgut contents of *R. santonensis* and *C. secundus* were used to amplify bacterial *fhs* genes. PCR reactions resulted in products of the expected length (~1100 bp), which were used to generate a clone library for each termite. Clones were screened by RFLP analysis and grouped according to their restriction pattern. Representatives from each group were sequenced and aligned on the basis of deduced amino acids. Clones with more than 99.5% DNA sequence identity were treated as representatives of the same genotype. Genotypes with similar deduced amino acid sequences formed distinct phylogenetic clusters and were grouped into phylotypes using a cut-off value of 93% amino acid sequence identity, which reflects the level of amino acid sequence identity between the *fhs* genes of *Clostridium aceticum* and *Clostridium formicoaceticum*, the most closely related *fhs* genes of authentic homoacetogens.

The clone library of *R. santonensis* comprised 50 distinct genotypes, which could be assigned to 13 phylotypes (Table 2). Eleven phylotypes (98% of the clones) grouped among the 'Termite Treponemes' (Fig. 1). This cluster contains only *fhs* genes obtained from termite guts and includes the homoacetogenic *Treponema primitia* strains ZAS-1 and ZAS-2 (Leadbetter et al., 1999; Graber et al., 2004) and the non-homoacetogenic *Treponema azotonutricium* strain ZAS-9 (Lilburn et al., 2001; Graber et al., 2004) isolated from *Z. angusticollis*. Moreover, all sequences in the cluster share a unique signature of six to eight amino acid residues distinct from the two amino acid residues (Asp232 and Gly233 in *Moorella thermoacetica*) typical for homoacetogenic Clostridiales (Salmassi and Leadbetter, 2003).

Table 2. Frequency and relative abundance of different phylotypes in the clone libraries from *Reticulitermes santonensis* and *Cryptotermes secundus* (this study) and *Zootermopsis nevadensis* (Salmassi and Leadbetter, 2003). For each phylotype, the corresponding genotypes and their terminal restriction fragments (T-RFs) are listed. T-RFs present in m-RNA based and DNA-based T-RFLP profiles (Fig. 2) are given in bold; T-RFs present in the DNA-based profiles only are marked in italics.

Phylotype [a]	Number of clones	T-RF [b] (bp)	Relative abundance (%)	Genotypes [c]
Reticulitermes santonensis				
RsI	32	**337**	36	Rs49, Rs66, Rs102, Rs107, Rs119, Rs142, Rs153, Rs163, Rs175, Rs181, Rs186, Rs202, Rs214, Rs236, Rs241, Rs243, Rs265, Rs271, Rs279, Rs293
		111	1	Rs256
		138	2	Rs100, Rs247
		201	1	Rs302
RsII	31	**429**	31	Rs5, Rs105, Rs122, Rs223, Rs239
		754	2	Rs54, Rs249
		763	4	Rs180, Rs195
		337	1	Rs87
RsIII	2	**347**	2	Rs264, Rs296
RsIV	3	**138**	2	Rs158
		192	1	Rs183
RsV	2	99	2	Rs57, Rs124
RsVI	2	205	2	Rs129, Rs231
RsVII	3	**413**	4	Rs44, Rs222
Rs10	1	186	1	Rs10
Rs13	1	99	1	Rs13
Rs23	1	192	1	Rs23
Rs131	1	1044	1	Rs131
Rs144	1	763	1	Rs144
Rs280	1	**337**	1	Rs280
Cryptotermes secundus				
CsI	43	**337**	91	Cs1, Cs4, Cs55, Cs 63, Cs101
		205	2	Cs3
Cs18	1	254	2	Cs18
Cs27	1	*138*	2	Cs27
Cs56	1	*138*	2	Cs56
Zootermopsis nevadensis [d]				
ZaH		**337**	12	ZaG2, ZaI, ZaL, ZaR, ZaU
		635	33	ZaE2, ZaF2, ZaH, ZaM
ZaP		**337**	19	ZaC, ZaG, ZaP, ZaZ
ZaN		**337**	2	ZaN
ZaA		138	11	ZaA
ZaF		188	2	ZaF
ZaY		1050	8	ZaY
ZaE		122	4	ZaE
ZaT		415	9	ZaT

a. Clones forming a cluster and sharing at least 93% amino acid sequence identity (see text).
b. Hypothetical T-RFs resulting from a simultaneous digestions with the restriction enzymes *Msp*I and *Rsa*I.
c. Clones with more than 99.5% DNA sequence identity.
d. Relative abundance of phylotypes was taken from Salmassi and Leadbetter (2003)

Most clones in the clone library belonged to phylotypes RsI and RsII. Among the non-'Termite Treponeme' phylotypes (2% of the clones), one grouped with *fhs* sequences of homoacetogenic Clostridiales (Rs10), and the other with *fhs* sequences of non-homoacetogenic bacteria (Rs131), both representing novel lineages without close relatives (Fig. 1).

The clone library of *C. secundus* was less diverse than that of *R. santonensis*. It contained only 9 distinct genotypes, which could be assigned to 4 phylotypes

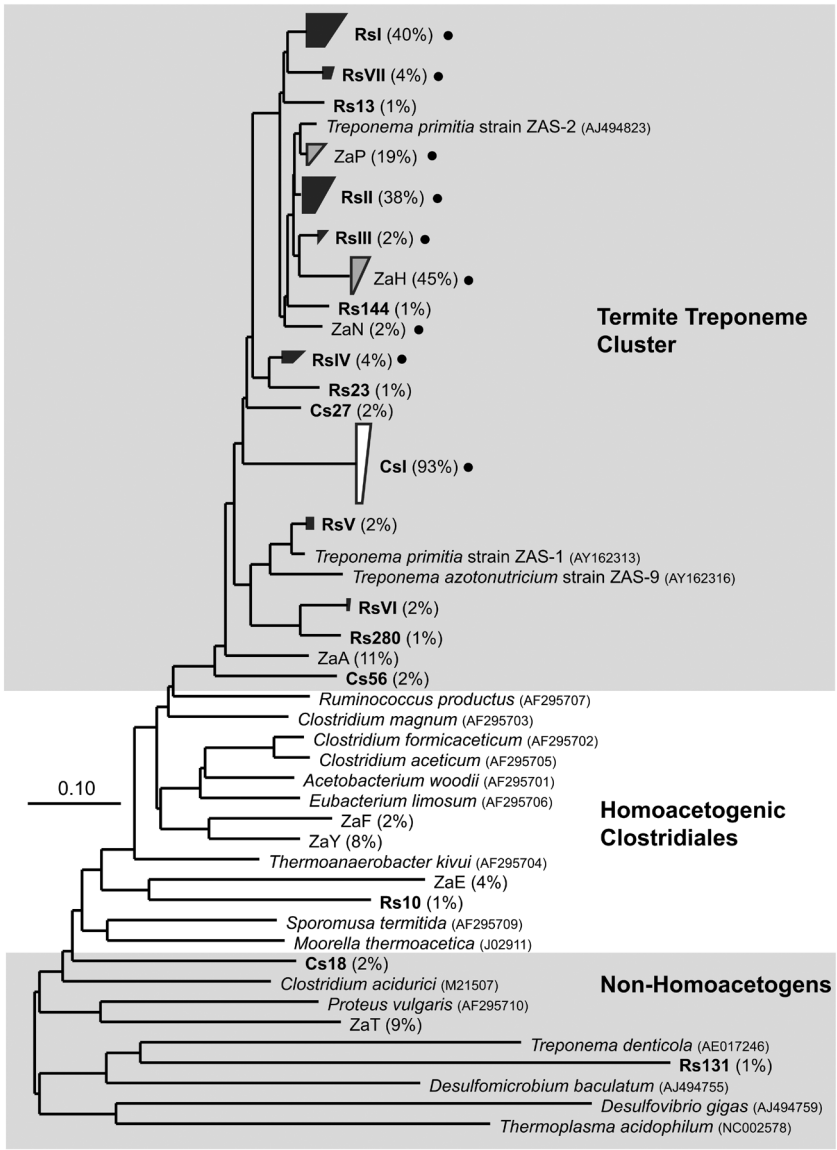

Figure 1. Phylogenetic tree of *fhs* genes from termite hindguts and of homoacetogenic and non-homoacetogenic isolates. Phylotypes obtained from *Reticulitermes santonensis* and *Cryptotermes secundus* (bold, this study) and from *Zootermopsis nevadensis* (Salmassi and Leadbetter, 2003) are preceded by Rs, Cs, or Za, respectively; their relative abundance in the respective clone library is given in parentheses. Phylotypes that are represented in the mRNA-based T-RFLP profiles are marked (•). The tree is based on a distance matrix of deduced amino acid sequences using 309 unambiguously aligned positions and was reconstructed using the Fitch algorithm (see Materials and methods); the bar indicates 10% sequence divergence.

(Table 2). Again, the majority of the clones (97%) grouped among the 'Termite Treponemes'. With two exceptions, all belonged to phylotype CsI, which was well separated from the sequences obtained from all other termites (Fig. 1). Only one clone (Cs18), representing a novel lineage without close relatives, could not be clearly assigned and was placed provisionally into the group of the non-homoacetogenic bacteria.

T-RFLP analysis of *fhs* genes and their transcripts

Aliquots of the nucleic acid extracts from the hindguts of the three termites were used, either directly or after pre-treatment with DNase and reverse transcription, for DNA-based or mRNA-based T-RFLP analysis. In all cases, PCR products had the expected length of ~1100 bp. In the case of *C. secundus* and *Z. nevadensis*, a second, less-abundant PCR product of ~1200 bp was formed, but only in the mRNA-based analysis. Because this product was not formed by RT-PCR with the unlabeled primer, it could not be cloned and sequenced. The product probably arose through nonspecific binding of the reverse primer during the reverse transcription reaction owing to the low annealing temperature (48 °C), which would result in a PCR product extended at the 5'-end of the coding DNA strand. However, such an extension would not be a problem because it would not affect the results of T-RFLP, which depend only on the binding site of the forward primer. This interpretation is supported by the observation that no unexpected T-RFs were present in the mRNA-based profiles (see below).

DNA-based profiles of *R. santonensis* were dominated by T-RFs assigned to the phylotypes RsI and RsII (Fig. 2), which is in good agreement with the large proportion of RsI and RsII clones in the clone library (Table 2). In the mRNA-based profiles, however, most of the T-RFs representing phylotypes RsI and RsII were relatively small. Instead, the T-RF of 138 bp was the most dominant peak (Fig. 2); it represents phylotype RsIV and two clones of phylotype RsI, which together comprise only 4% of the clones in the clone library.

The T-RFLP profiles for *C. secundus* were less complex than those for *R. santonensis* (Fig. 2), which reflects the levels of diversity in the respective clone libraries. Two of the three T-RFs in the DNA-based profiles could be assigned to the phylotype CsI, which also dominated the clone library. In contrast, the third T-RF, matching only with the predicted T-RFs of the clones Cs27 and Cs56, was severely underrepresented in the clone library (Table 2), and was also not present in the mRNA-based profiles. Here, a single T-RF representing the major subgroup of phylotype CsI was the only detectable peak (Fig. 2).

The T-RFs in the profiles of *Z. nevadensis* were assigned using the published sequence information from the study of Salmassi and Leadbetter (2003) (Table 2). DNA-based profiles showed a complexity similar to those of *R. santonensis* (Fig. 2). They were dominated by two T-RFs, one shared by the phylotypes ZaH, ZaP, and

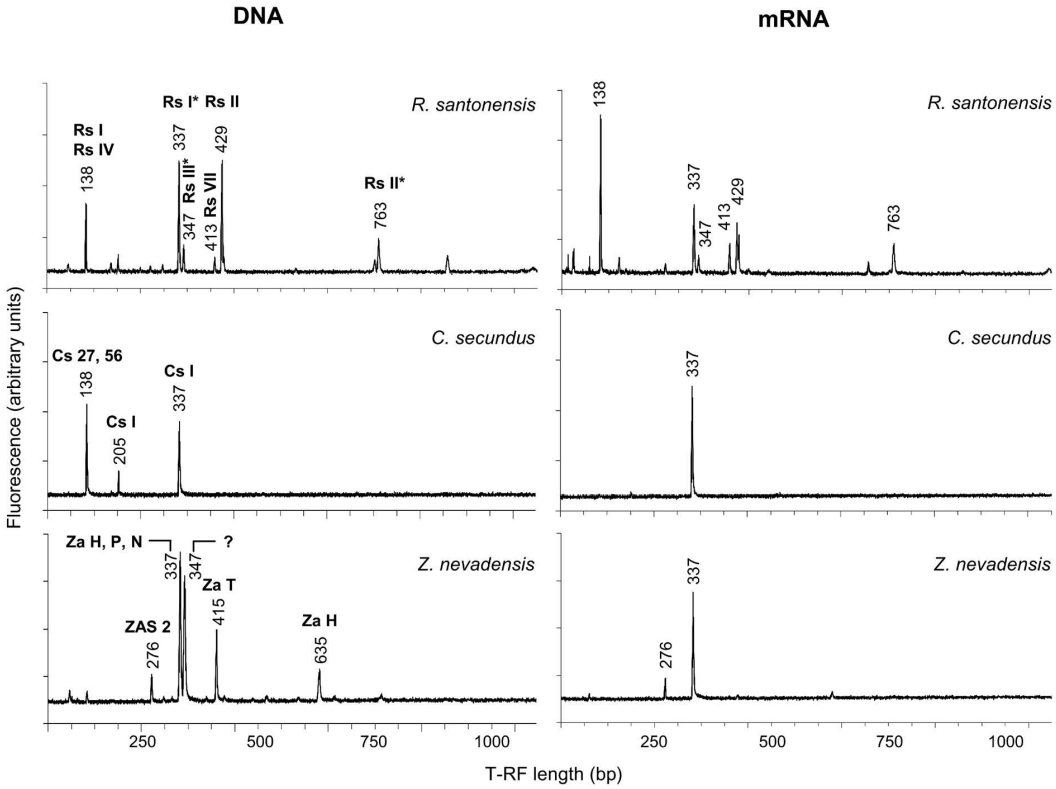

Figure 2. DNA-based and mRNA-based T-RFLP profiles of bacterial *fhs* genes from termite hindgut contents. PCR products were simultaneously digested with *Msp*I and *Rsa*I. All assignable T-RFs are labeled with the respective phylotype (Table 2; for phylogenetic positions refer to Fig. 1). T-RFs of phylotypes marked with an asterisk overlapped with those of single clones from other phylotypes (see Table 2) or, in the case of phylotype RsIII, with a potential pseudo-T-RF formed by clones in phylotype RsI. Each analysis was done in independent duplicates from the same batch of termites, which resulted in nearly identical profiles (not shown).

ZaN, and another at 347 bp. The latter could not be assigned to any phylotype and it is not a predicted pseudo-T-RF (Egert and Friedrich, 2003). Again, the complexity of the profiles decreased substantially in the mRNA-based analyses, where the T-RF assigned to the phylotypes ZaH, ZaP, and ZaN was the dominant peak. The minor peak of 276 bp could not be assigned to any clone in the clone library but matches the predicted T-RF of *T. primitia* strain ZAS-2, a homoacetogenic isolate from the closely related *Z. angusticollis*. All other T-RFs in the DNA-based profiles were not represented, including the T-RF assigned to the putatively non-homoacetogenic phylotype ZaT.

Discussion

Reductive acetogenesis is an important process in the hindgut fermentation of wood-feeding termites. The isolation of the homoacetogenic *Treponema primitia* from the hindgut of *Zootermopsis angusticollis* and the dominance of spirochete-related sequences among the formyl tetrahydrofolate synthetase genes (*fhs*) cloned from the hindgut community of *Zootermopsis nevadensis* indicated that spirochetes may contribute significantly to this activity (Leadbetter et al., 1999; Salmassi and Leadbetter, 2003).

In this study, we provide conclusive evidence that *fhs* genes from the 'Termite Treponeme' cluster are the only ones that are actively expressed in all termites investigated. This strongly supports the hypothesis that spirochetes dominate reductive acetogenesis in the hindgut of lower termites.

Our study comprised representatives of three of the six families of lower termites, namely the Rhinotermitidae (*Reticulitermes santonensis*), the Kalotermitidae (*Cryptotermes secundus*), and the Termopsidae (*Zootermopsis nevadensis*). In all species, potential rates of reductive acetogenesis, determined in gut homogenates, were slightly higher than previously published rates for closely related species (Breznak and Switzer, 1986; Brauman et al., 1992). This discrepancy is most likely not due to species-specific differences, but rather to our assays containing higher bicarbonate concentrations (10 mM) than those of previous studies (1 mM), as verified experimentally for *R. santonensis* (data not shown).

The majority of the *fhs* genes (77–98%) in the clone libraries from hindguts of *R. santonensis* and *C. secundus* (this study) and *Z. nevadensis* (Salmassi and Leadbetter, 2003) fall into a cluster that consists exclusively of sequences retrieved from the hindguts of these three termite species (Fig. 1). The fact that the cluster comprises also the *fhs* genes of the three spirochetal isolates from *Z. angusticollis*, two of which are *bona fide* homoacetogens (*Treponema primitia* strains ZAS-1 and ZAS-2), supports the hypothesis that at least some — if not the majority — of the clones in this 'Termite Treponeme' cluster originate from homoacetogenic spirochetes (Salmassi and Leadbetter, 2003).

In *R. santonensis* and *Z. nevadensis*, the most abundant phylotypes in the DNA-based T-RFLP profiles cluster together with the *fhs* gene of the homoacetogen *T. primitia* strain ZAS-2. Also in *C. secundus*, the dominating phylotypes in the T-RFLP analysis belong to the 'Termite Treponeme' cluster. However, they did not group with the dominating phylotypes in *R. santonensis* and *Z. nevadensis*, but constitute separate *fhs* lineages. This agrees with the hypothesis that the termite gut treponemes are co-evolving together with their hosts, as pointed out in a 16S-rRNA-based study (Lilburn et al., 1999), although it should be observed that the respective phylogenies of *fhs*, *nif*H, and *rrn* are not congruent for the *Treponema* strains ZAS-1, ZAS-2, and ZAS-9 (Lilburn et al., 2001; Salmassi and Leadbetter, 2003).

The number of phylotypes within the 'Termite Treponeme' cluster is considerably higher in *R. santonensis* than in *C. secundus* (this study) or *Z. nevadensis* (Salmassi and Leadbetter, 2003). Assuming that a phylotype is equivalent to a species, this indicates a higher species diversity of homoacetogenic treponemes in *R. santonensis*. A 16S-rRNA-based study detected 21 *Treponema* phylotypes in the hindgut of *Reticulitermes flavipes* (Lilburn et al., 1999), a species synonymous to *R. santonensis* (Austin et al., 2005), which is in good agreement with the 12–15 morphotypes described by Breznak and Pankratz (1977). The presence of 11 *fhs* phylotypes in *R. santonensis* suggests that a substantial portion of the treponemes in

R. santonensis are homoacetogens. A similar comparison is not possible for *Z. nevadensis* and *C. secundus* because an exhaustive analysis of the microbial diversity of their hindgut communities is lacking.

Some of the phylotypes from *Z. nevadensis* (Salmassi and Leadbetter, 2003) and a single clone from *R. santonensis* (this study) grouped loosely among the *fhs* genes of homoacetogenic Clostridiales. Their sequences differed considerably from each other and from the sequences of homoacetogenic Clostridiales, which suggests the presence of novel lineages of homoacetogenic bacteria. Although the proportion of such clones was relatively large in *Z. nevadensis* (14% of the clone library), they were not represented in the respective T-RFLP profiles. Conversely, the major T-RF at 347 bp in the DNA-based profiles could not be assigned to any phylotype in the clone library. Possibly, such discrepancies are explained by the different geographic origin of the termites used for the clone library (collected in California, USA; Salmassi and Leadbetter, 2003).

The mere presence of a marker gene in a DNA-based clone library or T-RFLP profile does not indicate that the gene is expressed. Detection of mRNA of a metabolic marker, however, documents transcription and allows conclusions on the activity of the respective pathway. Although the expression of certain genes, e.g., those coding for regulatory proteins, is also regulated at the post-transcriptional level, the mRNA levels of the majority of prokaryotic genes correlate well with the respective protein levels (reviewed by Conway and Schoolnik, 2003). Differences between DNA-based and mRNA-based T-RFLP profiles indicated that in all three termites, not all *fhs* genes are equally expressed. An extreme case is that of *C. secundus*, where only one of the phylotypes present expressed their *fhs* genes. In *R. santonensis*, the situation is completely different: all five phylotypes represented in the DNA-based profiles expressed their *fhs* genes, albeit at different levels. It remains open whether they represent co-existing species with the same kind of metabolism, i.e., reductive acetogenesis, because H_2 and CO_2 do not limit homoacetogenesis in termite guts (Ebert and Brune, 1997; Tholen and Brune, 2000). Alternatively, they may occupy different niches within the gut, either using different substrates or colonizing different microhabitats, e.g., the anoxic gut lumen or the microoxic gut periphery (Brune et al., 1995), or the surface of the protozoa (Breznak and Leadbetter, 2002).

Treponema spp. are one of the most numerous groups of bacteria in hindguts of wood-feeding termites. They represent up to 50% of all prokaryotic cells in microscope studies (Breznak, 1984; Paster et al., 1996) and dominate over other bacterial phyla in 16S-rRNA-based inventories of the hindgut community (Hongoh et al., 2003; Hongoh et al., 2005; Yang et al., 2005). At this point, it is not possible to exclude that some of the FTHFS produced by treponemes are merely involved in anabolic reactions. At least one isolate, *Treponema azotonutricium*, possesses an *fhs* gene closely related to that of homoacetogenic 'Termite Treponemes' but is not

homoacetogenic (Leadbetter et al., 1999; Graber et al., 2004). However, the high rates of reductive acetogenesis, both in gut homogenates (Brauman et al., 1992; this study) and under *in situ* conditions (Tholen and Brune, 2000, chapter 3), and the exclusive expression of *fhs* genes from the 'Termite Treponeme' cluster, lend strong support to the conclusion that at least some of the spirochetes in the 'Termite Treponeme Cluster' are responsible for reductive acetogenesis in the hindgut of lower termites.

Materials and methods

Termites

Worker termites of the wood-feeding species *Reticulitermes santonensis* (Rhinotermitidae), *Cryptotermes secundus* (Kalotermitidae), and *Zootermopsis nevadensis* (Termopsidae) were used in this study. *R. santonensis* was collected in the Forêt de la Coubre, near Royan, France, *C. secundus* stemmed from a mangrove forest near Darwin, Australia, and was kindly provided by Judith Korb. *Z. nevadensis* stemmed from Kawahishi, Japan, and was kindly provided by Ai Fujita. All termites were kept on a diet of pine wood (*Pinus silvestris* for *R. santonensis* and *Z. nevadensis*, *Pinus radiata* for *C. secundus*).

Species affiliation of the termites was checked by partially sequencing the cytochrome oxidase II gene (~700 bp, Liu and Beckenbach, 1992) and comparing it to previously published sequences using the ARB software package (http://www.arb-home.de). DNA was extracted from the respective termite heads by grinding them in liquid nitrogen, followed by extraction with the NucleoFood kit (Macherey-Nagel, Düren, Germany). Partial cytochrome oxidase II genes were then amplified by the primers C2-J-3096 (5'-AGA GCA TCA CCA ATC ATA GAA CA-3') and TK-N-3807 (5'-GTT TAA GAG ACC ATT ACT TA-3') (Thompson et al., 2000) using 4 mM $MgCl_2$ and the following PCR program: initial denaturation at 94 °C for 2 min 45 s, followed by 30 cycles of denaturation for 20 s at 94 °C, annealing for 20 s at 46 °C, and elongation for 50 s at 72 °C. The sequences of the studied termites were deposited in GenBank under the accession numbers DQ278260 to DQ278262.

$^{14}CO_2$ reduction by hindgut homogenates

Termites were dissected and hindguts (20 hindguts for *R. santonensis*, 10 hindguts for *C. secundus*, and 1 hindgut for *Z. nevadensis*) were homogenized in anoxic buffered salt solution (Breznak and Switzer, 1986) reduced with 1 mM dithiothreitol (DTT), using PVC pestles and Eppendorf tubes as mortars. Homogenates were dispensed into 2-ml glass vials and sealed with butyl rubber stoppers. The whole procedure was performed in an anoxic glove box under nitrogen (2 to 5% hydrogen); all equipment was pre-incubated in the glove box for at least 24 h. Following homogenization, the headspace in the glass vials was replaced by 100% hydrogen. Incubations were

started by adding 200 µl of an anoxic solution of $NaHCO_3$ (60 mM) in phosphate buffer (140 mM, pH 7.3, reduced with 1 mM DTT) and 50 µl of an aqueous solution of $NaH^{14}CO_3$ (1.2 mM, 2.1 MBq µmol^{-1}). The final pH of the assay was between 7.4 and 7.5, and the final concentration of total dissolved CO_2 (CO_2, HCO_3^-, and CO_3^{2-}) was 10 mM.

Vials were incubated at 30 °C on a rotary shaker (150 rpm). Samples were taken every 30 min over a period of 5 h and analyzed as described by Tholen and Brune (1999). Sample volumes were replaced by the same volume of hydrogen (1 bar).

Total nucleic acid extraction and PCR conditions

Termites were dissected and guts were placed immediately in ice-cold sodium phosphate buffer (Henckel et al., 1999), followed by a combined DNA/RNA extraction as described by Lueders et al. (2004). Samples were always placed on ice, and all steps were performed at 4 °C to prevent RNA degradation. Because of differences in gut size, nucleic acids were extracted from 20 guts of *R. santonensis*, 15 guts of *C. secundus*, and 3 guts of *Z. nevadensis*. Aliquots of the nucleic acid extracts were visualized by standard agarose gel electrophoresis to verify the quality of the extraction.

Fragments of *fhs* genes (~1100 bp) were amplified using the primers and protocol described by Leaphart and Lovell (2001), except that in the case of *R. santonensis*, no bovine serum albumin was used. The specificity of the PCR reaction was checked by standard agarose gel electrophoresis.

Clone libraries and phylogenetic analysis

Amplified *fhs* gene fragments were cloned into *Escherischia coli* cells using the TA cloning kit (Invitrogen). Clones were analyzed by RFLP using the restriction enzymes *Msp*I and *Hha*I (5 U each, Promega) and grouped according to their restriction pattern. Representatives of each group were sequenced from both strands. Sequences were checked for chimerae as described elsewhere (Pester et al., 2004) and aligned within the ARB software package (http://www.arb-home.de). A phylogenetic tree was reconstructed based on a distance matrix of deduced amino acid sequences inferred from the Dayhoff PAM 001 matrix as amino acid replacement model (Dayhoff et al., 1978). The tree was inferred from the distance matrix using the Fitch algorithm (Kimura, 1983) with global rearrangement and randomized input order of sequences, as implemented in ARB. Tree reconstruction, using the distance-based neighbor joining (Saitou and Nei, 1987) or the maximum-likelihood algorithm based on Dayhoff et al. (1978) as implemented in ARB, resulted in dendrograms with similar topology. All cloned sequences were deposited with GenBank under the accession numbers DQ278201 to DQ278259.

T-RFLP analysis

T-RFLP analysis was performed as described previously (Pester et al., 2004), using the nucleic acid extraction method and PCR conditions as described above, except that the forward primer was labeled with a fluorescent dye (IRD 700, pentamethine carbocyanine; MWG Biotech) and the number of PCR cycles was reduced to 26 (the minimum number of cycles yielding enough product for T-RFLP analysis). PCR products were digested simultaneously with the restriction endonucleases *Msp*I and *Rsa*I (3 U each; Fermentas), which gave the best resolution among the different clone groups and cultured homoacetogens in a computer analysis (data not shown). Great care was taken to avoid over-saturated T-RF signals, which would affect relative peak heights. If necessary, samples of the restriction digestion were diluted and analyzed again. Lengths of terminal restriction fragments (T-RFs) were calculated by comparison with molecular size markers (50–700 bp, LI-COR) and with selected *fhs* clones representing the major T-RFs, using the Gel-Pro Analyzer software (version 4.5, MediaCybernetics). The same clones were also analyzed for pseudo-T-RF formation (Egert and Friedrich, 2003).

Analysis of *fhs* gene expression

Total nucleic acid extracts were digested with RQ1 RNase-free DNase (1 U, Promega) as recommended by the manufacturer and used directly as template in RT-PCR reactions. RT-PCR was performed using the Access RT-PCR System kit (Promega) in 50 µl reactions. Each reaction contained 1× reaction buffer, 1 mM $MgSO_4$, 200 µM of each dNTP, 0.6 µM of fluorescently labeled forward primer (Leaphart and Lovell, 2001; IRD700, MWG Biotech), 0.6 µM of reverse primer (Leaphart and Lovell, 2001), 5 U of AMV reverse transcriptase, 5 U of *Tfl* DNA Polymerase, and 2 µl of the RNA extract. In the case of *C. secundus* and *Z. nevadensis*, 0.4 mg ml^{-1} bovine serum albumin were added. Thermal cycling started with reverse transcription for 45 min at 48 °C, immediately followed by an initial denaturation for 2 min at 94 °C, and proceeded in two phases: 9 cycles of a touchdown program (30 s at 94 °C, 1 min at 63 °C, decreasing 1 °C per cycle, and 2 min at 68 °C), followed by 17 cycles of a standard program (annealing temperature at 55 °C). The final extension step was 7 min at 68 °C. In all cases, parallel assays without AMV reverse transcriptase did not result in a PCR product, showing that the template was free of contaminating DNA. RT-PCR products were checked for the specificity of the PCR reaction by standard agarose gel electrophoresis and were further analyzed by T-RFLP as described above.

Acknowledgements

We thank Jared R. Leadbetter for sharing unpublished data and for critical comments on a previous version of this manuscript, Judith Korb and Ai Fujita for providing termites, and Katja Meuser for technical assistance.

References

1. Austin, J. W., Szalanski, A. L., Scheffrahn, R. H., Messenger, M. T., Dronnet, S., and Bagnères, A.-G. (2005) Genetic evidence for the synonymy of two *Reticulitermes* species: *Reticulitermes flavipes and Reticulitermes santonensis*. *Ann. Entomol. Soc. Amer.* 98: 395–401.

2. Boga, H. I., Ludwig, W., and Brune, A. (2003) *Sporomusa aerivorans* sp. nov., an oxygen-reducing homoacetogenic bacterium from the gut of a soil-feeding termite. *Int. J. Syst. Evol. Microbiol.* 53: 1397–1404

3. Brauman, A., Kane, M. D., Labat, M., and Breznak, J. A. (1992) Genesis of acetate and methane by gut bacteria of nutritionally diverse termites. *Science* 257: 1384–1387.

4. Breznak, J. A., and Leadbetter, J. R. (2002) Termite gut spirochetes. In *The Prokaryotes: An Evolving Electronic Resource for the Microbiological Community*. 3rd edition, release 3.10. Dworkin, M., Falkow, S., Rosenberg, E., Schleifer, K.-H. & Stackebrandt, E., (eds). New York: Springer-Verlag. http://link.springer-ny.com/link/service/books/10125/

5. Breznak, J.A. (1984) Hindgut spirochetes of termites and *Cryptocercus punctulatus*. In *Bergey's Manual of Systematic Bacteriology*. Krieg, N.R., and Holt, J.G. (eds). Baltimore: Williams & Wilkins, pp. 67–70.

6. Breznak, J. A., and Switzer, J. M. (1986) Acetate synthesis from H_2 plus CO_2 by termite gut microbes. *Appl. Environ. Microbiol.* 52: 623–630.

7. Breznak, J. A., Switzer, J. M., and Seitz, H. J. (1988) *Sporomusa termitida* sp. nov., an H_2/CO_2-utilizing acetogen isolated from termites. *Arch. Microbiol.* 150: 282–288

8. Breznak, J. A., and Pankratz, H. S. (1977) In situ morphology of the gut microbiota of wood-eating termites [*Reticulitermes flavipes* (Kollar) and *Coptotermes formosanus* Shiraki]. *Appl. Environ. Microbiol.* 33: 406–426.

9. Brune, A. (2006) Symbiotic associations between termites and prokaryotes. In *The Prokaryotes, 3rd edn., Vol. 1: Symbiotic Associations, Biotechnology, Applied Microbiology*, Dworkin, M., Falkow, S., Rosenberg, E., Schleifer, K.-H. and Stackebrandt, E., (eds). New York: Springer-Verlag. http://link.springer-ny.com/link/service/books/10125/

10. Brune, A., Emerson, D., Breznak, J. A. (1995) The termite gut microflora as an oxygen sink: microelectrode determination of oxygen and pH gradients in guts of lower and higher termites. *Appl. Environ. Microbiol.* 61: 2681–2687.

11. Cheng, Y. S., Halsey, J. L., Fode, K. A., Remsen, C. C., and Collins, M. L. (1999) Detection of methanotrophs in groundwater by PCR. *Appl. Environ. Microbiol* 65: 648–651.

12. Conway, T., and Schoolnik, G. K. (2003) Microarray expression profiling: capturing a genome-wide portrait of the transcriptome. *Mol. Microbiol.* 47: 879–889.

13. Dayhoff, M. O., Schwartz, R. M., and Orcull, B. C. (1978) A model of evolutionary change in proteins. In *Atlas of Protein Sequence and Structure*. Dayhoff, M.O. (ed). Silver Spring, Md: National Biomedical Research Foundation, pp. 345–352.

14. Drake, H. L., Küsel, K., and Matthies, C. (2001) Acetogenic Prokaryotes. In *The Prokaryotes: An Evolving Electronic Resource for the Microbiological Community, 3rd edn.* Dworkin, M., Falkow, S., Rosenberg, E., Schleifer, K.-H. and Stackebrandt, E., (eds). New-York: Springer-Verlag. http://link.springer-ny.com/link/service/books/10125/

15. Ebert, A., and Brune, A. (1997) Hydrogen concentration profiles at the oxic-anoxic interface: a microsensor study of the hindgut of the wood-feeding lower termite *Reticulitermes flavipes* (Kollar). *Appl. Environ. Microbiol.* 63: 4039–4046.

16. Egert, M., and Friedrich, M. W. (2003) Formation of pseudo-terminal restriction fragments, a PCR-related bias affecting terminal restriction fragment length polymorphism analysis of microbial community structure. *Appl. Environ. Microbiol.* 69: 2555–2562.

17. Graber, J. R., and Breznak, J. A. (2004) Physiology and nutrition of *Treponema primitia*, an H_2/CO_2-acetogenic spirochete from termite hindguts. *Appl. Environ. Microbiol.* 70: 1307–1314.

18. Graber, J. R., Leadbetter, J. R., and Breznak, J. A. (2004) Description of *Treponema azotonutricium* sp. nov. and *Treponema primitia* sp. nov., the first spirochetes isolated from termite guts. *Appl. Environ. Microbiol.* 70: 1315–1320

19. Henckel, T., Friedrich, M., and Conrad, R. (1999) Molecular analyses of the methane-oxidizing microbial community in rice field soil by targeting the genes of the 16S rRNA, particulate methane monooxygenase, and methanol dehydrogenase. *Appl. Environ. Microbiol.* 65: 1980–1990.

20. Hongoh, Y., Deevong, P., Inoue, T., Moriya, S., Trakulnaleamsai, S., Ohkuma, M., Vongkaluang, C., Noparatnaraporn, N., and Kudo, T. (2005) Intra- and interspecific comparisons of bacterial diversity and community structure support coevolution of gut microbiota and termite host. *Appl. Environ. Microbiol.* 71: 6590–6599.

21. Hongoh, Y., Ohkuma, M., and Kudo, T. (2003) Molecular analysis of bacterial microbiota in the gut of the termite *Reticulitermes speratus* (Isoptera; Rhinotermitidae). *FEMS Microbiol. Ecol.* 44: 231–242.

22. Kane, M. D., and Breznak, J. A. (1991) *Acetonema longum* gen. nov. sp. nov., an H_2/CO_2 acetogenic bacterium from the termite, *Pterotermes occidentis*. *Arch. Microbiol.* 156: 91–98.

23. Kane, M. D., Brauman, A., and Breznak, J. A. (1991) *Clostridium mayombei* sp. nov., an H_2/CO_2 acetogenic bacterium from the gut of the African soil-feeding termite, *Cubitermes speciosus*. *Arch. Microbiol.* 156: 99–104

24. Kimura, M. (1983) The neutral theory of molecular evolution. In *Evolution of genes and proteins*. Nei, M., and Koehn, R.K. (eds). Sunderland, Mass.: Sinauer, pp. 208–233.

25. Leadbetter, J. R., Schmidt, T. M., Graber, J. R., and Breznak, J. A. (1999) Acetogenesis from H_2 plus CO_2 by spirochetes from termite guts. *Science* 283: 686–689.

26. Leaphart, A.B., and Lovell, C.R. (2001) Recovery and analysis of formyltetrahydrofolate synthetase gene sequences from natural populations of acetogenic bacteria. *Appl. Environ. Microbiol.* 67: 1392–1395.

27. Leaphart, A. B., Friez, M. J., and Lovell, C. R. (2003) Formyltetrahydrofolate synthetase sequences from salt marsh plant roots reveal a diversity of acetogenic bacteria and other bacterial functional groups. *Appl. Environ. Microbiol.* 69: 693–696

28. Lilburn, T. G., Kim, K. S., Ostrom, N. E., Byzek, K. R., Leadbetter, J. R., and Breznak, J. A. (2001) Nitrogen fixation by symbiotic and free-living spirochetes. *Science* 292: 2495–2498.

29. Lilburn, T. G., Schmidt, T. M., and Breznak, J. A. (1999) Phylogenetic diversity of termite gut spirochaetes. *Environ. Microbiol.* 1: 331–345.

30. Liu, H., and Beckenbach, A. T. (1992) Evolution of the mitochondrial cytochrome oxidase II gene among 10 orders of insects. *Mol. Phylogenet. Evol.* 1: 41–52.

31. Lueders, T., Manefield, M., and Friedrich, M. W. (2004) Enhanced sensitivity of DNA- and rRNA-based stable isotope probing by fractionation and quantitative analysis of isopycnic centrifugation gradients. *Environ. Microbiol.* 6: 73–78.

32. Noda, S., Ohkuma, M., Usami. R., Horikoshi K, and Kudo, T. (1999) Culture-independent characterization of a gene responsible for nitrogen fixation in the symbiotic microbial community in the gut of the termite *Neotermes koshunensis*. *Appl. Environ. Microbiol.* 65: 4935–4942.

33. Nogales, B., Timmis, K. N., Nedwell, D. B., and Osborn, A. M. (2002) Detection and diversity of expressed denitrification genes in estuarine sediments after reverse transcription-PCR amplification from mRNA. *Appl. Envir. Microbiol* 68: 5017–5025.

34. Odelson, D. A., and Breznak, J. A. (1983) Volatile fatty acid production by the hindgut microbiota of xylophagous termites. *Appl. Environ. Microbiol.* 45: 1602–1613

35. Paster, B. J., Dewhirst, F. E., Cooke, S. M., Fussing, V., Poulsen, L. K., and Breznak, J. A. (1996) Phylogeny of not-yet-cultured spirochetes from termite guts. *Appl. Environ. Microbiol.* 62: 347–352.

36. Pester, M., Friedrich, M. W., Schink, B., and Brune, A. (2004) *pmoA*-based analysis of methanotrophs in a littoral lake sediment reveals a diverse and stable community in a dynamic environment. *Appl. Environ. Microbiol.* 70: 3138–3142.

37. Saitou, N., and Nei, M. (1987) The neighbour-joining-method – a new method for reconstructing phylogenetic trees. *Mol. Biol. Evol.* 4: 406–425.

38. Salmassi, T.M., and Leadbetter, J.R. (2003) Molecular aspects of CO_2-reductive acetogenesis in cultivated spirochetes and the gut community of the termite *Zootermopsis angusticollis*. *Microbiology* 149: 2529–2537

39. Schink, B., and Bomar, M. (1992) The genera *Acetobacterium*, *Acetogenium*, *Acetoanaerobium* and *Acetitomaculum*. In *The Prokaryotes, 2nd edn.* Balows A., Trüper H. G., Dworkin M., Harder W., and Schleifer K.-H., (eds). New York: Springer-Verlag. pp. 1925–1936. http://link.springer-ny.com/link/service/books/10125/

40. Tholen, A., and Brune, A. (1999) Localization and in situ activities of homoacetogenic bacteria in the highly compartmentalized hindgut of soil-feeding higher termites (*Cubitermes* spp.). *Appl. Environ. Microbiol.* 65: 4497–4505.

41. Tholen, A., and Brune, A. (2000) Impact of oxygen on metabolic fluxes and in situ rates of reductive acetogenesis in the hindgut of the wood-feeding termite *Reticulitermes flavipes*. *Environ. Microbiol.* 2: 436–449.

42. Thompson, G. J., Miller, L. R., Lenz, M., and Crozier, R. H. (2000) Phylogenetic analysis and trait evolution in Australian lineages of drywood termites (Isoptera, Kalotermitidae). *Mol. Phylogenet. Evol.* 17: 419–429.

43. Thorne, B., and Haverty, M. (1989) Accurate identification of *Zootermopsis* species (Isoptera Termopsidae) based on a mandibular character of nonsoldier castes. *Ann. Entomol. Soc. Am.* 82: 262–266.

44. Wilson, M. S., Bakermans, C., and Madsen, E. L. (1999) In situ, real-time catabolic gene expression: extraction and characterization of naphthalene dioxygenase mRNA transcripts from groundwater. *Appl. Envir. Microbiol.* 65: 80–87.

45. Wood, T. G. (1978) The role of termites (Isoptera) in decomposition processes. In *The role of terrestrial and aquatic organisms in decomposition processes*. Anderson, J. M, and Macfayden, A. (eds). Oxford: Blackwell, pp. 145–168.

46. Wood, T. G., and Johnson, R. A. (1986) The biology, physiology and ecology of termites. In *Economic Impact and Control of Social Insects*. Vinson, S. B. (ed). New York, USA: Praeger, pp. 1–68.

47. Yang, H., Schmitt-Wagner, D., Stingl, U., and Brune, A. (2005) Niche heterogeneity determines bacterial community structure in the termite gut (*Reticulitermes santonensis*). *Environ. Microbiol.* 7: 916–932.

48. Zani, S., Mellon, M. T., Collier, J. L., and Zehr, J. P. (2000) Expression of *nifH* genes in natural microbial assemblages in Lake George, New York, detected by reverse transcriptase PCR. *Appl. Environ. Microbiol.* 66: 3119–3124.

6 Supporting material

Hindgut metabolite pools in vivo compared to embedded guts

Hindgut metabolite pools of freshly dissected termites (referred to as in vivo) were compared to metabolite pools of hindguts embedded in agarose-solidified insect Ringer's solution (Brune et al., 1995) at different time points of incubation. These experiments were mainly flanking the microinjection experiments described in chapter 3 to find out to which extend pool sizes differ in vivo compared to embedded, dissected guts, and how pool sizes develop over time in embedded, dissected guts. To make correct estimations of the substrate turnover rate and the product turnover rates, it was of importance to know the exact pool size of a respective metabolite at the time point of injection, which was generally 10 min after guts were embedded (for details refer to chapter 2).

Great care was taken that only hindguts were used for pool size determination without any contamination by parts of the midgut. Detection of total CO_2 (CO_2, HCO_3^-, and CO_3^{2-}) was performed by flow injection analysis (FIA) coupled to a conductivity detector and detection of glucose, succinate, malate, lactate, and formate was done by HPLC analysis coupled to a refractive index detector (for details see chapter 3).

The main results are summarized in Table 1 and Table 2. In general, pool sizes were different under in vivo conditions compared to embedded guts and differed also in embedded guts over time. For total CO_2, a decrease of the pool size over time was observed in embedded guts of the three investigated termites *Reticulitermes santonensis*, *Zootermopsis nevadensis*, and *Cryptotermes secundus* (Table 1). For *R. santonensis*, where the pool size was determined at three different time points, this decrease could be modeled by a linear regression curve (data not shown). The CO_2 pools of the other two termites for which only two time points were sampled showed a similar trend and were assumed to behave the same.

Table 1. Change of total CO_2 pools (CO_2, CO_3^-, and CO_3^{2-}) in termite hindguts embedded in agarose and insect Ringer's solution over time.

Termite	CO_2 pool (nmol hindgut^{-1}) [a]		
	0 min (in vivo)	15 min	30 min
Reticulitermes santonensis	10.6 ± 0.7	6.9 ± 2.1	4.3 ± 0.6
Zootermopsis nevadensis	113.7 ± 33.8	39.1 ± 13.9	n. m. [a]
Cryptotermes secundus	56.4 ± 6.8	35.0 ± 3.9	n. m. [a]

a. At least three or more independent measurements were used for determinations of averages and standard deviations.
b. Not measured.

Table 2. Hindgut metabolite pools in vivo in comparison to hindgut metabolite pools in dissected guts embedded in agarose-solidified insect Ringer's solution after different time points of incubation.

Incubation time	Pool size (nmol hindgut^{-1}) [a]				
	Glucose	Succinate	Malate	Lactate	Formate
Reticulitermes santonensis					
0 min (in vivo)	2.4 ± 0.8	0.4 ± 0.1	0.1 ± 0.0	0.4 ± 0.0	1.7 ± 0.6
10 min	0.1 ± 0.2 [b]	0.4 ± 0.0	< 0.02	0.2 ± 0.1	1.6 ± 0.1
40 min [b]	< 0.02	0.2 ± 0.0	< 0.02	0.2 ± 0.0	2.8 ± 0.0
Zootermopsis nevadensis					
0 min (in vivo)	6.0 ± 1.6	10.3 ± 4.8	0.3 ± 0.2	2.1 ± 1.2	26.4 ± 4.8
10 min	2.7 ± 1.3	4.8 ± 0.9	2.5 ± 1.6	3.2 ± 0.5	4.7 ± 2.9
30 min	1.1± 0.3	4.6 ± 0.9	0.6 ± 0.4	0.8 ± 0.4	9.7 ± 3.5
Cryptotermes secundus					
0 min (in vivo) [b]	0.1 ± 0.1	0.2 ± 0.0	n. m. [c]	4.1 ± 1.8	1.1 ± 0.8
10 min [b]	0.1 ± 0.2	0.1 ± 0.0	0.4 ± 0.1	1.9 ± 1.7	0.8 ± 0.3
30 min [b]	0.5 ± 0.3	0.4 ± 0.1	< 0.02	1.5 ± 1.2	< 0.02

a. At least three or more independent measurements were used for determinations of averages and standard deviations. The detection limit was 0.02 nmol.
b. Mean and range of two independent measurements.
c. Not measured.

Table 3. Hindgut metabolite pools in vivo in comparison to hindgut metabolite pools of termites immobilized on ice or dissected after 5 min incubation in an anoxic chamber with an atmosphere of 95% N_2/5% H_2.

Incubation condition	Pool size (nmol hindgut^{-1}) [a]				
	Glucose	Succinate	Malate	Lactate	Formate
Reticulitermes santonensis					
In vivo [b]	2.4 ± 0.8	0.4 ± 0.1	0.1 ± 0.0	0.4 ± 0.0	1.7 ± 0.6
Ice	1.4 ± 0.1	0.3 ± 0.0	0.0 ± 0.0	0.3 ± 0.1	1.9 ± 0.5
Anoxic	7.3 ± 1.5	0.8 ± 0.1	0.1 ± 0.1	1.3 ± 0.3	< 0.02
Zootermopsis nevadensis					
In vivo [b]	6.0 ± 1.6	10.3 ± 4.8	0.3 ± 0.2	2.1 ± 1.2	26.4 ± 4.8
Ice [c]	29.9 ± 10.7	8.4 ± 2.6	0.5 ± 0.3	1.7 ± 0.4	22.0 ± 9.6
Anoxic	88.3 ± 37.1	8.6 ± 3.6	2.0 ± 1.3	13.1 ± 2.7	< 0.02

a. At least three or more independent measurements were used for determinations of averages and standard deviations. The detection limit was 0.02 nmol.
b. Data from Table 2.
c. Mean and range of two independent measurements.

For the remaining investigated metabolites, no clear trend was observed (Table 2). For example, in the case of lactate, which was analyzed by microinjection for *R. santonensis* and *C. secundus* in chapter 3, after 10 min of incubation the pool was half the size of the pool in vivo but remained constant thereafter. Formate, which was also analyzed by microinjection for the same two termites, behaved differently. Here the pool size stayed constant for the first ten minutes after embedding but was double as high after 40 min incubation in *R. santonensis* or was substantially decreased after 30 min incubation in *C. secundus*.

Pool sizes were also determined for termites immobilized on ice and for termites incubated for 5 min in an anoxic chamber containing an atmosphere of 95% N_2/5% H_2 (Table 3). The reason for these additional pool determinations were that termites, which are immobilized on ice, are easier to handle for dissection and that microinjection experiments were also planned under an anoxic atmosphere. In general, pool sizes under in vivo conditions and for termites dissected on ice were quite similar. The only exception was glucose, which showed pronounced differences in pool sizes under both conditions. Dissection of termites under anoxic conditions, where a change of metabolite pools due to the absence of inward diffusing oxygen is expected (Brune et al., 1995), revealed different trends of change for different metabolites. For example, pools of glucose and lactate increased under anoxic conditions, whereas the pool of formate decreased.

In conclusion, these experiments show that when performing microinjection experiments, it is important to determine the actual pool sizes at the time point of injection. This has important implications on the calculated turnover and formation rates, e.g., in the case of *C. secundus*, the rate of reductive acetogenesis would be three times larger when using the in vivo CO_2 pool simply because the turnover of label is mirrored onto a much larger pool than it is in reality. In this particular case, the overestimated rate of reductive acetogenesis would equal to almost 100% of the carbon flow through the termite and demonstrates how unrealistic such a determination would be. Of course, it would be ideal if pool sizes stayed constant over time, with influxes and effluxes in equilibrium. However, although this criterion cannot be fully met using dissected, embedded guts, the gut itself as the habitat of the intestinal microbiota stays absolutely intact as exemplified by the steep oxygen (Brune et al., 1995) and hydrogen gradients (Ebert and Brune, 1997; chapter 3) within the hindgut. In contrast, any alternative approach to measure turnover rates, e.g., homogenization, would destroy these gradients. Given the necessary precaution, i.e., calculation of the turnover rates based on data obtained shortly after injection (5–10 min), the effect of changing pools can be minimized, and agarose-embedded guts still provide the best model system to study metabolite fluxes in the termite hindgut.

Microinjection of malate and succinate

Comparison of the total carbon and electron balances in the hindgut (using the rates of the so far identified processes) revealed that a small part of the total carbon flow might still proceed through processes that are not yet accounted for (chapter 3). This raised the question, whether a minor portion of the carbon flow proceeds through additional metabolite pools like those of malate and succinate and how these intermediates are metabolized.

The role of malate and succinate was studied using microinjection as described in chapter 3 and in more detail in chapter 2. In the case of malate, 50 nl of L-(U-^{14}C)-malic acid with a specific radioactivity of 1.9 MBq μmol^{-1} was injected per gut. Due to the small malate pool at time point of injection (0.01 nmol hindgut^{-1}, Table 2), the injected amount of malate (0.19 nmol) exceeded the internal pool severalfold resulting in a quasi-constant specific radioactivity of malate in the initial phase of the experiment. In the case of succinate, 90 nl of (2,3-^{14}C)-succinic acid with a specific radioactivity of 3.1 MBq μmol^{-1} was injected per gut. Here, the succinate pool at time point of injection (0.42 nmol hindgut^{-1}, Table 2) was not considerably changed by the injected succinate (0.10 nmol).

Malate was rapidly consumed within the first five minutes after injection but thereafter turnover abruptly stopped with the result that the amount of remaining labeled malate stayed constant over time. The same result was obtained for the products acetate and CO_2, which resulted from the conversion of malate. Within the first five minutes after injection, label accumulated in both products but stayed thereafter constant (Fig. 1-A1). Interestingly, the decrease of label in the malate pool could not be explained by the sum of label recovered in the single products with a recovery gap approximating 50%. However, the total recovery of radioactivity as determined by liquid scintillation counting was after five minutes of incubation quite complete with a recovery of more than 80% (Fig. 1-A2). This imbalance indicates that one or more degradation product of malate were not detected by the analytical methods used.

A similar situation was observed after microinjection of labeled succinate. Also here, succinate was rapidly consumed within the first five minutes after injection with no turnover thereafter, resulting in a stable amount of label in the succinate pool. The sequence of product formation is more complex than in the case of malate. Overall, propionate, acetate, formate, and CO_2 resulted from succinate degradation. However, formation of these products was not simultaneously but in sequence. The first product accumulating was propionate with a slight decrease of label in its pool after five minutes of incubation. Formation of acetate was slightly shifted to the formation of propionate with no additional accumulation of label in its pool after five minutes of incubation. After 15 min of incubation label started accumulating in the formate pool. The amount of label entering the CO_2 pool was very small (Fig. 1-B1). As in the case of malate, the amount of label leaving the succinate pool within

the first five minutes of incubation could not be recovered by the sum of label in the single detected products. At the same time, total recovery of radioactivity was above 80% (Fig. 1-B2), again indicating that one or more degradation product of succinate were not detected by the analytical methods used.

In conclusion, the microinjection experiments of malate and succinate could not be explained by the label-dilution model described in chapter 2. In both cases, an abrupt cessation of substrate turnover during the first five minutes of incubation was observed. There is presently no obvious explanation for this phenomenon. One might argue that the microorganisms responsible for the turnover of malate or succinate, respectively, died or became inactive within the first five minutes of incubation. However, this stays in contrast to the successful microinjection experiments using CO_2, formate, and lactate (chapter 3), which suggest that the

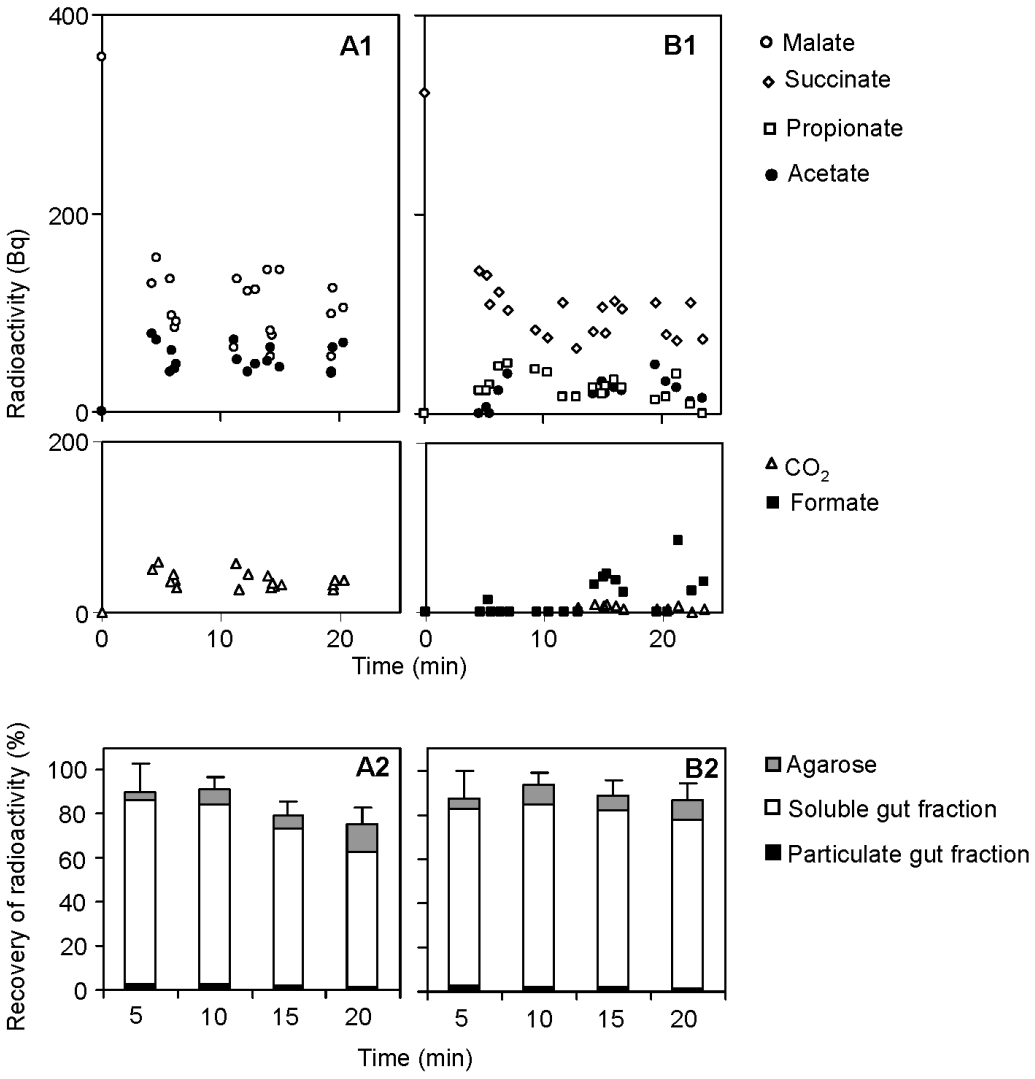

Figure 1. Microinjection of ^{14}C-labeled malate (A1) and ^{14}C-labeled succinate (B1) into hindguts of *R santonensis*. The recovery of total radioactivity around the indicated time points is given below for each experiment (A2 and B2, respectively).

integrity and the functioning of the hindgut community is given. Although a quantitative analysis of the malate and succinate microinjection experiments is not possible, they are still valuable because they show to which products both substrates are metabolized under in situ conditions. As described above, malate is degraded to acetate and CO_2, which indicates a turnover in the hydrogenosomes of the hindgut protozoa (for a detailed discussion see chapter 7). However, one should keep in mind that one or more degradation products of malate might not have been detected. In the case of succinate, an initial turnover to propionate was observed, which was accompanied by a slightly delayed formation of acetate either from succinate or from propionate or even from both. The formation of formate started relatively late after 15 min of incubation indicating that it originated from one of the intermediate products but not from succinate directly. As in the case of malate, one or more degradation products of succinate might not have been detected as indicated by the imbalance of recovery of total radioactivity compared to the sum of radioactivity in the single detected products.

Construction of polyribonucleotide probes targeting *fhs*-mRNA

Termite hindgut community studies that analyzed the phylogeny and transcription of the *fhs* gene, which encodes the formyl tetrahydrofolate synthetase, identified spirochetes of the genus Treponema as the dominating and exclusively active

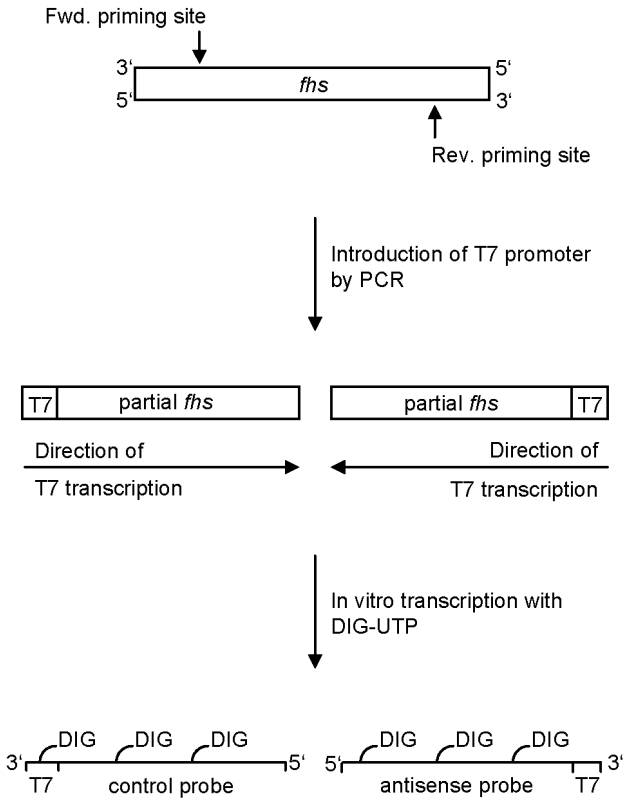

Figure 2. Flow diagram of polyribonucleotide probe synthesis.

homoacetogens in lower termites (chapter 5). To add further robustness to this finding, a co-localization of these spirochetes together with their respective *fhs* genes is desirable. Also a localization of the homoacetogens within the structured environment of the hindgut would provide important information. Combining mRNA-targeted fluorescent in situ hybridization (mRNA-FISH) of *fhs* genes that belong to the so-called "Termite Treponeme cluster" with 16S rRNA FISH would provide this missing information. This technique has been previously successfully applied to identify symbiotic methanotrophs in the hydrothermal vent mussel *Bathymodiolus puteoserpentis* by detection of mRNA of the particulate methane monooxygenase (Pernthaler and Amann, 2004). In the following, construction of a polyribonucleotide probe that targets *fhs*-mRNA of *Acetobacterium woodii*, which is used as a model organism to establish this method, is described.

The synthesis of polyribonucleotide probe is performed by in vitro transcription that requires a purified linear DNA template, which is preceded by a RNA polymerase promoter (Fig. 2). This linear DNA template was synthesized by PCR using the primers and PCR conditions targeting the *fhs* gene as described in chapter 5 (Fig. 3). The only exception was that either the forward primer or the reverse primer was modified by an extension of the 5'-end with a short sequence containing the T7 RNA polymerase promoter (5'-GGA TCC **TAA TAC GAC TCA CTA TAG GN**$_{(20\text{-}21)}$-3', T7 promoter is given in bold). PCR products, where the T7 promoter was introduced at the reverse priming site, were used for synthesis of the antisense probe. PCR products, where the T7 promoter was introduced at the forward priming site, were used for synthesis of the sense probe, which serves as control in the

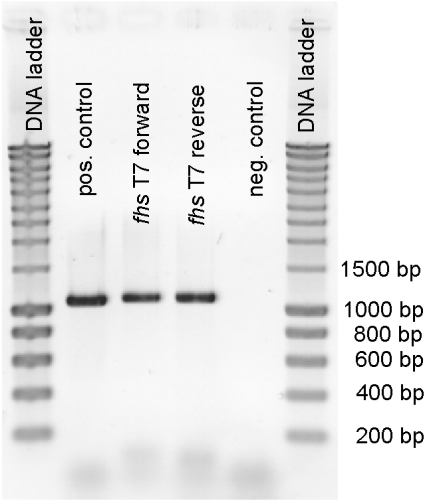

Figure 3. PCR targeting the *fhs* gene of *Acetobacterium woodii* with (i) the conventional *fhs* primers described in chapter 5 (pos. control), (ii) the T7-promoter elongated forward primer + the conventional reverse primer (*fhs* T7 forward), (iii) the conventional forward primer + the T7-promoter elongated reverse primer (*fhs* T7 reverse), (iv) and the conventional primers but no template (neg. control). Note the slightly larger PCR products resulting from the elongated primers in comparison to the positive control.

hybridization reaction. As template, genomic DNA of *Acetobacterium woodii* was used, which was obtained by three cycles of freezing 2 ml of a culture in the stationary phase in liquid nitrogen and subsequent thawing at 65°C.

To obtain enough template DNA for the in vitro transcription (1–2 µg DNA), several PCR reactions were combined and subsequently purified and concentrated by a PCR purification kit (QIAquick PCR purification kit, Qiagen, Hilden, Germany). Usually, it was necessary to combine the purified PCR products and concentrate them in a second round using the same kit to obtain a desirable template concentration. Subsequently, in vitro transcription was performed in a 20-µl reaction at 37 °C using a PCR cycler and the following reactants: 1 × transcription buffer (Promega, Mannheim, Germany), 10 mM DTT, 40 units recombinant RNasin® ribonuclease inhibitor (Promega), rNTP mix (Promega) with 0.25 mM of each NTP, except UTP, which was mixed with digoxigenin-labeled UTP in a ratio of 1:1 or 2:1 (Roche Applied Science, Mannheim, Germany), 2 µg DNA template, 20 units T7 RNA polymerase, and nuclease-free water (Sigma, Munich, Germany). After 4 h, in vitro transcription was stopped by addition of 1 unit DNase (Promega) to the reaction mixture and a further incubation at 37 °C for 15 min. The success of in vitro transcription was checked by loading 5 µl of the transcription reaction onto a 1% agarose gel and subsequent electrophoresis (Fig. 4). The remaining reaction mixture was stored in the meantime at -20°C.

Upon successful in vitro transcription, polyribonucleotide probes were purified using the following procedure. RNA was precipitated by a mixture of 0.5 volumes 7.5 M ammonium acetate, which was prepared with nuclease-free water, and 2.5 volumes of 100% ethanol. After mixing, the precipitation reaction was incubated at

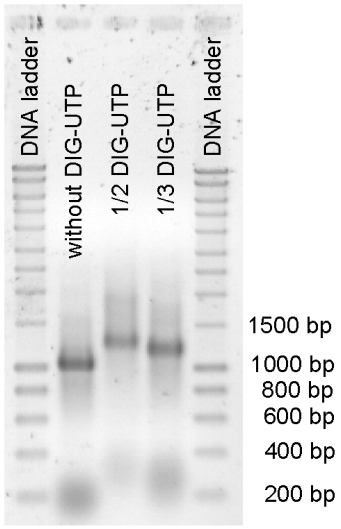

Figure 4. In vitro transcription of the partial *fhs* gene that was extended at the reverse primer binding site by the T7 RNA polymerase promoter with (i) unlabeled UTP, (ii) a mixture of unlabeled UTP and digoxigenin labeled UTP (DIG-UTP) in a ratio of 1:1, and (iii) a mixture of unlabeled UTP and DIG-UTP in a ratio 2:1. Note the decreasing mobility of transcripts with increasing amount of incorporated digoxigenin.

-70 °C for 30 min and RNA was subsequently pelleted by centrifugation (4 °C, 20.000 × g, 20 min). The supernatant was carefully removed and the pellet washed with 70% ethanol. After another centrifugation step (4 °C, 20.000 × g, 5 min), the supernatant was again carefully removed and the pellet was dried under a hood or next to a Bunsen burner (ideally not longer than 5 min). The dried pellet was dissolved in 20 µl nuclease-free water and the concentration of the produced probe stock solution was determined photometrically. The last step was a dilution of the stock solution to a working concentration of 10 ng μl^{-1} with nuclease-free water and storage in 10 µl aliquots at -70°C.

Future work will use the constructed probes to establish the mRNA-FISH method using first genetically transformed *Escherichia coli*, which harbor the partial *fhs* gene on a plasmid under the control of an inducible promoter, e.g., the pBAD TOPO® vector (Invitrogen, Karlsruhe, Germany), and later the homoacetogenic bacteria *A. woodii* and *Treponema primitia* in their exponential growth phase. Once the method is established, probes targeting the "Termite Treponeme cluster" can be constructed using clones obtained in the study described in chapter 5. Since it is expected that not all spirochetes in the termite hindgut are homoacetogens and therefore the mRNA of these spirochetes will not hybridize with *fhs*-probes of the "Termite Treponeme cluster", it would be desirable to distinguish homoacetogenic and non-homoacetogenic spirochetes also by 16S rRNA specific probes to get information about their phylogeny. Alternatively, microorganisms, which hybridize with the *fhs*-probes of the "Termite Treponeme cluster" could be separated from other microorganisms using a cell sorter. A subsequent 16S rRNA gene based clone library of the separated homoacetogens would reveal their phylogeny as well.

References

1. Brune, A., Emerson, D., and Breznak, J. A. (1995) The termite gut microflora as an oxygen sink: microelectrode determination of oxygen and pH gradients in guts of lower and higher termites. *Appl. Environ. Microbiol.* 61: 2681–2687.
2. Ebert, A., and Brune, A. (1997) Hydrogen concentration profiles at the oxic-anoxic interface: a microsensor study of the hindgut of the wood-feeding lower termite *Reticulitermes flavipes* (Kollar). *Appl. Environ. Microbiol.* 63: 4039–4046.
3. Pernthaler, A., and Amann, R. (2004) Simultaneous fluorescence in situ hybridization of mRNA and rRNA in environmental bacteria. *Appl. Environ. Microbiol.* 70: 5426–5433.

7 Discussion

Insects are one of the most successful groups of animals on earth. One of the reasons for their success is the often encountered specialization to particular food substrates, which is usually achieved by symbiosis with microorganisms (Breznak, 2004). Termites employ a whole network of such symbioses in their hindgut, which enables them to thrive on recalcitrant food like wood or soil. The impact of this symbiosis is tremendous since it opens termites the door to the most abundant food sources on earth with little or no competition with other organisms (Brune, 2003; Brune, 2005).

The aim of this study was to identify important intermediates during lignocellulose digestion in the hindgut of lower termites. The termites *Reticulitermes santonensis*, *Zootermopsis nevadensis*, and *Cryptotermes secundus*, which represent the three families of lower termites with the highest species number (Kambhampati and Eggleton, 2000), were studied for this purpose. Based on the obtained results, a quantitative model of the degradation network was proposed for each termite. Subsequently, the microbiota responsible for the turnover of the major intermediate was identified.

Individual results of this thesis have been discussed in detail in the respective chapters. In the following, the impact of these results on general aspects of lignocellulose digestion in lower termites and the responsible microbiota are addressed.

The role of hydrogen

Already early in termite gut research, evidence was accumulating that hydrogen could be an important intermediate (Hungate, 1943; Odelson and Breznak, 1983; Breznak and Switzer, 1986) but only the recent establishment of methods that keep the highly structured gut environment intact like substance gradient determination by microsensors (Revsbech et al., 1980; Brune et al., 1995; Ebert and Brune, 1997) and microinjection of tracer substances (Tholen and Brune, 1999; Tholen and Brune, 2000) made a reliable assessment possible.

Hydrogen accumulated to substantial amounts in the hindgut of *R. santonensis* and *Z. nevadensis*, whereas in *C. secundus* hydrogen was close to the detection limit of the hydrogen microelectrode (<1 kPa). Interestingly, almost no hydrogen escaped by direct emission, irrespective of the termite species. This indicated a high turnover within the hindgut, at least in *R. santonensis* and *Z. nevadensis* (chapter 3). Obviously, the pool size alone does not allow conclusions about the turnover of the respective

compound. Therefore, all hydrogen-consuming processes were studied in a comprehensive manner.

Reductive acetogenesis turned out to be the dominating hydrogen sink with rates corresponding to 18–25% of the total carbon and electron flow through the termite (chapter 3). Surprisingly, this was true not only for *R. santonensis* and *Z. nevadensis*, which showed a high accumulation of hydrogen, but also for *C. secundus*, where only a relatively low accumulation of hydrogen was observed. Since acetate is the major energy source of the termite (Odelson and Breznak, 1983), the recycling of hydrogen by reductive acetogenesis recovers about 20% of the energy that is released during lignocellulose digestion.

Other H_2-consuming processes, such as methanogenesis and aerobic hydrogen oxidation, played only a minor role. Moreover, an underestimation of gross methanogenesis by methane oxidation was explicitly ruled out since neither aerobic methane oxidizing bacteria nor archaea involved in anaerobic methane oxidation were active or even present in the hindgut (chapter 4). Using the sum of all hydrogen-consuming processes, it was determined that 22–26% of the total electron flow proceed through the hydrogen pool during lignocellulose digestion. Depending on the termite, this translates into 15–470 nmol H_2 produced per hour by the hindgut microbiota.

The high turnover rates of the hydrogen pool and CO_2 pool (chapter 3) as well as the high rate of total acetate production (ca. 80% of the total carbon flow, Odelson and Breznak, 1983) corroborate the hypothesis that the fermentation of wood polysaccharides to acetate, CO_2, and H_2 is the dominating primary degradation pathway. This type of fermentation has been shown in two cultures of hindgut protozoa (Yamin, 1980; Yamin, 1981; Odelson and Breznak, 1985b). Because protozoa make up the bulk of the hindgut volume (Berchtold et al., 1999), the assumption that protozoa are responsible for this process seems to be justified. Since hydrogen is the only reduced end product in this fermentation, it is likely that half of the produced hydrogen derived from the oxidation of reduced pyridine nucleotides (e.g., NADH), a reaction that is thermodynamically unfavorable at $pH_2 > 0.1$ kPa (Schink, 1997). In the human parasite *Trichomonas vaginalis*, which belongs to the phylum Parabasalia like many termite hindgut protozoa, malate serves as a shuttle to transport the reducing equivalents derived from reduced pyridine nucleotides into the hydrogenosome. In this organelle, malate is decarboxylated to pyruvate by the NAD^+-dependent malate enzyme (Rasoloson et al., 2002). The resulting NADH is then used to reduce H^+ to H_2 (Rasoloson et al., 2002), probably by means of a proton or sodium motive force, which drives this thermodynamically unfavorable reaction. The overall reaction could proceed via a membrane-bound NADH-ferredoxin oxidoreductase, which is driven by a proton or sodium motive force (Boiangiu et al., 2005). The reduced ferredoxin would be subsequently used as electron donor for a hydrogenase (Hrdy et al., 2004; Hrdy et al., 2005). Alternatively,

NADH could be directly used by an energy converting hydrogenase to produce hydrogen (Land et al., 2004; Dyall et al., 2004). A modified complex I that is related to such hydrogenases (Hedderich and Forzi, 2005) has been identified in hydrogenosomes of *T. vaginalis* (Dyall et al., 2004).

A question remaining is why hydrogen accumulates to different amounts in the individual termite species despite the fact that the relative turnover rate in all termites is more or less the same. A possible explanation lies in the relationship between the hydrogen concentration and the consumption rate as described, e.g., by the mathematics of the Michaelis-Menten model (e.g., Adam et al., 1995). This relationship is shaped by the affinity and kinetics of the involved enzymes but also by the number of consumers, which may differ in the studied termites.

Emerging model of lignocellulose degradation

The main degradation pathway of wood polysaccharides to acetate, CO_2, and H_2 and the subsequent recycling of CO_2 and H_2 by reductive acetogenesis have been pointed out in the previous subchapter. However, already the presence of other fermentation products in the hindgut, e.g., lactate, formate, malate, and succinate (chapter 3), indicate additional degradation pathways.

Lactate turnover rates were equal to 10% of the total carbon flow irrespective of the termite species studied. The two degradation products resulting from lactate turnover were acetate and CO_2, which is in agreement with a previous pilot study using *Reticulitermes flavipes* (Tholen and Brune, 2000). For *R. flavipes*, it was shown that this process takes place in the microoxic gut periphery and propionigenic bacteria were suggested to be responsible for lactate utilization (Tholen and Brune, 2000). In contrast to the termites analyzed in the current study, the lactate turnover rate in *R. flavipes* was determined to be equal to 33% of the total carbon flow (Tholen and Brune, 2000). However, this rate is very likely overestimated because the lactate concentration in vivo, which is higher than the lactate concentration at the time point of microinjection into embedded guts, was used for calculation (chapter 3 and chapter 6).

The origin of lactate is not clear at the moment. Results obtained with *R. flavipes* indicate that lactate originates directly from wood polysaccharide degradation (Tholen and Brune, 2000), which suggests that wood-phagocytizing protozoa are the main lactate producers. In the parabasalid protozoan *T. vaginalis*, which is a human parasite, lactate is one degradation product of glucose fermentation. *T. vaginalis* possesses hydrogenosomes and the parabasalid protozoa in the hindgut of termites are thought to posses these organelles as well (reviewed in Brune and Stingl, 2005). In contrast, oxymonads (phylum Oxymonadea), the other group of protozoa occurring in termite hindguts, seem not to possess hydrogenosomes (Bloodgood et al., 1974; Radek, 1994). Assuming that oxymonads cannot produce

hydrogen, an increased amount of reduced fermentation products like lactate can be expected.

In contrast to lactate, the role of formate differed between the model termites. In the case of *R. flavipes* (which is synonymous with *R. santonensis*, Austin et al., 2005), formate played only a minor role in the carbon flow and was completely oxidized to CO_2 (Tholen and Brune, 2000). The situation was different in *C. secundus*, where 11% of the carbon flow proceeded through the formate pool. Interestingly, formate was used both as carbon and electron donor in reductive acetogenesis, and formate-driven reductive acetogenesis constituted a second process independent from hydrogen-driven reductive acetogenesis. Although the origin of formate is also not known, it is likely that some protozoa release the reducing equivalents stemming from pyruvate oxidation not as hydrogen but as formate when they ferment wood polysaccharides to acetate.

Comparison of the total carbon and electron balances in the hindgut (using the rates of the so far identified processes) revealed that a small part of the total carbon flow might still proceed through processes that are not yet accounted for (chapter 3). This finding is corroborated by results obtained for *R. flavipes*, where the rate of total acetogenesis from ^{14}C-labeled cellulose accounted for 78% of the total carbon flow (Odelson and Breznak, 1983). The easiest explanation for this recovery gap would be that glucose and other mono- and oligosaccharides, which are produced by hydrolysis of cellulose and hemicellulose in the fore- and midgut, are absorbed in the midgut and utilized as energy substrate. There is evidence that termites are able to do so (Itakura et al., 1997) and that they possess all enzymes to respire glucose completely to CO_2 and H_2O (O'Brien and Breznak, 1984; Itakura et al., 2003).

Another explanation for the incomplete recovery is the production of additional fermentation products, e.g., malate and succinate. Hydrogenosomes of the parabasalid protozoa *Trichonympha vaginalis* and *Tritrichonympha foetus*, which are parasites of humans and bovines, respectively, produce in addition to acetate, CO_2, and H_2 also malate from pyruvate. In the presence of a high partial pressure of CO_2 as is the case in the termite hindgut, the fraction of produced malate even increases (Steinbüchel and Müller, 1986a). Alternatively, malate could also be produced as an intermediate after glycolysis and than be further converted to pyruvate and subsequently to acetate, CO_2, and H_2 in the hydrogenosomes (discussed in detail above). Succinate, on the other hand, is known to be a major fermentation product of glucose in *T. foetus* (Steinbüchel and Müller, 1986b). Therefore, the importance of malate and succinate as intermediates was analyzed as well. Malate was converted to acetate and CO_2 indicating a turnover in the hydrogenosomes, a process, which would already be included in the measured carbon flow. However, degradation in the microoxic gut periphery as shown for lactate (Tholen and Brune, 2000) cannot be excluded. In the case of succinate, propionate and acetate were the main

fermentation products, but formate and CO_2 were formed in small amounts as well (chapter 6).

The cumulative results of this study allowed the proposal of a robust quantitative model of the degradation network in the different termites studied (Fig. 7, chapter 3). The degradation of wood polysaccharides to acetate, CO_2, and H_2 and the subsequent recycling of CO_2 and H_2 by reductive acetogenesis were identified as the two main degradation pathways. Nevertheless, the hindgut metabolism is not completely homoacetogenic as proposed previously (Breznak and Switzer, 1986) but possesses additional routes of lignocellulose digestion as discussed above. Interestingly, the metabolites produced by these additional pathways, be it lactate, formate, malate, or succinate, are mainly intermediates that are degraded further, and acetate is always one of their degradation products. Obviously, the metabolic network in the termite hindgut is optimized to produce as much acetate as possible, which in turn is used by the termite as the main energy substrate (Odelson and Breznak, 1983).

Spirochetes drive reductive acetogenesis

The importance of reductive acetogenesis necessitated the identification of the responsible microorganisms. The first hint for the identity of homoacetogens in lower termites came from the isolation of the homoacetogenic spirochete *Treponema primitia* (Leadbetter et al., 1999; Graber and Breznak, 2004; Graber et al., 2004). This finding was surprising because the majority of isolated homoacetogens belong to the class Clostridia (Drake et al., 2001). However, in the termite hindgut, where spirochetes can account for as many as 50% of all prokaryotes (Breznak, 1984), the hypothesis of spirochete-driven reductive acetogenesis seems realistic.

A diversity analysis of the functional marker gene *fhs* in the three studied termites indicated that indeed spirochetes of the "Termite Treponeme Cluster" are the dominating homoacetogens (chapter 5). This was in good agreement with previous results obtained for *Z. nevadensis* (Salmassi and Leadbetter, 2003). However, the presence of a gene is not proof of the associated activity. Using an expression analysis, finally evidence was provided that only *fhs* genes of the 'Termite Treponeme cluster' are transcribed in all three studied termites (chapter 5). The cumulative evidence presented in this and previous studies strongly indicates that spirochetes are indeed the dominating and most active homoacetogens in the hindgut of lower termites. However, not all spirochetes found in the termite hindgut can perform reductive acetogenesis and a role in the nitrogen economy of the termite was proposed for these bacteria (Lilburn et al., 2001). Using fluorescent in situ hybridization techniques targeting the mRNA of functional genes (Pernthaler and Amann, 2004) like *fhs* or *nif*H and a subsequent identification by cell sorting and analysis of the 16S rRNA genes could help to distinguish the different

populations of spirochetes. The designing of a probe targeting the *fhs*-mRNA is described in chapter 6.

Applied aspects of termite gut research

Lignocellulose is the most abundant form of biomass on earth, which makes it at the same time the most abundant renewable organic energy source (Claassen et al., 1999 and references therein). Lower termites are very efficient in utilizing lignocellulose by dissimilating a large proportion of the cellulose (74–99%) and hemicellulose (65-87%) components (Esenther and Kirk, 1974; Wood, 1978), which makes them a very good model to study energy access from wood or plant litter.

Using the results of this study (chapter 3) and assuming that the termite uses acetate as its main energy source, as has been shown by Odelson and Breznak (1983), the energy gain of the termite from the symbiotic degradation of lignocellulose can be estimated. The underlying calculations are based on the energy gain from aerobic oxidation of acetate by the termite (-854 kJ mol^{-1}) and the amount of acetate produced by the individual processes in the hindgut (chapter 3) using the aerobic oxidation of the glucosyl units of cellulose as a reference (-2872 kJ mol^{-1}) (Brune, 2005). In total, it can be calculated that approximately 80% of the energy stored in the degraded parts of lignocellulose is provided to the termite in form of acetate with the remaining 20% mainly used by the hindgut microbiota for its own energy needs. Acetogenesis of primary fermentations (presumably by the protozoa) provides the main energy contribution (53–54%), followed by H_2-dependent reductive acetogenesis (16–22%) and acetogenesis from lactate (5–6%). In *C. secundus*, formate-dependent reductive acetogenesis provides an additional energy contribution (5%). These calculations show once more how important the recycling of hydrogen by reductive acetogenesis is for the termite. If homoacetogens would be absent from the termite hindgut, most likely methanogens would take over hydrogen recycling as known from the rumen (Wolin et al., 1997). Since methane cannot be used by animals as an energy substrate, this would result in a substantial energy loss for the termite.

Comparison of the termite hindgut to reactors that produce instead of acetate ethanol from wood quickly reveals that nature is still more efficient than mankind. Using the wood consumption rate of *Reticulitermes* spp. (19.3 mg wood (g. f. wt. termite)$^{-1}$ day^{-1}; Wood, 1978) and their acetate production rate (chapter 3), it can be estimated that these termites produce 13 mol acetate per kg wood. In comparison, reactors, which use a simultaneous saccharification and fermentation process of softwood, gain 5 mol ethanol per kg wood (Galbe and Zacchi, 2002). However, there is one point where these reactors are superior to the termite hindgut. With a production rate of 5 mol ethanol (liter reactor)$^{-1}$ day^{-1} (calculated using data from Galbe and Zacchi, 2002 and Wingren et al., 2003) they have a higher turnover rate

then the termite hindgut, which produces 1 mol acetate (liter termite hindgut)$^{-1}$ day^{-1} (calculated using data from chapter 3 and Wood, 1978).

An additional interesting aspect of termite hindgut biology is the internal production of hydrogen. Hydrogen is viewed as an emerging "clean" energy carrier of the near future and the production from lignocellulose has been suggested as one possibility (Claassen et al., 1999; Dunn, 2002). As discussed in detail in the previous subchapters, the termite hindgut harbors symbiotic protozoa, which can produce 4 mol of hydrogen per glycosyl unit of cellulose. The interesting fact here is that they are able to do so even at high hydrogen partial pressures, which can be close to saturation as observed in the hindgut of *Z. nevadensis*. In contrast, bacteria like the Clostridia, which are widely used in biotechnological research concerning hydrogen production (Collet et al., 2004; Morimoto et al., 2004 and references therein), can achieve such a high hydrogen yield only at $pH_2 < 0.1$ kPa (Schink, 1997). Certainly, termite hindgut protozoa are to difficult to maintain for a direct biotechnological use. However, there is still a lot to learn from their biochemistry including the efficient hydrolysis of wood polysaccharides and the subsequent fermentation that produces hydrogen as the sole reduced end product, even under a high hydrogen partial pressure.

Outlook

Currently, we are just beginning to understand the tripartite interaction between the termite host, its symbiotic protozoa, and the highly diverse prokaryotic community. The identification of homoacetogenic spirochetes and the importance of reductive acetogenesis was the first step in elucidating the structure and function of the microbial hindgut community. From phylogenetic studies it is known that besides spirochetes there is a second dominant group of bacteria, which were termed the Endomicrobia (Hongoh et al., 2003; Stingl et al., 2005; Yang et al., 2005). As the name implies, these bacteria are endosymbionts of the hindgut protozoa and interestingly enough represent a novel phylum (Stingl et al., 2005). However, as was previously the case with the spirochetes, the function of these symbionts is unknown. Using modern techniques like genome and transcriptome analysis of Endomicrobia representatives in combination with the transcriptome analysis of the host protozoa could help to understand how, among many other aspects, the fermentation of wood polysaccharides proceeds in detail.

It should also be emphasized that there is still a lack in knowledge about the physiology of the diverse protozoa that are known to occur in different termites (Yamin, 1979). It is very likely, that not all protozoa strictly ferment wood polysaccharides to acetate, CO_2, and H_2, which is already indicated by the many fermentation products found in the hindgut (chapter 3). Their metabolism is probably more versatile or could in other cases even be completely unrelated to the primary fermentation of wood polysaccharides. Evidence pointing towards this

direction is the description of the termite hindgut protozoan *Tricercomitus divergens*, which does not utilize cellulose at all (Yamin, 1978). An approach to study the physiology of single protozoa species in more detail could be a short-time incubation of picked protozoa with a subsequent analysis of their released fermentation products by microanalytics, which would employ, e.g., a detection by mass spectrometry. The obtained results could then be corroborated by transcriptome analysis using a cDNA library. Nevertheless, traditional approaches using cultivation techniques should still be employed in parallel since they have proven to work in the past (Yamin, 1978; Yamin, 1980; Yamin, 1981; Odelson and Breznak, 1985b).

References

1. Adam, G., Läuger, P., and Stark, G. (1995) Physikalische Chemie und Biophysik. 3rd edn. Berlin: Springer.
2. Austin, J. W., Szalanski, A. L., Scheffrahn, R. H., Messenger, M. T., Dronnet, S., and Bagnères, A.-G. (2005) Genetic evidence for the synonymy of two *Reticulitermes* species: *Reticulitermes flavipes* and *Reticulitermes santonensis*. *Ann. Entomol. Soc. Amer.* 98: 395–401.
3. Berchtold, M., Chatzinotas, A., Schönhuber, W., Brune, A., Amann, R., Hahn, D., and König, H. (1999) Differential enumeration and in situ localization of micro-organisms in the hindgut of the lower termite *Mastotermes darwiniensis* by hybridization with rRNA-targeted probes. *Arch. Microbiol.* 172: 407–416.
4. Boiangiu, C. D., Jayamani, E., Brugel, D., Herrmann, G., Kim, J., Forzi, L., Hedderich, R., Vgenopoulou, I., Pierik, A. J., Steuber, J., and Buckel, W. (2005) Sodium ion pumps and hydrogen production in glutamate fermenting anaerobic bacteria. *J. Mol. Microbiol. Biotechnol.* 10: 105–119.
5. Bloodgood, R. A., Miller, K. R., Fitzharris, T. P., and McIntosh, J. R. (1974) The ultrastructure of *Pyrsonympha* and its associated microorganisms. *J. Morphol.* 143: 77–106.
6. Breznak, J. A. (1984) Hindgut spirochetes of termites and *Cryptocercus punctulatus*. In *Bergey's Manual of Systematic Bacteriology*. Krieg, N. R., and Holt, J. G. (eds). Baltimore: Williams & Wilkins, pp. 67–70.
7. Breznak, J. A. (2004) Invertebrates–Insects. In *Microbial Biodiversity and Bioprospecting*. Bull, A. T. (ed). Washington, D. C.: ASM Press, pp. 191–203.
8. Breznak, J. A., and Switzer, J. M. (1986) Acetate synthesis from H_2 plus CO_2 by termite gut microbes. *Appl. Environ. Microbiol.* 52: 623–630.
9. Brune, A. (2003) Symbionts aiding digestion. In *Encyclopedia of Insects*. Cardé, R. T. and Resh, V. H. (eds). New York: Academic Press, pp. 1102–1107.
10. Brune, A. (2005) Symbiotic associations between termites and prokaryotes. In *The Prokaryotes. An Online Electronic Resource for the Microbiological Community, 3rd edn.* Dworkin, M., Falkow, S., Rosenberg, E., Schleifer, K-H., and Stackebrandt, E., (eds). New York: Springer-SBM, http://link.springer-ny.com/link/service/books/10125/
11. Brune, A., and Stingl, U. (2005) Prokaryotic symbionts of termite gut flagellates: phylogenetic and metabolic implications of a tripartite symbiosis. In *Molecular Basis of Symbiosis*. Overmann, J. (ed). Berlin: Springer, pp. 39–60.

12. Brune, A., Emerson, D., and Breznak, J. A. (1995) The termite gut microflora as an oxygen sink: microelectrode determination of oxygen and pH gradients in guts of lower and higher termites. *Appl. Environ. Microbiol.* 61: 2681–2687.

13. Claassen, P. A. M., van Lier, J. B., Lopez Contreras, A. M., van Niel, E. W. J., Sijtsma, L., Stams, A. J. M., de Vries, S. S., and Weusthuis, R. A. (1999) Utilisation of biomass for the supply of energy carriers. *Appl. Microbiol. Biotechnol.* 52: 741–755.

14. Collet, C., Adler, N., Schwitzguébel, J.-P., and Péringer, P. (2004) Hydrogen production by *Clostridium thermolacticum* during continuous fermentation of lactose. *Int. J. Hydrogen Energy* 29: 1479–1485.

15. Drake, H. L., Küsel, K., and Matthies, C. (2001) Acetogenic Prokaryotes, 3rd edition, release 3.7. In *The Prokaryotes: An Evolving Electronic Resource for the Microbiological Community*. Dworkin, M., Falkow, S., Rosenberg, E., Schleifer, K.-H. and Stackebrandt, E. (eds). New York: Springer-Verlag. http://link.springer-ny.com/link/service/books/10125/

16. Dunn, S. (2002) Hydrogen futures: toward a sustainable energy system. *Int. J. Hydrogen Energy* 27: 235–264.

17. Dyall, S. D., Yan, W., Delgadillo-Correa, M. G., Lunceford, A., Loo, J. A., Clarke, C. F., and Johnson, P. J. (2004) Non-mitochondrial complex I proteins in a hydrogenosomal oxidoreductase complex. *Nature* 431: 1103–1107.

18. Ebert, A., and Brune, A. (1997) Hydrogen concentration profiles at the oxic-anoxic interface: a microsensor study of the hindgut of the wood-feeding lower termite *Reticulitermes flavipes* (Kollar). *Appl. Environ. Microbiol.* 63: 4039–4046.

19. Esenther, G. R., and Kirk, T. K. (1974) Catabolism of aspen sapwood in *Reticulitermes flavipes* (Isoptera: Rhinotermitidae). *Ann. Entomol. Soc. Am* 67: 989–991.

20. Galbe, M., and Zacchi, G. (2002) A review of the production of ethanol from softwood. *Appl. Microbiol. Biotechnol.* 59: 618–628.

21. Graber, J. R., and Breznak, J. A. (2004) Physiology and nutrition of *Treponema primitia*, an H_2/CO_2-acetogenic spirochete from termite hindguts. *Appl. Environ. Microbiol.* 70: 1307–1314.

22. Graber, J. R., Leadbetter, J. R., and Breznak, J. A. (2004) Description of *Treponema azotonutricium* sp. nov. and *Treponema primitia* sp. nov., the first spirochetes isolated from termite guts. *Appl. Environ. Microbiol.* 70: 1315–1320.

23. Hedderich, R., and Forzi, L. (2005) Energy-converting [NiFe] hydrogenases: more than just H_2 activation. *J. Mol. Microbiol. Biotechnol.* 10: 92–104.

24. Hongoh, Y., Ohkuma, M., and Kudo, T. (2003) Molecular analysis of bacterial microbiota in the gut of the termite *Reticulitermes speratus* (Isoptera; Rhinotermitidae). *FEMS Microbiol. Ecol.* 44: 231–242.

25. Hrdy, I., Cammack, R., Stopka, P., Kulda, J., and Tachezy, J. (2005) Alternative pathway of metronidazole activation in *Trichomonas vaginalis* hydrogenosomes. *Antimicrob Agents Chemother* 49: 5033–5036.

26. Hrdy, I., Hirt, R. P., Dolezal, P., Bardonová, L., Foster, P. G., Tachezy, J., and Embley, T. M. (2004) *Trichomonas* hydrogenosomes contain the NADH dehydrogenase module of mitochondrial complex I. *Nature* 432: 618–622.

27. Hungate R. E. (1967) Hydrogen is an intermediate in the rumen fermentation. *Arch. Microbiol.* 59: 158–164.

28. Hungate, R. E. (1943) Quantitative analyses of the cellulose fermentation by termite protozoa. *Ann. Entomol. Soc. Am.* 36: 730–739.

29. Itakura, S., Tanaka, H., and Enoki, A. (1997) Distribution of cellulases, glucose and related substances in the body of *Coptotermes formosanus*. *Mater. Org.* 31: 17–29.

30. Itakura, S., Tanaka, H., Enoki, A., Chappell, D. J., and Slaytor, M. (2003) Pyruvate and acetate metabolism in termite mitochondria. *J. Insect Physiol.* 49: 917–926.

31. Kambhampati, S., and Eggleton, P. (2000) Taxonomy and phylogenetics of Isoptera. In *Termites: Evolution, Sociality, Symbiosis, Ecology*. Abe, T., Bignell, D. E., and Higashi, M. (eds). Dordrecht: Kluwer Academic Publishers, pp. 1–23.

32. Land, K. M, Delgadillo-Correa, M. G., Tachezy, J., Vanacova, S., Hsieh, C. L., Sutak, R., and Johnson, P. J. (2004) Targeted gene replacement of a ferredoxin gene in *Trichomonas vaginalis* does not lead to metronidazole resistance. *Mol. Microbiol.* 51: 115–122.

33. Leadbetter, J. R., Schmidt, T. M., Graber, J. R., and Breznak, J. A. (1999) Acetogenesis from H_2 plus CO_2 by spirochetes from termite guts. *Science* 283: 686–689.

34. Leaphart, A. B., and Lovell, C. R. (2001) Recovery and analysis of formyltetrahydrofolate synthetase gene sequences from natural populations of acetogenic bacteria. *Appl. Environ. Microbiol.* 67: 1392–1395.

35. Lilburn, T. G., Kim, K. S., Ostrom, N. E., Byzek, K. R., Leadbetter, J. R., and Breznak, J. A. (2001) Nitrogen fixation by symbiotic and free-living spirochetes. *Science* 292: 2495–2498.

36. Madigan, M. T., Martinko J. M., and Parker, J. (2003) Brock biology of microorganisms. 10th ed. London: Pearson Education Ltd.

37. Miller T. L. (1995) Ecology of methane production and hydrogen sinks in the rumen. In *Ruminant physiology: Digestion, Metabolism, Growth and Reproduction*. Engelhardt, W. V., Leonhardt-Marek, S., Breves, G., and Gieseke, D. (eds). Stuttgart: Ferdinand Enke Verlag, pp. 317-331.

38. Morimoto, M., Atsuko, M., Atif, A. A. Y., Ngan, M. A., Fakhru'l-Razi, A., Iyuke, S. E., and Bakir, A. M. (2004) Biological production of hydrogen from glucose by natural anaerobic microflora. *Int. J. Hydrogen Energy* 29: 709–713.

39. O'Brien, R. W., and Breznak, J. A. (1984) Enzymes of acetate and glucose metabolism in termites. *Insect Biochem.* 14: 639–643.

40. Odelson, D. A., and Breznak, J. A. (1983) Volatile fatty acid production by the hindgut microbiota of xylophagous termites. *Appl. Environ. Microbiol.* 45: 1602–1613.

41. Odelson, D. A., and Breznak, J. A. (1985) Nutrition and growth characteristics of *Trichomitopsis termopsidis*, a cellulolytic protozoan from termites. *Appl. Environ. Microbiol.* 49: 614–621.

42. Pernthaler, A., and Amann, R. (2004) Simultaneous fluorescence in situ hybridization of mRNA and rRNA in environmental bacteria . *Appl. Environ. Microbiol.* 70: 5426–5433.

43. Radek, R. (1994) *Monocercomonides termitis* nov. sp., an Oxymonad from the lower termite *Kalotermes sinaicus*. *Archiv für Protistenkunde* 144: 373–382.

44. Rasoloson, D., Vanacova, S., Tomkova, E., Razga, J., Hrdy, I., Tachezy, J., and Kulda, J. (2002) Mechanisms of in vitro development of resistance to metronidazole in *Trichomonas vaginalis*. *Microbiology* 148: 2467–2477.

45. Revsbech, N .P., Jorgensen, B. B., and Blackburn, T. H. (1980) Oxygen at the sea bottom measured with a microelectrode. *Science* 207: 1355–1356.

46. Salmassi, T. M., and Leadbetter, J. R. (2003) Molecular aspects of CO_2-reductive acetogenesis in cultivated spirochetes and the gut community of the termite *Zootermopsis angusticollis*. *Microbiology* 149: 2529–2537.

47. Schink, B. (1997) Energetics of syntrophic cooperation in methanogenic degradation. *Microbiol. Mol. Biol. Rev.* 61: 262–280.

48. Steinbüchel A., and Müller, M. (1986) Anaerobic pyruvate metabolism of *Tritrichomonas foetus* and *Trichomonas vaginalis* hydrogenosomes. *Mol. Biochem. Parasitol.* 20: 57–65.

49. Steinbüchel A., and Müller, M. (1986) Glycerol, a metabolic end product of *Trichomonas vaginalis* and *Tritrichomonas foetus*. *Mol. Biochem. Parasitol.* 20: 45–55

50. Stingl, U., Radek, R., Yang, H., and Brune, A. (2005) '*Endomicrobia*': Cytoplasmic symbionts of termite gut protozoa form a separate phylum of prokaryotes. *Appl. Environ. Microbiol.* 71: 1473–1479.

51. Tholen, A., and Brune, A. (1999) Localization and in situ activities of homoacetogenic bacteria in the highly compartmentalized hindgut of soil-feeding higher termites (*Cubitermes* spp.). *Appl. Environ. Microbiol.* 65: 4497–4505.

52. Tholen, A., and Brune, A. (2000) Impact of oxygen on metabolic fluxes and in situ rates of reductive acetogenesis in the hindgut of the wood-feeding termite *Reticulitermes flavipes*. *Environ. Microbiol.* 2: 436–449.

53. Wingren A., Galbe M., and Zacchi G. (2003) Techno-economic evaluation of producing ethanol from softwood: comparison of SSF and SHF and identification of bottlenecks. *Biotechnol. Prog.* 19: 1109–1117.

54. Wolin, M. J. (1982) Hydrogen transfer in microbial communities. In *Microbial interactions and communities*, vol. 1. Bull, A. T., and Slator, J. H, (eds). New York: Academic Press, pp. 323–356.

55. Wolin, M. J., Miller, T. L., and Stewart, C. S. (1997) Microbe-microbe interactions. In *The rumen microbial ecosystem*. Hobson P. N., and Stewart, C. S. (eds). London: Blackie Academic and Professional, pp. 478–481.

56. Wood, T. G. (1978) Food and feeding habits of termites. In *Production Ecology of Ants and Termites*. Brian, M. V. (ed). Cambridge: Cambridge Univ. Press, pp. 55–80.

57. Yamin, M. A. (1978) Axenic cultivation of the flagellate *Tricercomitus divergens* Kirby from the termite *Cryptotermes cavifrons* Banks. *J. Parasitol.* 64: 1122–1123.

58. Yamin, M. A. (1979) Termite flagellates. *Sociobiology* 4: 1–119.

59. Yamin, M. A. (1980) Cellulose metabolism by the termite flagellate *Trichomitopsis termopsidis*. *Appl. Environ. Microbiol.* 39: 859–863.

60. Yamin, M. A. (1981) Cellulose metabolism by the flagellate *Trichonympha* from a termite is independent of endosymbiotic bacteria. *Science* 211: 58–59.

61. Yang, H., Schmitt-Wagner, D., Stingl, U., and Brune, A. (2005) Niche heterogeneity determines bacterial community structure in the termite gut (*Reticulitermes santonensis*). *Environ. Microbiol.* 7: 916–932.

Summary

This thesis summarizes a series of studies concerning the quantitative analysis of lignocellulose degradation in the hindgut of lower termites. Emphasis was put on the intermediates of symbiotic digestion, especially hydrogen, and the processes as well as microorganisms involved in their turnover.

The termites *Reticulitermes santonensis*, *Zootermopsis nevadensis*, and *Cryptotermes secundus*, which represent the three lower termite families with the highest species numbers, were used as model organisms. The three species showed pronounced differences in the degree of hydrogen accumulation in their hindguts, ranging from almost no accumulation in *C. secundus* to nearly saturation in *Z. nevadensis*.

Despite these differences in accumulation, hydrogen was the most important intermediate of the metabolic network in the three termites. About 22–26% of the total electron flow proceeded through the hydrogen pool. Reductive acetogenesis was identified as the dominating hydrogen-utilizing process, whereas hydrogenotrophic methanogenesis, aerobic hydrogen oxidation, and loss of hydrogen by emission from the termite played only a minor or no role. Moreover, an underestimation of gross methanogenesis by methane oxidation was explicitly ruled out by the finding that neither aerobic methane oxidizing bacteria nor archaea involved in anaerobic methane oxidation were active or even present in the hindgut. Further experiments identified lactate as second important intermediate in the studied termites. Formate played a role as additional intermediate in *C. secundus* only, where it was used in formate-dependent reductive acetogenesis. Based on these carbon and electron flux measurements, quantitative models of the degradation processes in the different termites were proposed.

Using the functional marker gene *fhs*, which encodes the formyl tetrahydrofolate synthetase, the identity and diversity of homoacetogens was assessed. In all studied termites, *fhs* genes were dominating that fell into the "Termite Treponeme cluster". Subsequent expression analyses revealed that only *fhs* genes of the "Termite Treponeme cluster" were transcribed. The cumulative evidence of this study together with the previous isolation of a homoacetogenic spirochete from the termite hindgut strongly indicate that spirochetes of the genus *Treponema* are responsible for reductive acetogenesis in the hindgut of lower termites.

In summary, the structure and function of the homoacetogenic populations in the termite hindgut were successfully elucidated. Spirochetes were shown to be responsible for the efficient recycling of hydrogen by reductive acetogenesis thereby making the termite hindgut to one of the most efficient bioreactors in nature.

Zusammenfassung

Die vorliegende Arbeit umfasst eine Reihe von Studien, die sich mit der quantitativen Analyse des Lignocelluloseabbaus im Enddarm von niederen Termiten beschäftigt. Das Hauptaugenmerk der Untersuchungen lag auf den Zwischenprodukten des Abbaus, im Besonderen auf Wasserstoff, sowie deren Umsatz und den dafür verantwortlichen Mikroorganismen.

Die Termiten *Reticulitermes santonensis*, *Zootermopsis nevadensis* und *Cryptotermes secundus*, welche die drei artenreichsten Familien niederer Termiten repräsentieren, wurden als Modellorganismen verwendet. Untersuchungen zur intestinalen Wasserstoffkonzentration offenbarten extrem hohe Unterschiede in den verschieden Termitenarten, wobei in *Z. nevadensis* Wasserstoff in Mengen nahe dem Sättigungsbereich vorlag, während in *C. secundus* sich die Konzentration des Wasserstoffs nahe der Nachweisgrenze befand (<1 kPa).

Trotz dieser unterschiedlichen Konzentrationen war Wasserstoff das wichtigste Zwischenprodukt des Lignocelluloseabbaus in den drei Termitenarten. Dabei betrug der Anteil des gesamten Elektronenflusses, der durch den Wasserstoffpool fließt, 22–26%. Die reduktive Acetogenese war der dominierende Wasserstoff-verbrauchende Prozess, während die hydrogenotrophe Methanogenese, die aerobe Wasserstoffoxidation sowie die Emission von Wasserstoff aus der Termite eine unwesentliche oder keine Rolle spielten. Eine Unterbestimmung der Methanogeneserate durch aerobe bzw. anaerobe Methanoxidation wurde experimentell ausgeschlossen. Weiterhin wurde Laktat als zweites wichtiges Zwischenprodukt in allen untersuchten Termiten identifiziert. Formiat stellte ebenfalls ein Zwischenprodukt dar. Allerdings war Formiat nur in *C. secundus* von Bedeutung, wo es durch die Formiat-abhängige reduktive Acetogenese umgesetzt wurde. Basierend auf diesen Kohlenstoff- und Elektronenflussmessungen wurden quantitative Modelle der Abbauprozesse im Enddarm der einzelnen Termitenarten postuliert.

Die Identität und Diversität homoacetogener Bakterien im Enddarm wurde mit Hilfe des funktionellen Markergens *fhs* analysiert. Dieses Gen kodiert die Formyl-Tetrahydrofolat-Synthetase – ein Enzym des Acetyl-CoA-Weges. In allen untersuchten Termiten dominierten zahlenmässig *fhs*-Gene, die dem „Termiten-Treponemen-Cluster“ angehören. Weiterhin ergaben Expressionsanalysen, dass ausschließlich *fhs*-Gene des „Termiten-Treponemen-Cluster“ transkribiert wurden. Zusammenfassend deuten die Ergebnisse dieser Studie und die vorangegangene Kultivierung eines homoacetogenen Spirochäten aus dem Termitenenddarm stark darauf hin, dass Spirochäten der Gattung *Treponema* für die effiziente Wiederverwertung des Wasserstoffs durch die reduktive Acetogenese verantwortlich sind.

Publikationsliste

Pester, M., Friedrich, M. W., Schink, B., and Brune, A. (2004) *pmoA*-based analysis of methanotrophs in a littoral lake sediment reveals a diverse and stable community in a dynamic environment. *Appl. Environ. Microbiol.* 70: 3138–3142.

Bussmann, I., Pester, M., Brune, A., and Schink, B. (2004) Preferential cultivation of type II methanotrophic bacteria from littoral sediments (Lake Constance). *FEMS Microbiol. Ecol.* 47: 179–189.

Brune, A., and Pester, M. (2005) In situ measurements of metabolite fluxes: microinjection of radiotracers into insect guts and other small compartments. In *Methods in Enzymology*. Leadbetter, J. R. (ed). London: Elsevier, pp. 200–212.

Pester, M., and Brune, A. (2006) Expression profiles of *fhs* (FTHFS) genes support the hypothesis that spirochaetes dominate reductive acetogenesis in the hindgut of lower termites. *Environ. Microbiol.* 8: 1261–1270.

Pester, M., and Brune, A. Hydrogen recycling is a key process in the hindgut metabolism of lower termites. In Vorbereitung.

Pester, M., Tholen, A., Friedrich, M. W., and Brune, A. Methane oxidation in termite hindguts – absence of evidence and evidence of absence. In Vorbereitung.

Brune, A., and Pester, M. Symbiotic processes in the hindgut metabolism of lower termites. In Vorbereitung.

Beiträge zu wissenschaftlichen Tagungen (nur Promotion)

Pester, M., and Brune, A. (2004). Hydrogenotrophic methanogens and homoacetogens in termite guts: Competition or co-existence? VAAM Jahrestagung, März 2004, Braunschweig (Poster).

Pester, M., and Brune A. (2004). Hydrogenotrophic methanogens and homoacetogens in termite guts: Competition or co-existence? 4th INRA-RRI Symposium, June 2004, Clermont-Ferrand, Frankreich (Poster).

Pester, M., and Brune, A. (2005). Why termites need microbes – acetogenesis in the hindgut of wood-feeders. 1st PhD student meeting of the Mas Planck Institutes in Marburg and Bremen. Februar 2005, Marburg (Vortrag).

Pester, M., Ikeda-Ohtsubo, W., Desai, M., and Brune, A. (2006). *Candidatus* Endomicrobium trichonymphae – role in the endosymbiosis. Begutachtung des SFB TR1, April 2006, München (Poster).

Pester, M. and Brune, A. (2006). Spirochetes are the dominating homoacetogens in the hindgut of lower termites. VAAM Jahrestagung, März 2006 (Vortrag).

Pester M., and Brune, A. (2006) High performance of spirochete-driven reductive acetogenesis in lower termites. Joint meeting of the Dept. of Biogeochemistry, MPI Marburg and the Microbial Physiology Research Group, University of Wageningen, NL. May 2006, Marburg (Vortrag).

Pester M., and Brune, A., (2006). Top-performance of spirochete-driven homacetogenesis in the termite hindgut. 11th ISME Symposium. August 2006, Wien (Poster).

Abgrenzung der Eigenleistung

Soweit nicht anders erwähnt, wurden alle Experimente von mir selbst geplant und durchgeführt, sowie anschließend in Form eines Manuskriptes ausgewertet. Das abschließende Verfassen der Manuskripte erfolgte zusammen mit meinem Betreuer Prof. Dr. A. Brune.

Kapitel 2 besteht aus einem Übersichtsartikel über Mikroinjektion, bei dem die Literatursuche sowie das primäre Abfassen des Manuskripts vorwiegend von mir übernommen wurde. Das endgültige Erstellen des Manuskripts erfolgte zusammen mit meinem Betreuer Prof. Dr. A. Brune.

Die Messung von Methanoxidationsraten mit $^{14}CH_4$ in Kapitel 4 wurden von Anne Tholen durchgeführt. Die Entwicklung und Bewertung des PCR-Tests für die Detektion von Archaea, die an der anaeroben Methanoxidation beteiligt sind, erfolgte in der Arbeitsgruppe von PD Dr. Michael W. Friedrich. Die PCR-Tests mit funktionellen Markergenen erfolgte in Zusammenarbeit mit Katja Meuser.

Die RFLP-Analyse der *fhs*-Klonbibliothek aus dem Endarminhalt von *Cryptotermes secundus* wurde in Zusammenarbeit mit Katja Meuser durchgeführt.

Die in vitro Transkription sowie die Aufreinigung der mRNA-Sonden, die in Kapitel 6 beschrieben sind, wurden von Julia Riekmann im Rahmen einer von mir betreuten Diplomarbeit durchgeführt.